Austrian Journal of Technical and Natural Sciences

№ 7–8 2016
July–August

«East West» Association for Advanced Studies and Higher Education GmbH

Vienna
2016

Austrian Journal of Technical and Natural Sciences

Scientific journal

№ 7–8 2016 (July–August)

ISSN 2310-5607

Editorial office European Science Review
"East West" Association for Advanced Studies
and Higher Education GmbH, Am Gestade 1
1010 Vienna, Austria

Email: info@ew-a.org

Homepage: www.ew-a.org

Austrian Journal of Technical and Natural Sciences is an international, German/English/Russian language, peer-reviewed journal. It is published bimonthly with circulation of 1000 copies.

The decisive criterion for accepting a manuscript for publication is scientific quality. All research articles published in this journal have undergone a rigorous peer review. Based on initial screening by the editors, each paper is anonymized and reviewed by at least two anonymous referees. Recommending the articles for publishing, the reviewers confirm that in their opinion the submitted article contains important or new scientific results.

East West Association GmbH is not responsible for the stylistic content of the article. The responsibility for the stylistic content lies on an author of an article.

Instructions for authors

Full instructions for manuscript preparation and submission can be found through the "East West" Association GmbH home page at: http://www.ew-a.org.

Material disclaimer

The opinions expressed in the conference proceedings do not necessarily reflect those of the «East West» Association for Advanced Studies and Higher Education GmbH, the editor, the editorial board, or the organization to which the authors are affiliated.

East West Association GmbH is not responsible for the stylistic content of the article. The responsibility for the stylistic content lies on an author of an article.

Typeset in Berling by Ziegler Buchdruckerei, Linz, Austria.
Printed by «East West» Association for Advanced Studies and Higher Education GmbH, Vienna, Austria on acid-free paper.

Section 1. Mathematics

Druzhinin Victor Vladimirovich,
Alekseev Vladimir Vasilevich
National research University "MEPHI"
Sarov physical-technical Institute
E mail: vvdr@newmail.ru

The construction of the sums of a geometric progression to a degree

Abstract: The analytical expressions for the erection of sums of geometric progressions to a degree. The results are used for the summation of series, complex finite sums, solving algebraic equations.

Keywords: geometric progression, complex finite and infinite sums.

In analytical mathematics there are many examples of finite sums and series, with a relatively simple formula the result. These include the binomial theorem, sums of arithmetic and geometric progressions, sums of Bernoulli — ordered amount of the one power, whole and fractional numbers, arithmetic-geometric progressions and other subjects [1; 2; 3; 4]. In this article we focus on the construction in the natural degree *m* amounts of a geometric progression

$$G(a,n,m) = \left(\sum_{k=0}^{n} a^k\right)^m = \left(1+a+a^2+a^3+\ldots+a^n\right)^m = \left(\frac{a^{n+1}-1}{a-1}\right)^m. \quad (1)$$

In reference books and educational literature we have not found this problem. Meanwhile here there is a large set of new deemed according to the formula amounts and ranks as well as taking the integrals and the solution of algebraic equations. In (1) the final result is the right side, but as reveals the amount of degree, what its symmetry and structure are we show below. First we write the polynomial theorem

$$\left(\sum_{k=0}^{n} x_k\right)^m = \sum \frac{m!}{(t_1!)(t_2!)\ldots(t_n!)} (x_1)^{t_1} (x_2)^{t_2} \ldots (x_n)^{t_n}, \quad (2)$$

where $(t_1+t_2+\ldots+t_n)=m$ and the sum goes through all combinations of these numbers. With the special structure of numbers $x_k = x^k$ (our case) the left part is much easier. Number of terms is $(nm+1)$, the highest degree is a^{nm}. General record in nm even has a view

$$G(a,n,m) = \sum_{k=0}^{n} c_k a^k + \sum_{k=n+1}^{s-1} b_k a^k + d_s a^s + \sum_{k=s+1}^{2s-n-1} e_k a^k + \sum_{k=2s-n}^{mn} f_k a^k. \quad (3)$$

Coefficients with increasing k monotonically increase up to including d_s. The central coefficient d_s has the greatest value. The following ratios monotonically decrease symmetrically, and $c_k = f_{nm-k}$ and $b_k = e_{nm-k}$. We have identified the coefficients of the different letters as they are considered by different formulas. The basic factors are calculated using binomial coefficient $(n \geq 2)$

$$c_k(n,m) = \frac{(m+k-1)!}{(m-1)!k!} = C^k_{m+k-1}. \quad (4)$$

For the coefficients b_k and d_s we have not received General formula, but found them to specific $m = 2,3,4$. If nm is an odd number, then in the middle of the right row (3) there is not one greatest factor, and two of the same factor. If $n = 2t+1, m = 2p+1$ that are coefficients $d_{2pt+t+p} = d_{2pt+t+p+1}$. Subsequently the coefficients of mirror symmetry occurs.

If $m = 2$ then

$$G(a,n,2) = \left(\sum_{k=0}^{n} a^k\right)^2 = \sum_{k=0}^{n} (k+1)a^k + \sum_{k=n+1}^{2n} (2n+1-k)a^k. \quad (5)$$

For example,

$$\left(1+a+a^2\right)^2 = 1+2a+3a^2+2a^3+a^4, \quad (6)$$

$$\left(1+a+a^2+a^3\right)^2 = 1+2a+3a^2+4a^3+3a^4+2a^5+a^6. \quad (7)$$

From identities (6 –7) a symmetry of the right and left parts and an algorithm for the construction of any geometric progression is in the square.

In the construction of $G(a,n,3)$ in the cube we obtain the following result. If n is even, $n = 2t$, if $2t+1 \leq k \leq 3t-1, b_k = 1+3t(t+1)-(mt-k)^2$; $d_{3t} = 1+3t(t+1)$. Examples

$$G(a,2,3) = 1+3a+6a^2+7a^3+6a^4+3a^5+a^6. \quad (8)$$

$$G(a,4,3) = 1+3a+6a^2+10a^3+15a^4+ \\ +18a^5+19a^6+18a^7+\ldots+a^{12}. \quad (9)$$

$$G(a,6,3) = 1+\ldots 21a^5+28a^6+33a^7+ \\ +36a^8+37a^9+36a^{10}\ldots+a^{18}. \quad (10)$$

If n is odd, $n=2t+1$, then $2t+2\le k\le 3t, b_{3t+1-q}=$ $=d_{3t+1}-q(q+1);\ 1\le q\le t-1$. The highest coefficients $d_{3t+1}=d_{3t+2}=3(t+1)^2$. Examples

$$G(a,3,3)=1+3a+6a^2+10a^3+12a^4+ +12a^5+10a^6+6a^7+3a^8+a^9. \quad (11)$$

$$G(a,5,3)=1+3a+6a^2+10a^3+15a^4+ +21a^5+25a^6+27a^7+\ldots+a^{18}. \quad (12)$$

These amounts are calculated according to right side (1). In the construction of $G(a,n,4)$ in the fourth degree we get such formulas, regardless of the evenness or unevenness of n. If $k=2n, d_{2n}=1+5n+$ $+2n(n-1)(n+4)/3$, the maximum value of the coefficient. If $k=2n-1$ have the greatest $b_{2n-1}=d_{2n}-(n+1)$. The other coefficients b_{2n-l}, with $1\le l\le n-2$ are calculated by recurrent relations $b_{2n-l-1}=b_{2n-l}-(2l+1)n+(3l^2-l-2)/2$. Examples

$$G(a,2,4)=1+4a+10a^2+16a^3+ +19a^4+16a^5+\ldots+a^8. \quad (13)$$

$$G(a,3,4)=1+4a+10a^2+20a^3+31a^4+ +40a^5+44a^6+40a^7+..+a^{12}. \quad (14)$$

$$G(a,4,4)=1+\ldots+35a^4+52a^5+68a^6+ +80a^7+85a^8+80a^9\ldots+a^{16}. \quad (15)$$

It is also possible to obtain other degrees $G(a,n,m)$. Consider the possible applications of these structures.

1. The sum of a convergent series of generalized geometric progression with $0<|a|<1$ species arises

$$\sum_{k=0}^{\infty}\frac{(m+k-1)!}{(m-1)!k!}a^k=\frac{1}{(1-a)^m}. \quad (16)$$

2. If we take the derivative at a, we get the new calculated amount. For example, $\partial G(a,2,3)/\partial a$ gives

$$1+4a+7a^2+8a^3+5a^4+2a^5=\frac{(a^3-1)^2(2a^2-a-1)}{(a-1)^3}. \quad (17)$$

3. There appears the possibility of analytical solutions of algebraic equations of high order. The equation $a^6+3a^5+6a^4+7a^3+6a^2+3a-26=0$ is reduced to the equation $a^2+a-2=0$ which has two $a_1=1, a_2=-2$.

4. Combinations of sums and products of $G(a,n,m)$ form a new hope of final amount and series and also give the opportunity to find the integral analytically.

References:

1. Sizyi S. V. Lectures on the theory of numbers, FIZMATGIZ, – M., 2007.
2. Korn. G., Korn. T. Handbook of mathematics, Science, GHML, – M., 1974. P. 31, 135.
3. Gradshteyn I. S., Ryzhik I. – M. Tables of integrals, sums, series and products. GIFML, – M, 1962. P. 15–16.
4. Druzhinin V. V., Sirotkina A. G. NTVP, No. 4, 2016, P. 15–16.

Section 2. Medical science

Anoshina Tatiana Nikolaevna,
PhD, Assistant of the Department of Obstetrics,
Gynecology and Reproduction,
Shupik National Medical Academy
of Postgraduate Education, Kyiv, Ukraine
E-mail: tanyakolom@gmail.com

Clinical course of genital herpes in HIV-infected pregnant women

Abstract: HIV-infected pregnant women have severe manifestations of the clinical course of genital herpes, which was accompanied by a characteristic colpo- and vulvoscopic picture (inflammatory background, herpes vesicles, ulcers, erosion, hyperemia, apparent edema, serous-inflammatory discharge, multi-vessels, severe reaction on acetic acid, rough epithelial relief with micropapillary needled like outgrowths of the connective tissue). It was demonstrated the expediency of express diagnostics (Tzanck sample, Schiller test). There were specific for HSV cytologic manifestations: increased sizes of nuclei in epithelial cells, form of watch-glass, multinucleated cells, muddy unstructured chromatin. In 40.0% of patients the Cowdry bodies were found. In 40.0% of HIV-infected patients a tendency to recurrence of HSV was revealed.

Keywords: HIV, herpes, pregnancy, colposcopy, cytology.

Introduction. The course of pregnancy in HIV-infected women is often accompanied by fetal growth retardation, low birth weight, fetal death, premature delivery, ill-timed discharge of amniotic fluid [1]. It is believed that these complications occur more frequently as a result of HIV-associated infections, but not HIV [2; 3].

Numerous studies demonstrated that in HIV-infected women the herpes virus detected with high rates in the structure of associated infections. It is known that herpes viruses may activate HIV gene in provirus stage and there is cofactors for progress of HIV infection to AIDS [4; 5].

The clinical manifestations of herpes simplex virus infection (HSV) in HIV-positive patients are more aggressive, with frequent relapses and systemic lesions, and this compromised the course of underlying disease [6].

Objective: To characterize the clinical course of genital herpes infections in HIV-infected pregnant women.

Materials and methods. The evidences of the study of specific Ig M, Ig G and IgG avidity are demonstrated the activity of virus herpes simplex virus (HSV) type 2 in 24 of the 50 infected women (8 women — primary infection, 16 — reactivation process). In 18 women observed a typical clinical picture of genital herpes (6 — with the primary infection and 12 — with the reactivation). Ten of these women have the first clinical episodes.

HSV-2 diagnosis was based on the identified changes of genitals using colposcopic techniques with accounting the data of cytological investigations. Colposcopy (vulvoscopy) is conducted with 10–20x magnifications. Simple colposcopy means the examination of the mucous membrane without diagnostic solutions. Further extended colposcopy performed with a 3-percent solution of acetic acid (acetic acid test). Tzanck sample and Schiller test with Lugol were used. Cytological and direct microscopic study was performed according to the conventional techniques. Staining of preparations was performed according to Papanicolaou, Papengeym, and Romanovsky-Giemsa.

Results and discussion. We observed the following stages of the clinical form of HSV-2 primary episodes: 1 — incubation period (2–7 days); 2 — initial-prodromal (minimally symptomatic) — 1–2 days; 3 — culmination (multi-symptomatic period of rash), symptomatic — from 3 to 14 days; 4 — regressive (reparative) — from 2 to 10 days; 5 — subclinical period (recovery) — to relapse.

As can be seen from Table 1, the initial phase was characterized by small number of symptoms, mainly

complaints on itching (70.0%); 20.0% of women felt a tingling, 20.0% — pain, 20.0% — edema, 10.0% — redness. In 10.0% there was an increase of whole body temperature.

The appearance of herpetic vesicles with clear contents in all women (in 80.0% — the ulcers with sharp margins and flat bottoms) indicated on the culminating stage, that in all women accompanied by pain, redness, purulent and serous discharges, positivity of Tzanck samples. The vast majority of patients mentioned the tingling and itching, 20.0% — myalgia, 20.0% — increasing of regional lymph nodes, 40.0% — rise of temperature. Almost in all (90.0%) the vessels with response on diagnostic solution, bleeding vessels, and negative Schiller test were observed. In 60.0% was noted a rough, granular, lumpy relief of mucous, in 10.0% — micropapillary papillae (needle-like hyperplasia of the connective tissue), acetowhite epithelium.

Table1 – Clinical diagnostic manifestations of genital herpes in HIV-infected pregnant women according to the period of process (2 — initial; 3 — culmination; 4 — reparative; 5 — subclinical),%

Diagnostic manifestations		Period of herpes process			
		2	3	4	5
Tingling		20,0	60,0	10,0	–
Redness		10,0	100,0	60,0	20,0
Itching		70,0	30,0	20,0	10,0
Pain		40,0	100,0	40,0	20,0
Development of herpetic vesicles		–	100,0	40,0	10,0
Ulcers with sharp margins and flat bottom		–	80,0	30,0	10,0
Myalgia		–	20,0	10,0	–
Enlarged of regional lymph nodes		–	20,0	10,0	–
Rise of temperature		10,0	40,0	20,0	10,0
Edema		20,0	90,0	30,0	10,0
Purulent and serous discharges		–	100,0	20,0	10,0
Vessels with response on diagnostic solution		–	90,0	40,0	10,0
Bleeding vessels		–	90,0	30,0	10,0
Rough, grainy, and lumpy relief		–	60,0	40,0	30,0
Micropapillary papillae		–	10,0	40,0	20,0
Acetowhite epithelium,		–	10,0	10,0	50,0
Sheeler Test in affected area	positive	–	–	20,0	40,0
	slightly positive	20,0	10,0	50,0	10,0
	negative	70,0	90,0	30,0	30,0
Tzanck sample	positive	–	100,0	70,0	10,0
	negative	–	–	30,0	90,0

In the reparative period, the number of vesicles decreased (40.0%), being replaced with hyperpigmentation crusts, accompanied by pain; in 40.0% with a decrease of complaints on tingling (10.0%) and pruritus (20.0%). At the transition to the subclinical stage (30 hours from the onset of clinical signs) in HIV-infected pregnant women observed some clinical diagnostic manifestations of genital herpes.

The initial process on the vulvar and cervical mucosa was characterized by redness of varying intensity, moderate edema, presence of translucent vesicles with different sizes, a small number of vessels, reaction to acetic acid (constriction — dilatation), mild severity of pain syndrome. Cytologically, the period was characterized by a large number of white blood cells with prevailing of polynuclear cells, in a presence of macrophages, lymphocytes, and histiocytes. The epithelium has dystrophic changes. It was noted the isolated double-nucleated cells. The viral cytopathic typical for herpes changes in this period not be detected (Table 2).

The culmination period — the number of vesicles increases, it size enlarges, part of the vesicles dissilientes with forming of ulcers on their place, true erosion, inflammation background, hyperemia, apparent edema, serous-inflammatory discharges, multi-vessels, pronounced reaction on acetic acid (rapid constriction — dilatation), severe pain. Cytologically, the HSV-specific changes were developed on inflammatory background (large amount of neutrophilic, eosinophilic and lymphoid elements, including plasma cells, histiocytes, and cells of fibroblastic family). The nuclei of epithelial cells considerably enlarged. The large number of multinucle-

ated cells which are formed not as a result of mitotic division, but at adhesion and stratification of nuclei are present. Typical features of nuclei: turbid (opaque) unstructured chromatin; nuclei looked as if through frosted glass; grain structure of chromatin is absent, the presence of regional (marginal) chromatin. The swelling of the nucleus, the nucleus are looked as «watch glass». In 40.0% of patients the Cowdry bodies (nuclear bodies with a light halo) were detected, that was apparent sign of herpes virus infection.

Table 2 – Cytological features of genital herpes in HIV-infected pregnant women according to the period of process (2 – initial; 3 – culmination; 4 – reparative; 5 – subclinical),%

Cytological features	Period of herpes process			
	2	3	4	5
Increased nuclei	10,0	90,0	20,0	10,0
Loosening nuclei	10,0	90,0	30,0	10,0
Changes in nuclei forms (polymorphism)	10,0	60,0	20,0	–
Hyperchromatosis of nuclei	–	30,0	20,0	10,0
Swelling of nuclei	10,0	80,0	40,0	20,0
Multinucleated cells	20,0	90,0	30,0	20,0
Margination of thickened chromatin	–	70,0	40,0	10,0
Erased, dirty, and grayish chromatin	10,0	100,0	40,0	20,0
Unstructured chromatin, appearance as «watch glass»	10,0	90,0	40,0	20,0
Structured chromatin	30,0	–	30,0	60,0
Muddy chromatin structure	20,0	100,0	70,0	30,0
Intranuclear inclusions with illumination area (Cowdry bodies)	10,0	40,0	10,0	10,0
Enlarged cytoplasm		60,0	30,0	20,0
Vacuolated cytoplasm		30,0	20,0	–
Packed cytoplasm		20,0	10,0	10,0
Fuzzy contour of cytoplasm		40,0	20,0	10,0

In reparative period, the majority of patients had a relief or absence of pain, reduction of congestion, little or no blood vessels, lack of response to acetic acid, absence of vesicles, ulcer epithelialization without rough relief, isolated small ulcers, and lack of needled-like reaction of connective tissue. In some HIV-positive patients (40.0%) are still noted the presence of ulcers, red color, uneven relief with raised portions, lesions, rough epithelial relief with micropapillary needled-like outgrowths of the connective tissue.

Cytologically, this period characterized by a small amount of leukocytes, most of which are presented by macrophage and lymphoid elements. In the majority of patients herpes-specific viral cytopathic changes in this period were not observed, reparative changes in the cells were mild. In 40% of patients preserved the cytological background (typical for herpetic changes), namely: the presence of white blood cells, small number of macrophages, isolated double- and multinucleated cells with a weak violation of chromatin structure, blurred chromatin, pronounced reparative changes in cells.

Subclinical period (at a month after the onset of symptoms) in most patients vulvo- and colposcopically characterized by a flat uniform relief of the mucosa surface, whitish and slightly red coloring, and absence of granular raised acetowhite erosive vesical areas. In 10.0% of patients the slightly grainy relief was detected, that can be explained by normal teratogenesis of the vulva mucous membrane. In some patients (40.0%) colposcopy and vulvoscopy characterized by a motlier picture, coloring was diverse: from white to red, the surface of some areas was raised, micropapillary, round-granular; in 10.0% the small vesicles in the 1st cervix uteri zone were observed by colposcopy.

Cytologically, this period in the majority of patients characterized by the following picture: squamous epithelium without structure, cytoplasm and nuclei disturbing, well-structured chromatin in the nuclei, the absence of double- and multinucleated cells, the vulva epithelium without hyper-, para- and dyskeratosis, isolated leukocytes. However, in some women it was noted an increased number of white blood cells, the dystrophic and degenerative changes of epithelium, presence of isolated double-nucleated cells with a weak structuring of chromatin, some clouding of the nuclei, which is typical for the recurrence risk.

Conclusions. Thus, this study found that HIV-positive pregnant women have severe manifestations of the clinical course of genital herpes (pain, redness, herpetic vesicles, purulent and serous discharges, in 20.0% — an enlarging of regional lymph nodes, in 40.0% — fever), which was accompanied by a characteristic colpo- and vulvoscopic picture (the presence of vesicleing, ulceration, erosion, hyperemia, apparent edema, serous-inflammatory discharges, multi-vessels, intense reaction on acetic acid — fast constriction-dilatation, rough epithelial relief with micropapillary needled-like outgrowths of the connective tissue on the inflammatory background). The expediency of express-diagnostics (at the culmination period 100% patients have a positive Tzanck test and negative or slightly positive Schiller test) was established.

The diagnosis of genital herpes confirmed by HSV-specific cytological manifestations: nuclei of epithelial cells have much larger sizes, looked as watch-glass, multinucleated cells, turbid (opaque) unstructured chromatin). In 40.0% of patients Cowdry bodies were found, that is also typical for HSV.

In HIV-infected patients revealed a tendency to recur (in 40.0% observed the colposcopic and cytological signs of relapse at the end of 1 month).

References:

1. Фризе К. Инфекционные заболевания беременных и новорождённых/К. Фризе, В. Кахель. – М.: Медицина, 2003. – 423 с.
2. The Role of Co-Infections in Mother-to-Child Transmission of HIV/C. C. King, S. R. Ellington, A. P. Kourtis//Current HIV Research. – 2013. – № 11. P.10–23.
3. Вплив перинатальних факторів на швидкість прогресування ВІЛ-інфекції в дітей/Л. І.Чернишова, Ю. С. Степановський, І. В. Раус, О. В. Юрченко//Перинатология и педиатрия. – 2012. – № 4 (52). – С. 8–13.
4. Кузьмин В. Н. Генитальный герпес в акушерстве и гинекологии — проблема и пути решения /В. Н. Кузьмин//Гинекология. – 2010. – № 4. – С. 4–7.
5. ВИЧ_инфекция, вторичные и сопутствующие заболевания. Тематический архив./Под ред. Н. А. Белякова, В. В. Рассохина, Е. В. Степановой. – СПб: Балтийский медицинский образовательный центр, 2014. – 368 с.
6. Вепрык Т. В., Матейко Г. Б. Герпетическая инфекция у ВИЧ-инфицированных пациентов//Современные проблемы науки и образования. – 2013. – № 5. – С. 365.

Section 3. Food processing industry

Kakhramon Sanoqulovich Rakhmonov,
Science researcher, faculty chemical technological,
Bukhara engineering technological institute, city Bukhara.
Isabaev Ismail Babadjanovich,
Doctor of Technical Sciences,
Professor faculty chemical technological,
Bukhara engineering technological institute, city Bukhara.
Bukhara engineering-technological institute
E-mail: qaxa8004@mail.ru

Wheaten ferments spontaneous fermantation in biotechnological methods

Abstract: In article are shown results of research of biotechnological properties of wheaten leavens of spontaneous fermentation (in the example of pea–anisetree leaven) and their analysis. Also is established influence of the given type of leavens on the basic biopolymers of the flour, on the property of the pastry and quality of bread from wheaten flour.

Keywords: Bread, microbial contamination, the spontaneous fermentation, bakery products

In modern conditions of an intensification of technologies of bread production in regions with hot climate and ecologically adverse zones, requirements to biotechnological properties of flour half-finished products, in particular wheaten leavens have raised. Traditionally at preparation of national bakery products in Republic of Uzbekistan leavens of spontaneous fermentation are used. The greatest distribution has received pea–anisetree leaven, which technological potential practically is not learned. Pea–anisetree leaven concerns to polystrain spontaneously soured leavens. This type of leavens is characterized by instability of biotechnological indicators of quality, and even short storage is accompanied by decrease in their barmy activity and development of nonspecific microflora for the wheaten pastry.

Pea-anistree leaven on traditional technology was prepared.

The mixture of peas and anistree was filled in with 1 l of water in temperature 80±2 °C, surface was strewed with flour and mixture maintained at temperature 30±1 °C within 24 hours. Fermented leaven pounded to homogeneous mass and added a nutritious substratum. A substratum for leaven prepared from 100 g of wheaten floor of the second grade, 200 ml of water, ferment preparation of Amilorizin P10x (0.01% to weight of flour in the mixture) and cultivated at temperature 28±1 °C. In each 24 hours within 8 days in leaven without updating were defined titratable and active (pH) acidity, mass fraction of sugars, quantity of yeast and acid-forming bacteria, and their regenerative activity.

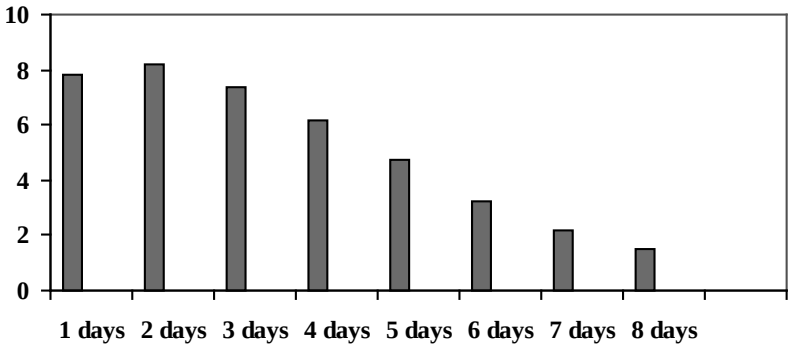

Figure 1. Dependence of glycogenesis (% on SV) in leaven from duration of cultivation (days)

Results of research are represented in drawing and presented at tab. 1–4.

The analysis of experimental data (fig.) has shown that in the first days of fermentation the mass fraction of sugars in leaven made 7.8 … 8.2%, then their maintenance naturally decreased, and by the fermentation end was within 1.2 … 1.5% that is caused by active accumulation of a biomass of microorganisms.

It was established (tab. 1) that the leaven which has started to fermentation spontaneously, reached optimum acidity only on 4–5 days. Thus bacteria were differed the best regenerative activity which made 40–35 minutes, then natural deterioration of the given indicator was marked.

Table 1. – Indicators of quality of leavens at spontaneous fermentation

The name of indicators	Values of indicators of quality of leaven at fermentation, during days								
	Initial	1	2	3	4	5	6	7	8
Acidity	1.6	10.0	12.6	15.0	17.5	17.0	22.0	26.8	32.4
pH	6.30	3.70	3.65	3.55	3.50	3.50	3.40	3.00	2.80
Quantity of acid-forming bacteria, million/g	–	226	1329	2385	2320	2769	2851	2512	2192
Restorative activity, minutes	–	70	65	50	40	35	55	60	75

Plating of biologically active mixture on diagnostic medium made in 3 multiple frequencies. As diagnostic mediums were used meat infusion agar and mash agar. Plating was observed since 4 hours after preparation of a mixture and further in each 24 hours within 5 days. Mixtures stored at temperature 28±1 °C.

Microbiological plating on firm mediums, microscoping and subsequent identifications of microorganisms shown that within 5 days of cultivation in leaven remained the various microflora: rod form bacteria, yeast, moldy mushrooms.

In information from specialized sources (1.2) were defined that in spontaneously soured wheaten leavens dominate family of Enterobacteriaceal bacteria, fermenting sugar with formation of carbon dioxide, hydrogen and quantity of organic acids (lactic, acetic, formic and succinic acids).

Simultaneously in the medium started to breed barmy cells which in the process beginning were present only at individual examples. In leaven yeast of sort Saccharomyces and Zygomycetes has been found out. The given microorganisms, along with bacteria and microscopic mushrooms, contain in the flour. On the average the quantity of yeast of sort Saccharomyces in the first days of maturing made $16 \cdot 10^6$ … $18 \cdot 10^6$. Zygomycetes — $10 \cdot 10^6$ … $12 \cdot 10^6$ cells in 1 g of leaven. In process of increase in a period of storage of leaven was marked gradual dying off of barmy cells of both sorts so after 3 days the quantity of cells of cultural race of yeast Saccharomyces has decreased to $15.8 \cdot 10^6$. and Zygomycetes — to $3.4 \cdot 10^6$ cells in 1 r leavens. The parity of bacteria and yeast on 1, 3 and 5 days of cultivation made accordingly 13:1. 151:1 and 181:1.

Because work is directed on studying of possibility of use of leavens of spontaneous fermentation as an alternative substitute of yeast, have been conducted comparative researches of properties of the pastry and condition of the basic biopolymers of a flour in variants without leaven, on leaven without yeast, on leaven and yeast at a parity 1:1.

For intensification of the process of pastry preparation it is important that by the fermentation end in the pastry there was enough quantity of sugars. Therefore, was studied influence of investigated leaven on dynamics of change of the maintenance of sugars in half-finished products (tab. 2).

Table 2. – Formation and consumption of sugars at fermentation of half-finished products

Variants	The maintenance of sugars,% on SV					
	In dense sourdough			In sourdoughless pastry		
	Initial	In 3.0 h	In 5.0 h	Initial	In 3.0 h	In 5.0 h
Mixture of a flour, water and salt	1.9	–	–	1.5	–	–
With addition: – Yeast	2.4	3.4	2.0	2.2	2.7	1.4
– Leavens	2.0	4.8	3.4	1.9	3.6	2.9
– Yeast and leaven	2.6	4.0	2.9	2.4	3.1	1.8

Comparison of the data on consumption of sugars by microorganisms shows that in half-finished products with yeast sugar are much more intensively consumed than with leaven and a mixture of yeast and leavens. So, in 3 hours of fermentation the residual maintenance of sugars in sourdough and the pastry in variants with leaven exceeded similar value in variants with yeast and yeast with leaven, accordingly, on 1.4 … 0.8 and 0.9 … 0.5%.

The increase in duration of fermentation of half-finished products in variants with leaven and yeast with leaven even to 5 h did not lead to an exhaustion of a mass fraction of sugars, moreover, in the given variants the maintenance of residual sugars exceeded similar value in half-finished products on yeast on 0.9 … 1.4% at sourdough way of pastry making and on 1.5 … 0.4% — at sourdoughless way.

Natural decrease in an exit crude and dry gluten in the process of the pastry maturing, prepared with addition of spontaneously soured leaven, and also increase of the maintenance of water-soluble substances concerning the control sample (tab. 3) is established.

Table 3. – Change of albuminous connections of the flour in the process of pastry fermentation

Variants	Duration of fermentation, h	Quality indicators of gluten					The maintenance of water-soluble substances,% on SV the pastry
		Quantity of gluten from 50 g of the pastry, r	The maintenance of gluten,% on SV the pastry		Hydration ability,%	Deformation of compression, Unit of IDK	
			The crude	The dry			
Mixture of a flour, water and salt	0	10.23	36.8	13.9	165	65	12.1
	3.0	10.11	36.4	13.8	164	71	14.8
With addition: – Yeast	0	10.04	36.1	13.9	160	65	11.7
	3.0	9.15	33.0	13.1	152	70	12.7
– Leavens	0	10.10	36.2	13.9	160	64	13.3
	3.0	6.63	23.8	9.6	148	43	19.2
– Yeast and leaven	0	10.00	35.9	13.8	160	64	13.7
	3.0	5.80	20.8	8.6	142	45	17.2

The above-stated suggests that changes in the pastry with leaven are caused basically by acid hydrolysis of albuminous connections of the flour, caused by the products of vital activity of acid-forming bacteria.

Further have been prepared the dough from first-rate wheaten flour in sourdough and sourdoughless ways. At sourdough way of pastry making leaven was brought in sourdough in quantity of 4% to prescription quantity of the flour, the pressed yeast — in the dough, and at sourdoughless way — 8% of leaven to prescription quantity of the flour. As the control samples without leaven served.

Entering mesophyll leavens in an initial stage of pastry making as at sourdough so and sourdoughless ways reduces pH indicator of half-finished products to the values 5.5-5.3 which are optimum for vital activity of microorganisms. At such pH values of flour half-finished products inhibits action of α-amylase that allows receiving qualitative production from a flour with raised autolytic activity.

Use of mesophyll leavens leads to reduction of durability of structure of the pastry that, obviously, is connected with an intensification of processes aerogenesis, hydrolytic splitting of biopolymers of the flour, increase of the maintenance of water-soluble substances in the pastry.

Influence of analyzed leaven on quality of bread from the first-rate wheaten flour was estimated by results of laboratory baking quality test. Finished goods analyzed through 16-18 h after the baking quality test.

Results of researches are presented at tab. 4.

Table 4. – Influence of leaven on quality of bread from the first-rate wheaten flour

The name of indicators	Indicators of quality of the bread prepared			
	in the sourdoughless way		on dense sourdough	
	Without leaven	With leaven	Without leaven	With leaven
Humidity,%	43.80	43.80	43.60	43.70
Acidity, degree	2.60	3.00	3.10	3.40
Porosity,%	69	70	70	74
Specific volume, sm^3/g	2.44	2.59	2.60	2.74
Stability of shape (N: D)	0.44	0.45	0.45	0.48
Organoleptic estimation, point	78	80	80	84

It is established that the improving effect of action of leaven depends on a way of preparation of the pastry.

From results of the researches resulted in tab. 4 follows that the bread with the best quality is received at use of sourdough way of pastry making with entering of leaven in dense sourdough, and yeast — in the pastry. The increase in specific volume of bread on the average on 5.4% and porosity — on 5.7%, and improvement of structurally-mechanical properties of a crumb is established, products were characterized by lighter color of a crumb, strongly pronounced taste and aroma in comparison with the similar production prepared on dense sourdough without leaven.

As a result of the carried out researches it is established that leavens have an influence to the condition of the basic biopolymers of the flour, intensity of their acid hydrolysis, and structurally-mechanical properties of the pastry.

Sharing of yeast and leavens is especially effective at sourdough way of pastry making that will allow to intensify technological process of preparation of bread, to lower pH indicator of the half-finished products to values 5.5 … 5.3 at which decreases activity of of α-amylase and is synthesized sufficient quantity of sugars for proof and baking.

Also it is established that irrespective from the way of pastry making, use of investigated leaven of spontaneous fermentation promotes improvement of quality of finished goods.

The way of preparation of bread on dense sourdough with entering of lactic leaven in sourdough, and yeast in the pastry has been recognized as the optimum way. The given way allows receiving finished goods with stable quality, which are meeting the requirements of State Standard 27842-88.

References:

1. Matveeva I.V., Belyavskaya I.G. Biotechnological basis of preparation of bread. – M: DeLi print, 2001, P. 150.
2. Bogatyryova T.G., Polandova R. D. Novelty in production of wheaten bread on leavens. – M: CSRITER of bakery products, 1994, P. 45.

Section 4. Technical sciences

Yorkin Sodikovich Abbasov,
Fergana Polytechnic Institute
Doctor of Technical Sciences,
the Faculty of Construction
E-mail: education.fer@yandex.ru
Mirsoli Odiljanovich Uzbekov,
Fergana Polytechnic Institute
Senior Researcher,
the Faculty of Construction

Studies efficiency solar air collector

Abstract: The article presents an analysis of the existing solar air collectors. A description of the design and the results of experimental studies on the effectiveness of the solar air collector with an absorber of from metal shavings.

Keywords: mankind, ecology, energy crisis, alternative energy sources, solar radiation, solar air collectors, efficiency.

For almost the entire history of mankind, the population increased very slowly because of the large dependence of man from nature, frequent wars, epidemics, hunger. Population growth in the 18TH-19th centuries became extremely gather momentum and accelerated sharply in the first half of the 20th century. The growth rate of population is associated with an enormous leap in development and discoveries in the field of basic sciences, medicine, and materials science. As a result of modern life has become much more convenient and easier, which causes an increase in the birth rate and life expectancy of the person.

As of January 1, 2016 years Earth's population totaled almost 7.3 billion. Predictable number of the world's population stood at 1.01.2016 at 7 295 889 256 people, thus having increased for 1 year at 78 million inhabitants or 1.08 percent.

Main and the obligatory condition of existence man and mankind as a whole, is the consumption of energy and energy resources, the existence of available for energy consumption has always been required to meet human needs.

However, global growth in energy consumption in addition to the positive effect of such a rapid energy development and population growth exists and the negative impact of progress:

– environmental pollution;

– depletion of mineral reserves and others.

The International Energy Agency and the World Energy Council predicts a 400 percent increase in energy consumption in the world by 2050, which will lead to further climate change [1, 9 –11].

One way to deter this threat is greater use of renewable energy sources (RES) [1, 8–10].

Among the renewables, solar radiation on the scale of the resources, environmental friendliness and omnipresence is the most promising energy source for heat and cold [2, 25–26].

According to the data of 2011, more than 180 million.m2 solar collectors are used in the world, which provide different heat consumers. The most common of these technologies in China (59%), in second place — Europe (14%). 186 large are firms producing solar collectors in 41 countries [3, 9–10].

One of the first decisions made when choosing a solar power system is the choice of the working fluid for the type of heat transfer. The heat transfer can be considered as liquids and gases. Currently prevailing heat transfer fluids: water, antifreeze, aqueous solutions of ethylene — and propylene glycol, oil. The only gas became widespread as a coolant is the air [1, 11–12].

When choosing a set of coolant is necessary to consider various factors (Table 1). If we analyze all the

factors, the air-type collectors are usually cheaper than the identical liquid, but generally have a lower level of the coolant temperature and efficiency. However, the scope of the air collectors (due to temperature stratification in the battery or due to the fact that air is taken from outside or from the premises) located near the low value of reduced temperature and high efficiency, while the water collectors have to be used at higher values of the reduced temperature and consequently, at lower efficiency [5, 17–19].

Table 1. – Comparison of air and water systems

Factor	Air system	Water system
The possibility of corrosion	Potentially low probability	Potentially high probability
Influence of leaks	Negligible, if they are small	Significant damage to the system
The problems associated with phase transitions coolant (freezing, boiling)	–	Potentially high probability; needed protection
Pipelines, canals	An air duct of larger cross section (higher cost)	Pipes with relatively small cross sections (the lower value)
The cost of the pump (fan)	relatively high	relatively low
Tank capacity — Battery	More than in water systems	Less than air systems
collector weight	Relatively lightweight design	Relatively heavy construction
Fabrication and installation	It does not require high accuracy	Requires high precision (tightness)

For air heating buildings and drying agricultural products have received widespread solar air collectors, which are ways of moving the absorber air is relatively divided into two types: convective (contact) and matrix (transposition) [6, 15–16]. In the first — air flow washes impervious surface absorber, heated by solar radiation, and in the second — there is filtration of air movement through the structure of the absorber.

According to an overview of the world market of solar heating, performed Franz Mautner and Werner Weiss from the institute AEE INTEC (Austria) under the «Solar heating and cooling,» the International Energy Agency (May 2013), at the end of 2011 in the world operated by air solar total area 2,213,434 m^2, including the majority (71%, 15 68549 m^2) — without glazed collectors. Glazed collectors constitute for 29% (644,885 m^2). The following table shows the distribution of air solar collector in volumes of more than 100 thousand m^2 installations by country.

Table 2. — Air air solar collector area of the countries of the world [4].

Countries	don't vitrified	vitrified	Total, m^2	Countries	don't vitrified	vitrified	Total, m^2
Australia	264000	6600	270600	Japan	–	475199	475199
Austria	–	1078	1078	Mexico	–	7664	7664
Canada	334426	11781	346207	Norway	–	1019	1019
Denmark	3133	17280	20413	Switzerland	876000	–	87600
Germany	–	32256	32256	United Kingdom	14000	–	14000
Hungary	1440	1152	2692	USA	75000	75185	150185
India	–	15667	15667	Total	1568549	644885	2213434
Israel	550	–	550				

As a result of structural analysis USED solar air collectors currently in practice [1; 3; 6; 8; 9] may be developed which are the most effective collector matrix type air because of the greater area of contact with the absorber and the greater the value of convection coefficient heat absorber in the air.

In recent decades, much research conducted to improve the efficiency of solar air collectors. To improve the efficiency of the solar air collectors heat must be effectively transferred from the absorber to around his air [3, 1–2], reducing radiation and reduce overall heat loss coefficient of absorber in the surrounding environment [1, 13–15].

To achieve these goals, the authors' are proposing variant design solar air collector with absorber convection-matrix type.

The main technical indicators of the solar air collector is showed in Figure 1. Solar air heater is made from durable and lightweight two-chambered plastic frame

from lambri (1) that allows to exploit by the collector without insulation, reducing its weight and increasing mobility. First absorber (3) represents the profiled sheeting with a thickness of 1 mm, total area 0.7 m^2, painted with Matt black light from the side the sun, underneath the absorber (2) mounted 3 partitions, to increase the length of the path of air through the collector, over the profile sheet set second absorber (4) from metal shavings (made by steel metal NH 78t) with a diameter of 0.5 to 0.7 cm, thickness 1÷2 mm, total area of 0.725, painted bluish light. As a transparent insolation (5) used glass with thickness 4 mm.

The basic idea of the design of such a solar collector, that the use of metal shavings as absorber of the solar heater, allows you to maximize the heat exchanging surface heating and air contact area with the absorber and absorbers of from a profile sheet and of metal shavings intensify heat that increases efficiency.

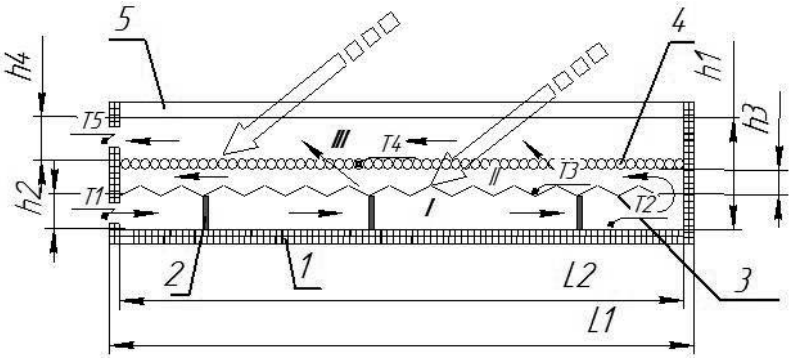

1 — insulation;
2 — partitions;
3 — absorber of from profiled sheet;
4 — absorber of from metal shavings;
5 — transparent insulation;
T1 ...T5 — point temperature measurement

Figure 1. Air Solar Collector scheme.

Table 3. – The dimensions of the designed constructions:

№	The name of the	Value	№	The name of the	Value
1	The length of the collector (channels) L2, m	1.45	7	The thickness of the channel h2, m	0.01
2	The length of the collector, L1, m	1.5	8	The thickness of the channel h3, m	0.01
3	The width of the manifold (channel) b, m	0.5	9	The thickness of the channel h4, m	0.015
4	The width of the manifold, b, m	0.6	10	Absorber area AU 1 m^2	0.7
5	The height of the collector (channels) h1, m	0, 072	11	Area of heating surface 2, m^2	0, 725
6	Area of heating surface 2, m^2	0,7	12	Unit weight, kg	20

Solar radiation falling on the collector, passing through a transparent coating, part is absorbed by the absorber of metal shavings, the remainder absorbed the second absorber, which heated up. Air is fed into the solar air collector heater using a fan is blown through the inlet tube (Figure 1), air enters the space between the bottom of the absorber and the collector (I). The heated air passing the lower openings enters the space between the absorbers (II), where intensify heating air. The air then enters the space between the absorber and the transparent insulation (III), after the air goes through the exit tube.

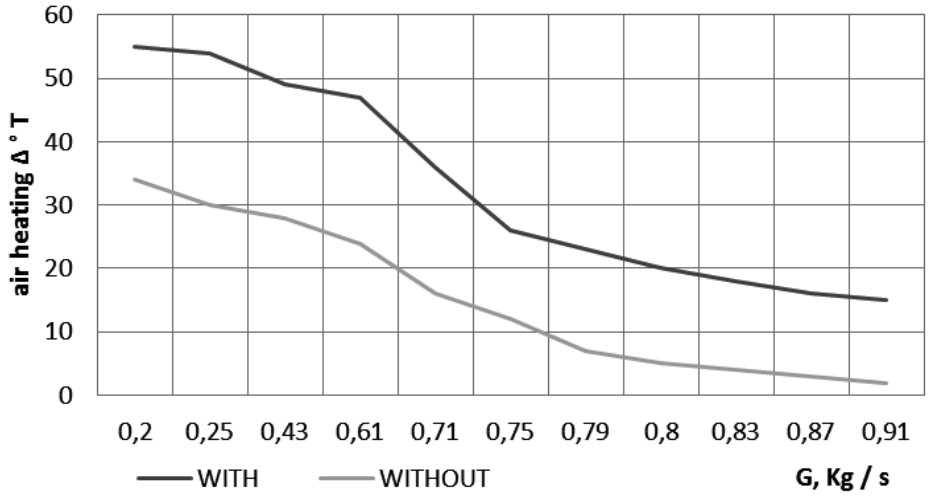

Figure 2. The dependence of the efficiency of the collector from the heating absorbers for with / without absorber of METAL SHAVINGS

Experimental studies on the thermal characteristics of a solar collector were carried out in field conditions and in the following order: For a fixed value of the angle of inclination of the 45°, to measure the in collector temperature used chromel — copel thermocouple connected to the TRACE MODE software, through TRM 138 — measuring system, air flow rate was varied by changing the fan speed.

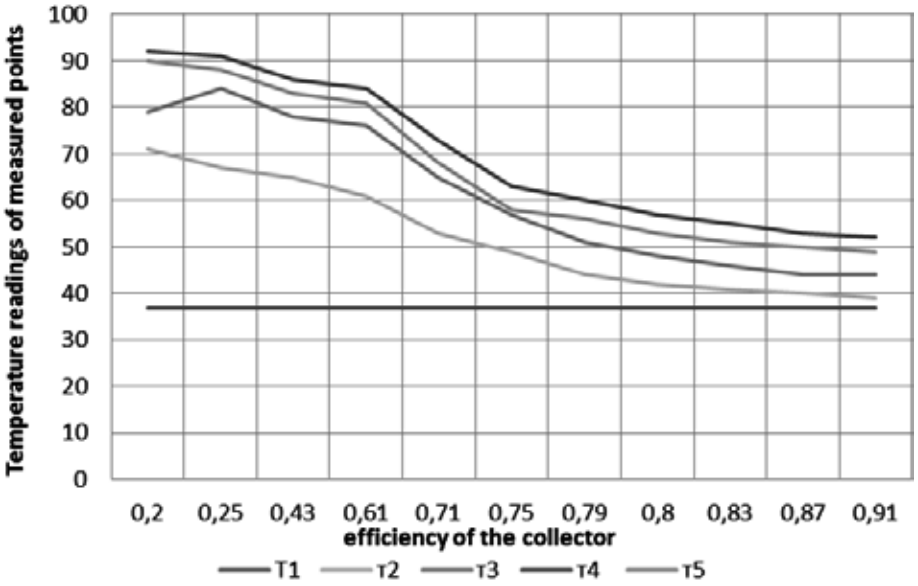

Figure 3. The dependence of the temperature characteristics of the measured points of FROM the efficiency of air heaters

Coefficient of efficiency solar air collector, which is the ratio of the amount of usable energy obtained air in the collector, to the amount of energy coming from solar radiation at the surface of the absorber solar air collector, based on dependencies:

$$\eta = \frac{Q_{ug}}{Q_s} = \frac{G \cdot c_p \cdot (T_{outp} - T_{inp})}{A_c \cdot H_t} = \frac{p \cdot Q \cdot c_p \cdot (T_{outp} - T_{inp})}{A_c \cdot H_t}$$

where Q_{ug} — the amount of usable energy, W; Q_s — the amount of energy coming from solar radiation at the surface of the absorber, W; G — coolant mass flow rate, kg/s; C_p — specific heat capacity, J/(kg K); T_{output}, T_{input} — output, input air temperature, °C; A_C — the area of a collector, m^2; H_t — parish of total solar radiation at the surface of the collector, w/m^2; p — density, kg/m^3; Q — volumetric flow rate, m^3/s.

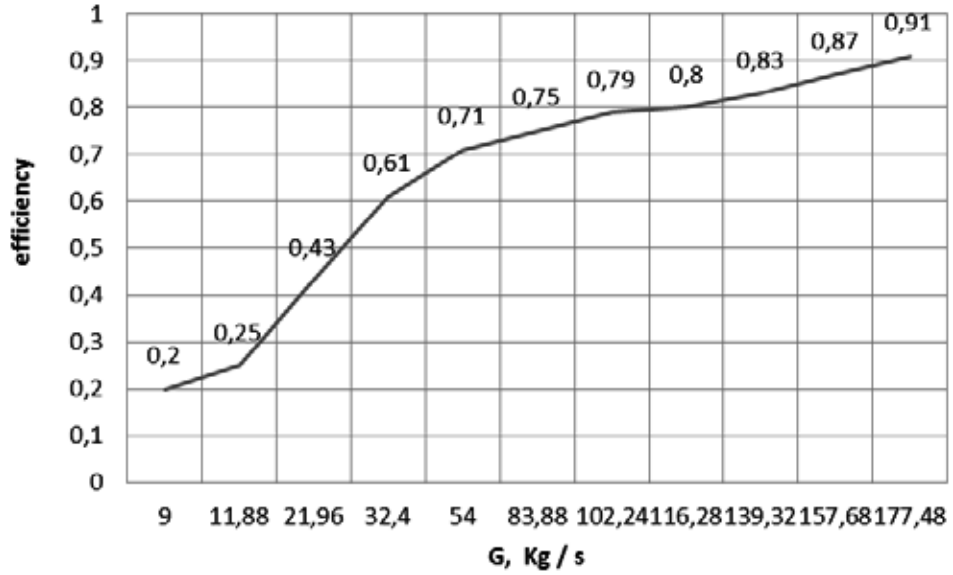

Figure 4. The dependence of the efficiency of heater from the air flow

Test results for the year May 5, 2016 in total solar radiation on inclined surface H_t = 0.9 kW/m^2, diffuse radiation S = 0, 1 kW/m^2, at an ambient temperature T_{input} = 37 ° C, the amount of energy coming from solar radiation at the surface of the absorber Q_s = 0.6525.

Table 4.

(G) flow rate, kg/s	° $\Delta T = T_{out} - T_{in}$	Q_{ug}, W	Efficiency,%	t_2, °C	t_3, °C	t_4, °C
0.0025	53	0.1331	0.204	71	85	92
0.0033	51	0.1631	0.2592	67	84	91
0.0061	46	0.4321	0.4321	65	78	86
0.009	44	0.3379	0.6099	61	76	84
0.015	31	0.4673	0.7132	53	65	73
0.0233	21	0.4917	0.706	49	57	63
0.0284	19	0.5137	0.787	44	51	60
0.0323	16	0.599	0.796	42	48	57
0.0387	14	0.5445	0.83	41	46	55
0.0438	13	0.5722	0.87	40	44	53
0.0493	12	0.5945	0.91	39	44	52

Conclusions:

1. Produced a literary analysis of the existing solar air collectors

2. Experimentally proved high efficiency of the collector.

3. Analysis of the results of experimental studies showing the high efficiency of the use of metal shavings in the air collector systems.

4. Proved an experimental use metal shaving as the absorber will reduce the cost of air solar collectors.

5. Proposed options for increasing the area of the heating surface heat transfer agent using metal shavings as an absorber.

6. The results can be used by developers when designing solar air systems.

References:

1. Takaev B. V. "Design air solar collector with transparent thermal insulation and optimization solar systems" – M, 2003.
2. Kharchenko H. B. Individual solar installations. – M, 1991.
3. Virlan, M. S. Development and research of solar collector. SOK No. 6., 2013. Internet resource http://www.c-o-k.ru/articles/razrabotka-i-issledovanie-solnechnogo-vozdushnogo-kollektora
4. Butuzov V. A. Air solar collectors SOK – № 7. 2013 Internet resource. http://www.c-o-k.ru/articles/vozdushnye-solnechnye-kollektory
5. Edited by Pryor T. L. Theory and design of solar thermal systems, University of Melbourne, 1980, 238 p.
6. Ion V. I., Martins G. J. Design, developing and testing of a solar air collector. The annals of «Dunarea de Jos» University of Galati Fascicle IV Refrigerating technique, internal combustion engines, boilers and turbines, 2006. ISSN 1221–4558.
7. Kurtas I., Turgut E. Experimental Investigation of Solar Air Heater with Free and Fixed Fins: Efficiency and Exergy Loss//International Journal of Science & Technology, 2006, 1 (1).
8. Plesca M. The Experimental studies of a flat plate air collector. Proceedings of National Conference of Power Engineering CNE-M-2000. Vol. 2. Chisinau: Moldpres Agency, 2000.
9. Tarnizhevsky B. V., Alekseev V. B., Kabilov Z. A. Solar collectors and water heating installations//Thermal Engineering, – № 6, 1995.

Iskenderov Akhmed Maksetbaevich,
Tashkent Chemical Technological Institute,
the associate professor
of the faculty of chemical technology of inorganic substances
E-mail: axmed_73g@mail.ru

The influence of additives of distilled liquids, containing NaCl and $CaCl_2$ on the process of mineralformation at roasting of sulphate containing blend

Abstract: In this paper the question of use of distilled liquid-withdrawal of the soda manufacture, containing $CaCl_2$ and NaCl as the intensifying additive at burning of a raw mix of sulfo-aluminate-silicate cement, made on the basis of phosphogypsum and a small with drawal of slaked from lime damper of soda factory, for decrease in temperature of burning at 100 °C and cement improvement of quality has been considered. The amount of distilled liquids, providing maintenance in a raw mix of 1% NaCl and $CaCl_2$ is optimum.

Keywords: distilled liquids, phosphogypsum, klinker, sulfo-silicate, cement.

Development of the building industry, accompany increase in volumes of building, causes to raise of manufacture of high-quality building materials, to expand their assortment, to introduce new, effective methods of construction. A variety of building designs, feature constructions and essential distinctions of service conditions by different kinds of aggressive influences invoked the requirement of creation of cements with special technical properties. Regulating the structure of new kinds of cement or the structure created on the basis of their composite binding, it is possible to achieve necessary technical characteristics of construction materials.

The important problem, facing the cement industry, is the expansion of a raw-material base at the expense of use of (technogenic) anthropogenic products of other industries. Recycling of industrial wastes is one of rational solutions of a problem of liquidation of environmental contamination, and the large-tonnage of the cement industry will allow to "consume" them in significant amount. In connection with this it is kept an urgency use of large industrial wastes, such as the waste of the soda industry, phospho gypsum, etc. as secondary raw materials.

As is known that the manufacture of soda is accompanied by a considerable quantity of difficultly utilizable liquid waste (in particular — distilled liquid) in the form of solutions of salts $CaCl_2$ and NaCl in the ratio 2:1. Such waste is formed annually in a considerable amount that substantially pollute environment by the manufacture of soda.

For increase of clinkerformation speed, the additives are used, accelerating processes of decarbonization and mineralformation, The action mechanism of additives consists in the formation at smaller temperatures on the border of contact of particles of a raw mix of a layer or from the fused mineralizer, or from eutectic melt of mineralizer with components of a raw mix. As such additives chlorine-containing reagents are most effective and in particular, a distilled liquid of Kungrad soda factory.

According to researches by T. A. Atakuziyev and others it is known that products of roasting blend calcium sulfoaluminate with 0,5% Na_2O represent almost practically pure calcium sulfoaluminate. The increase in Na_2O content to 1–3% leads to its formation in a small amount. Sodium oxide decelerates reactions of mineralformation of calcium sulfosilicate as well [1].

In connection with this, it presents an interest to investigate the influence of chloride calcium and sodium on roasting blend of the sulfomineral cements.

To this purpose, it has been prepared a raw mix with KH=0,67, for n_s=1, to which has been added in various percentage ratio 1–3% NaCl and $CaCl_2$, from raw materials (Almalyk phosphogypsum, Angren deposit enriched clay, soda manufacture solid waste is used as a calcareous component). The chemical composition of raw materials are resulted in table 1.

Table 1. – Chemical composition of raw materials

Components	SiO_2	Al_2O_3	Fe_2O_3	CaO	MgO	SO_3	R_2O	TiO_2	P_2O_5	MnO	Cl	пп
1	*2*	*3*	*4*	*5*	*6*	*7*	*8*	*9*	*10*	*11*	*12*	*13*
Almalyk phospho-gypsum	7,9	0,39	0,15	29,1	0,3	40,44	–		1,53	–	–	18,8

1	2	3	4	5	6	7	8	9	10	11	12	13
Angren deposit enriched clay	52,46	31,4	0,61	0,74	0,5	–	1,16	0,52	–	–	–	12,2
soda manufacture solid waste	0,11	0,11	0,01	88,25	11,3	0,1	0,43	0,01	0,01	0,01	–	10,2

Prepared raw blends with mineralizers have been exposed to roasting at temperatures 1000, 1100, 1150, 1200, 1250 and 1300° C within 60 minutes.

For comparison, sulphate-containing blend without additives in parallel has been burnt and exposed to the roentgenophase analysis (fig. 1).

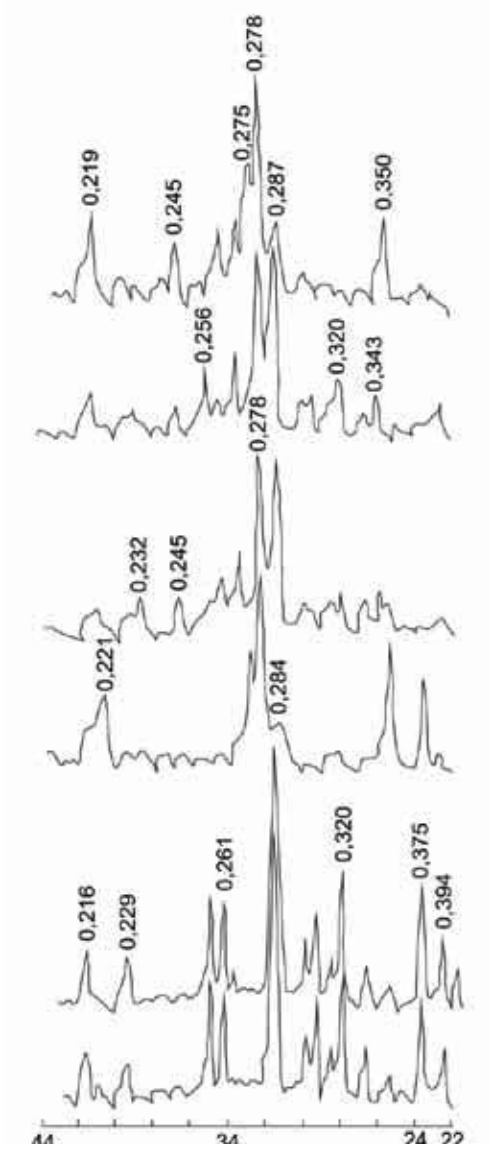

Figure 1. X-rayogram of roasting products

In the burnt products with n_s = 1,0 at temperature 1250° C the height of lines of intensity of a diffraction maximum of minerals $C_4A_3\bar{S}$, $C_5S_2\bar{S}$, $C\bar{S}$, also C_2S making accordingly 120, 82, 15 and 45 mm. The obtained product can be carried to SAS (sulfoaluminate silicate cement) clinker with the small content of belite.

Rise in temperature to 1250° C showed that at value of ns =1,0 there generally generated minerals $C_4A_3\bar{S}$, $C_5S_2\bar{S}$, and $C\bar{S}$, lines of intensity which made accordingly 116, 45 and 34 mm, and lines of intensity C_2S were insignificant (6 mm).

1–3 1% NaCl; 4–6 3% $CaCl_2$.

1,4–1100° C; 2,5–1200° C; 3,6–1300°C.

Rise in temperature to 1350° C showed the following changes in process of mineralformation: lines of intensity C_2S and $C_4A\bar{S}$ have decreased to 146 and 140 mm, and the line of intensity $C\bar{S}$ has increased slightly at n_s =1,0. Formation of a fourth mineral (5 mm) is observed. Thus, at temperature of roasting of blend 1150° C and n_s =1,0 it is obtained the clinker, containing minerals $C_4A_3\bar{S}$, $C_5S_2\bar{S}$, and C_2S. At temperature 1350° C and n_s =1,0 it is obtained the SAS clinker with the large content of C_2S and $C\bar{S}$.

Rise in temperature to 12500 C showed that at value of n_s =1,0 there generally generated minerals $C_4A_3\bar{S}$, $C_5S_2\bar{S}$, and $C\bar{S}$ lines of intensity which made accordingly 116, 45 and 34 mm, and lines of intensity C_2S were insignificant (6 mm).

Rise in temperature to 1350° C showed the following changes in the process of mineralformation: lines of intensity C_2S and $C_4A\bar{S}$ have decreased to 146 and 140 mm, and the line of intensity $C\bar{S}$ has increased slightly at n_s =1,0. Formation of a fourth mineral (5 mm) is observed. Thus, at temperature of roasting of blend 1150° C and n_s =1,0 it is obtained the clinker containing minerals $C_5S_2\bar{S}$, $C_5S_2\bar{S}$, and C_2S. At temperature 1350° C and n_s =1,0 it is obtained SAS clinker with the large content of C_2S and $C\bar{S}$.

Results of roentgenophase analysis testify that already at 1100° C $C_5S_2\bar{S}$, $C_4A_3\bar{S}$, unbound $C\bar{S}$ are generated, lines of intensity which make accordingly 82, 31 and 13 mm. However, it is necessary to notice that thus the content of unbound $C\bar{S}$ is much less than in products of roasting without mineralizer on which X-rayograms which the line of intensity $C\bar{S}$ makes 32 mm. Besides, $C_4A_3\bar{S}$ which defines strength characteristics of sulphate containing cement, forms in rather small amount (32 mm) whereas lines

of intensity $C_4A_3\overline{S}$ without mineralizer in roasting products are equal to 41 mm.

Calcium chloride has been applied as mineralizer for a long time in the USA at roasting of the glauconite containing rocks in revolving furnaces for industrial obtaining of cement and salts of potassium [2].

Introduction of Portland cement $CaCl_2$ (1%) in a raw mix rather activates the process of assimilating lime in kiln charge [2].

The researches, carried out with addition of calcium chloride, show that the presence of $CaCl_2$ in sulphate containing mixture in amount of 1, 2 and 3% and roasting at 1000° C, leads to assimilating lime practically full.

Results of roentgenophase analysis testify that at addition 3% $CaCl_2$ and temperatures 1100° C C_2S and unbound $C\overline{S}$ are generated, lines of intensity, which make accordingly 51 and 10 mm. It is necessary to notice that thus $C_5S_2\overline{S}$ does not generate, and the height of diffraction maximum $C_4A_3\overline{S}$ is equal to 500 mm, i. e. formation of SAS clinker does not occur, but a sulfoaluminate-belite clinker generates.

Rise in temperature to 1200° C at roasting of sulphate containing blend with addition the halogen containing mineralizer the following changes occur in the process of clinkerformation.

When 1% NaCl was added in roasting products there generated minerals $C_5S_2\overline{S}$, $C_4A_3\overline{S}$ and unbound $C\overline{S}$, the intensity of lines, which make accordingly 80, 39 and 8 mm. Thus the line of intensity $C_5S_2\overline{S}$ is less than in roasting products without mineralizer where lines of intensity of the specified mineral make 95 mm, unbound calcium sulfate are absent, i. e. NaCl opposes the formation of calcium sulfosilicate a little. However, at addition of NaCl the content of $C_4A_3\overline{S}$ is more than in products of roasting with the same additive at temperature 1100° C where the line of intensity of the last is equal to 32 mm. At roasting of blend with an additive 3% $CaCl_2$ only minerals C_2S and $C_4A_3\overline{S}$ (d=0,287 of nanometer) generate, lines of intensity which are equal to accordingly 49 and 54 mm whereas in the products of roasting, obtained without mineralizers, there generate $C_5S_2\overline{S}$ and $C_4A_3\overline{S}$. The amount of $C_4A_3\overline{S}$ increases in comparison with products of roasting at 1373 K with an additive of $CaCl_2$, where the line of intensity $C_4A_3\overline{S}$ is 50 mm.

Rise in temperature to 1300° C shows that addition of the halogen containing of mineralizer gives other character to the process of clinkerformation.

Roasting with NaCl testify that are thus minerals C_2S, unbound $C\overline{S}$ and $C_4A_3\overline{S}$, lines of intensity which make accordingly 49,39 and 28 mm whereas in products of roasting without mineralizers there generate $C_5S_2\overline{S}$, C_2S, $C_4A_3\overline{S}$ and unbound $C\overline{S}$, lines of intensity which are equal to accordingly 43, 29, 35 and 8 mm.

Absence of $C_5S_2\overline{S}$ at addition of NaCl is connected with the decomposition of $C_5S_2\overline{S}$ into C_2S and $C\overline{S}$, therefore the contents of C_2S and $C\overline{S}$ (unbound calcium sulfate) increase. Besides, it are necessary to notice that at temperatures 1100° C and 1200° C in roasting products with an additive of NaCl there generated only $C_5S_2\overline{S}$, $C_4A_3\overline{S}$, and unbound $C\overline{S}$, and the line of intensity C_2S is absent.

In roasting products with an additive of $CaCl_2$ only C_2S, $C_4A_3\overline{S}$ and $C\overline{S}$ with lines of intensity 63,18 and 22 mm accordingly, whereas in the roasting products obtained without mineralizer, $C_5S_2\overline{S}$, $C_4A_3\overline{S}$ and unbound $C\overline{S}$ generate. Similarly previous, here, there is a decomposition of sulfosilicate into belite and unbound calcium sulfate too (fig. 1).

With CaF_2 minerals C_2S, $C\overline{S}$, $C_4A_3\overline{S}$ with lines of intensity accordingly 45, 31 and 48 mm are generated, and sulfosilicate is not generated, whereas in the roasting products obtained without mineralizer, the line of intensity makes 43 mm. It is necessary to notice that the line of intensity unbound $C\overline{S}$ is more six times than in the roasting products obtained at temperatures 1100° C and 1200° C (with an additive of CaF_2). The line of intensity $C_5S_2\overline{S}$ is much more — accordingly 75 and 72 mm. The line of intensity $C_4A_3\overline{S}$ at 1300° C is less (31 mm) than in roasting products at 1100° C and 1200° C where the intensity of line $C_4A_3\overline{S}$ is accordingly 38 and 37 mm.

Thus, results of the carried out researches at temperatures 1000–1300° C with addition of 1–3% $CaCl_2$ in the sulphate containing mix of NaCl, leads to the following conclusions:

– assimilation of lime at addition of $CaCl_2$ completes at temperature 1000° C, i. e. the temperature of roasting falls to 100° C;

– application of $CaCl_2$ (3%) as mineralizer at 1100° C opposes the formation of $C_5S_2\overline{S}$, i. e. SAB clinker is generated;

– the additive of $CaCl_2$ (3%) at 1200° C opposes the formation of mineral $C_5S_2\overline{S}$, where there are generated only C_2S and $C_4A_3\overline{S}$;

– addition of 1% NaCl at 1300° C leads to the formation of SAB clinker, i. e. sulfosilicate is absent;

– at 1200° C the additive of 1% NaCl reduces the content of $C_5S_2\overline{S}$ and increases the amount of unbound $C\overline{S}$.

References:

1. Атакузиев Т. А. Физико-химические исследования сульфатсодержащих цементов и разработка низкотемпературной технологии их получения. / Ташкент, – Фан, – УзССР, – 1983, – С. 102.
2. Бутт Ю. М., Тимашев В. В. Портландцементный клинкер. – М.,/Стройиздат, – 1967, – С. 303.

Iskenderov Akhmed Maksetbaevich,
Tashkent chemical technological institute,
the associate professor of the
faculty of chemical-technology of inorganic substances
E-mail: axmed_73g@mail.ru

Erkaev Akhtam Ulashevich,
Tashkent chemical technological institute,
the associate professor
of the faculty of chemical-technology of inorganic substances

Toirov Zokirjon Kalandarovich,
Tashkent chemical technological institute,
the associate professor
of the faculty of chemical-technology of inorganic substances

Begdullaev Akhmed Kobeysitnivich,
the main specialist on the innovation
and new technology UE "Kungrad Sodium Plant."

Research on the purification process of low-grade sodium chloride

Abstract: The theoretical analysis on the purification process of brine has been carried out with the usage of solubility isotherms of reciprocal systems $Ca^{2+}, 2Na^{+} // 2Cl^{-}, SO_4^{2-} - H_2O$. By experimental investigations it has been determined that the purification of low-grade sodium chloride with the application of distilled fluid in the production of soda ash can increase the coefficient of sodium chloride to 0,5–2, 0% and decrease water consumption and lime to 3–8%.

Keywords: sodium chloride, distilled fluid, theoretical analysis, soda ash, water consumption.

In Uzbekistan the reserves of salt deposits of Barsakelmes, located in 30 km from UE «Kungrad Sodium Plant» (UEKSP), have been chosen as the base of chlorine-sodium raw materials.

Salts must be subjected to the purification from additives of salt calcium and magnesium. For example, for this purpose in the Crimea Sodium Plant a new two-staged lime-sodium method of brine purification [1] has been developed and implemented. With the purpose of intensification of this process, the suspension of calcium hydroxide is quenched by crude brine and the formed suspension is fed to the mixing with brine, and it is subjected to the purification (purification stage of brine from magnesium).

In the technology of obtaining soda ash in UE KSP, solid salt from storehouse is delivered with the help of grab crane in the capacity for dissolving salt, where dissolved by water (volume — 2500 m^3) with the obtaining of crude brine, containing 26,41% NaCl. The dissolution occurs in the cylindrical apparatus with a square hopper for receiving solid salt with the inner distributing devices for inputting water and steam and overflow the top of the chute. The crude brine with the temperature of 44 °C overflows into the container, intermediate container of brine, which is cylindrical vessel with the volume flat cap of 2500 m^3 [2].

The initial brine is pumped in the capacity of raw brine with the volume of 3500 m^3, which is delivered to the container for mixing. Solutions of lime milk and soda ash are delivered into this container at the temperature of 50 °C. In the reactors the binding of cations Ca^{2+} and Mg^{2+} is occurred with the formation of insoluble combi-

nations of $Mg(OH)_2$ and $CaCO_3$, which are in the form of slime, are removed periodically in slime container — a cylindrical vessel with a mixer. The purification process occurs at the temperature of 43 °C.

The brine travels from reactor into the container with baffles, where it is mixed with the solution of polyacrylamide (PAA) for better coagulation. Further, the purified solution of sodium chloride is given to the ammoniation stage. The ammoniated brine undergoes to the preliminary and final carbonation. The formed bicarbonate sodium is separated on filters and further it is delivered to the calcination for obtaining the commercial soda ash. The filtered fluid is delivered to the distillation of ammonia and carbon dioxide with the blowout of distilled fluid in wastes slurry tank.

The advantages of this method: availability, abundance, large reserves and low cost of raw materials (table salt and limestone); the basic reactions, except roasting of limestone and calcination process, which occur at low (up to 100 °C) temperatures and at atmospheric pressure; stability of technological processes; high-quality of products; relatively low cost of soda ash.

Disadvantages: low degree of raw material usage — sodium is used only by two-thirds, calcium and chloride are not used at all; the large amount of solid and liquid wastes, demanding utilization, dumping or long-term storage; significant energy resource consumption; high specific investments which lead to the long-term payback of built factories; the impossibility of carrying out the purification of low-grade sodium chloride with the content of 3–4% of insoluble part, for example, in UE KSP from sulphate ions, the content of which increases to 2.4 times of regulated amount. Besides that, it is necessary to consider that when sodium chloride is added to the solution of soda ash in the process of purification the additional amount of sulphate ion is produced due to the presence of sulphate calcium in the solution according to the reaction:

$$CaSO_4 + Na_2CO_3 \rightarrow CaCO_3 + Na_2SO_4$$

While producing well-dissolved salt Na_2SO_4, in the further process the regeneration of ammonia from filtered fluid complicates, as at the interaction of it with the limestone suspension the gypsum deposit is generated (instructing of distiller walls). Real methods of decreasing of contents of ions SO_4^{2-} in crude brine to the level, excepting the generation of gypsum incrustation at the distillation stage, in the sodium industry it hasn`t been yet in this sphere. Intensive works are being held though [1–10].

These shortcomings prove that the given method of brine purification is imperfect and noneconomic, especially, at the usage of low- grade sodium chloride.

The aim of the present investigations is the development of purification technology of low-grade sulphate containing sodium chloride with the partial return in the process of distiller fluid-waste production of soda ash.

So, the low-grade of sodium chloride has to dissolve in the presence of distilled fluid at 25–45 °C, and the ratio of ions SO_4^{2-}/Ca^{2+} and Mg^{2+}/Ca^{2+} must be in the interval of 0,55–0,98, which regulates the amount of distiller fluid, returned to the stage of salt dissolution from the regeneration part of the production of soda ash.

In comparison with the mentioned in [1; 2; 9; 10], the suggested purification method of low-grade sodium chloride has the series of existing essential features.

Firstly, in the suggested technology the regime of dissolving process of low-grade sulphate containing sodium chloride and the amount of return distilled fluid is regulated on the basis of isotherms of dissolution of quaternary mutual systems $Ca^{2+}, 2Na^+//2Cl^-, SO_4^{2-}$-$H_2O$, at 25 and 45 °C (Fig. 1 and table. 1).

The given system consists of four ternary and four binary systems. Binary and ternary systems are rather highlighted in the literature [3, 8], in which the equilibrium is established in 6–7 days.

At 25 °C, lines of six fields of salts crystallization break the surface of solubility diagrams, hereupon, that five fields correspond to the release of initial components, one field to the double combinations. Fields converge in four nodal points, corresponding to the release of three different phases.

From the solubility diagram analysis of systems $2Na^+, Ca^{2+}//2Cl^-, SO_4^{2-}$ H_2O at 25 °C it is necessary that its main part belongs to the crystallization field of two dihydrate sulphate calcium, which is due to its poor solubility in water. It is clear from the diagram that solubility of sulphate calcium in the saturated solution of sodium chloride reaches to 0,598%, and with the increase of chloride calcium content to more 0,6%, it effects salting-out of chloride sodium. The solubility of sulphate calcium decreases to 0,123% with the content of 1,61% chloride calcium. However, an excessive increase in the content of the last is also not desirable, since at the purification stage of brine from calcium ions it is required the increased consumption of soda solutions.

The second distinguishing feature of the controlling process is the separation in collections of salt solutions of its insoluble part and the formed calcium sulphate. That allows significantly the number of stops of sinkers to decrease for the purification and to prevent the conversion of calcium sulphate by carbonate sodium with the formation of well-soluble sulphate sodium, which

Table 1. – Dat a on solubility of components in the syste m $2Na^+$, $Ca^{2+}//2Cl^-$, SO_4^{2-} -H_2O at 25°C

№ Composition points	Composition of fluid phase,%					Composition of fluid phase, mole/100g r/r				Indices of Ineke			Solid phase
	NaCl	Na_2SO_4	$CaCl_2$	$CaSO_4$	H_2O	NaCl	Na_2SO_4	$CaCl_2$	$CaSO_4$	Ca^{2+}	SO_4^{2-}	Moles H_2O /MO moles Σ salts	
1.	26,41	–	–	–	73,59	0,2257	–	–	–	–	–	18,1139	NaCl
2.	–	21,8	–	–	78,2	–	0,1535	–	–	–	1	28,3023	$Na_2SO_4 \cdot 10H_2O$
3.	–	–	47,10	–	53,0	–	–	0,4234	–	1	–	6,954	$CaCl_2 \cdot 4H_2O$
4.	–	–	–	0,21	99,79	–	–	–	0,0015	1	1	3695,933	$CaSO_4 \cdot 2H_2O$
5.	25,85	–	–	0,4666	73,6834	0,2209	–	–	0,0034	0,0152	0,0152	18,2501	$NaCl+CaSO_4 \cdot 2H_2O$
6.	23,10	6,89	–	–	70,01	0,1974	0,0485	–	–	–	0,1972	15,817	Na_2SO_4+NaCl
7.	13,67	14.82	–	–	86,33	0,1168	0,1044	–	–	–	0,4727	24,53	$Na_2SO_4+Na_2SO_4 \cdot 10H_2O$
8.	1,02		43,59	–	55,39	0,0087	0	0,3927	–	0,9783	–	7,666	$NaCl+CaCl_2 \cdot 6H_2O$
9.		21,21		0,219	78,79	–	0,149	–	0,0016	0,6288	1	29,065	$Na_2SO_4 \cdot 10H_2O + CaSO_4 \cdot 2H_2O$
10.	23,87	3,90	–	0,0644	72,1656	0,204	0,0275	–	0,0005	0,0022	0,1207	17,281	$NaCl+3Na_2SO_4 \cdot 2CaSO_4+CaSO_4 \cdot 2H_2O$
11.	22,21	5,66	–	–	72,13	0,1898	0,0399	–	–	–	0,1737	17,4454	$3Na_2SO_4 \cdot 2CaSO_4+CaSO_4 \cdot 2H_2O$
12.	12,88	13.41	–	–	87,12	0,1101	0,0944	–	–	–	0,4616	23,607	$3Na_2SO_4 \cdot 2CaSO_4+CaSO_4 \cdot 2H_2O$
13.	22,71	6,70	–	–	70,59	0,1941	0,0472	–	–	–	0,1956	16,2524	$NaCl+Na_2SO_4+3Na_2SO_4 \cdot 2CaSO_4$
14.	18,88	9,58	–	0,0228	71,5172	0,1614	0,0675	–	0,0002	0,0009	0,2955	17,3426	$Na_2SO_4+3Na_2SO_4 \cdot 2CaSO_4$
15.	16,42	12,15	–	0,0223	71,4077	0,1403	0,0856	–	0,0002	0,0009	0,3795	17,5458	$Na_2SO_4+3Na_2SO_4 \cdot 2CaSO_4$
16.	13,63	15,45	–	0.0251	70,92	0,1165	0,1088	–	0,0002	0,0009	0,4834	17,47	$Na_2SO_4+Na_2SO_4 \cdot 10H_2O+3Na_2SO_4 \cdot 2CaSO_4$
17.	11,78	14,42	–	0,0256	73,7744	0,1007	0,1015	–	0,0002	0,001	0,5025	20,25	$Na_2SO_4 \cdot 10H_2O+3Na_2SO_4 \cdot 2CaSO_4+CaSO_4 \cdot 2H_2O$
18.	7,64	16.16	–	0,1353	92,2247	0,0653	0,1138	–	0,001	0,0056	0,6374	28,45	$Na_2SO_4 \cdot 10H_2O+CaSO_4 \cdot 2H_2O$
19.	4,58	18,06	–	0,1570	77,203	0,0391	0,1272	–	0,0012	0,0072	0,7666	33,89	$Na_2SO_4 \cdot 10H_2O+CaSO_4 \cdot 2H_2O$
20.	2,29	19.74	–	0,1795	97,5305	0,0196	0,1390	–	0,0013	0,0081	0,8774	33,89	$Na_2SO_4 \cdot 10H_2O+CaSO_4 \cdot 2H_2O$
S	–	–	–	–	54,2	–	–	–	–	1	0,015	7,20	$CaCl_2 \cdot 4H_2O+CaSO_4 \cdot 2H_2O$
S_1	–	–	–	–	54,3	–	–	–	–	0,978	0,0151	7,00	$CaCl_2 \cdot 4H_2O+NaCl+CaSO_4 \cdot 2H_2O$

causes incrustations of pipelines, carbo- and distillation columns in the production of soda ash.

The initial, intermediate and final solutions have been analyzed in the content of ions Cl^-, Ca^{2-}, Mg^{2+}, SO_4^{2-} and insoluble part with the usage of common methods of analysis [11–12]. In the researches there has been used the low-grade sodium chloride of composition mass. Mass%: NaCl – 94,01; Ca^{2+} –0,49; Mg^{2+} –0,115; SO_4^{2-} –1,15; i. r. – 4,10 and distiller fluid composition mass %: NaCl – 5,67; $CaCl_2$ –9,57; Mg^{2+} –0,03; SO_4^{2-} –0,003; i. r. –0,13.

The amount of distiller fluid for 1000 kg of low-grade sodium chloride at the given weight ratio of SO_4^{2-}: Ca^{2+} is calculated on the formula:

$$A_{dist.f} = \frac{(100 \cdot a_{SO_4^{2-}} - 100N \cdot a_{Ca^{2-}})}{N \cdot b_{Ca^{2-}}}$$

$$A_{H_2O} = \begin{bmatrix} (100 \cdot a_{NaCl} + A_{dist.f.} \cdot b_{NaCl}) \cdot 100 - \\ -\{(100 \cdot a_{NaCl} + A_{dist.f.} \cdot b_{NaCl}) + \\ + A_{dist.f}(1 - b_{NaCl})\}26,4 \end{bmatrix} / 26,4$$

where $A_{dist.f}$; A_{H_2O} – amount of distiller fluid and recycled water, respectively for the dissolution of sodium chloride, kg; $a_{SO_4^{2-}}$, $a_{Ca^{2-}}$, a_{NaCl} — the content of SO_4^{2-}, Ca^{2+} and NaCl in sodium chloride %; $b_{Ca^{2-}}$, b_{NaCl} – contents of Ca^{2+} and NaCl in distiller fluid,%; N-controlled weight ratio of SO_4^{2-}; Ca^{2+} at the dissolution stage, which fluctuates in the interval of 0,55–0,98.

The dissolution process of salt has been carried out at the temperature 45 °C with the settling of obtained suspension for 120 min. After release of the clarified part of the produced thick suspension has been filtrated, the wet residue has been expressed with the obtaining of clarified desulfated solution. It can be seen on the experimental data (tables 2,3) that at the salt dissolution by only the recycled water the clarified solution of sodium chloride with the content is obtained, mass%: NaCl – 26,41; Ca^{2+} –0,13; Mg^{2+} –0,03; SO_4^{2-} –0,32; i. r. –0.13 and ratio SO_4^{2-}/Ca^{2+}, equal to 2,46.

By salt dissolution in the presence of distiller fluid and ratio of SO_4^{2-}/Ca^{2+} = 0,86 it is obtained the dissulfated clarified solution of sodium chloride with the content, mass %: NaCl — 26,20; Ca^{2+} –0,29; Mg^{2+} –0,04; SO_4^{2-} –0,20; i. r. –0,14. With the decrease of SO_4^{2-}/Ca^{2+} to 0,55 the content of ion SO_4^{2-} decreases to 0,15%, however, the content of ion Ca^{2+} is more than 0.44%. Therefore, the decrease of ratio SO_4^{2-}/Ca^{2+} is lower to 0,55 undesirably.

The decrease of ratio of ions SO_4^{2-}/Ca^{2+} and Mg^{2+}/Ca^{2+} at the dissolution stage to less than 0,55 leads to the increase of content of chloride calcium in the solution, which requires the increased consumption of sodium solution at the purification stage from calcium ions, at the indicated ratio more than 0,98 it is observed incomplete desulfation.

The fall of temperatures to 25 °C leads to the minor decrease of content of ions SO_4^{2-} in clarified solution. As analysis of isotherms shows the volume diagram of solubility systems

$Na^+, \frac{1}{2}Ca^{2+} // \frac{1}{2}SO_4^{2+}, Cl^- - H_2O$ at 25 °C, occupying $CaSO_4 \cdot 2H_2O$ the volume is more than at 45 °C. The increase of content of SO_4^{2+} is defined due to the formation of small crystals $CaSO_4 \cdot 2H_2O$ and the slow precipitation due to the viscosity of brine.

At the temperature less than 25 °C the reduction of solubility of sodium chloride occurs.

The increase of temperature more than 45 °C practically does not affect to the solubility of sodium chloride and leads to the overspending of heating steam.

Therefore, it is desirable to carry out the dissolution process at 40–45 °C temperature.

Various factors influence on the kinetics of sedimentation and condensation of sludge. Thus, by the purification of brine from calcium ions and magnesium sludge, which is rich with calcium carbonate, it can be gelatinous and have a large volume at the beginning of condensation.

For achieving high sedimentation rates and minimum final volume of sludge, it is desirable that the ratio of ions Ca^{2+} and Mg^{2+} in the suspension has been as large as possible.

Therefore, at the purification of brine, which is rich with magnesium, more rationally the usage of lime, as at the purification from Mg^{2+} ions Ca^{2+}, forming during dissociation $Ca(OH)_2$, transit in the final result to $CaCO_3$, increasing the ratio of calcium and magnesium ions in the suspension [9; 10].

Implementation of the obtaining process of soda ash from low-grade sulphate containing halites on the suggested technology provides all the primary requirements on the creation of conditions for the formation of large well precipitating crystals with the obtaining purified brine, according to the technological regulations [2; 9; 10].

Composition of purified brine: NaCl — no less than 100 n.d, Ca^{2+} — no more than 10 mg/l, Mg^{2+} — no less than 5 mg/l, insoluble residue — no more than 40 mg/dm^3, temperature of brine — 35–40 °C [2].

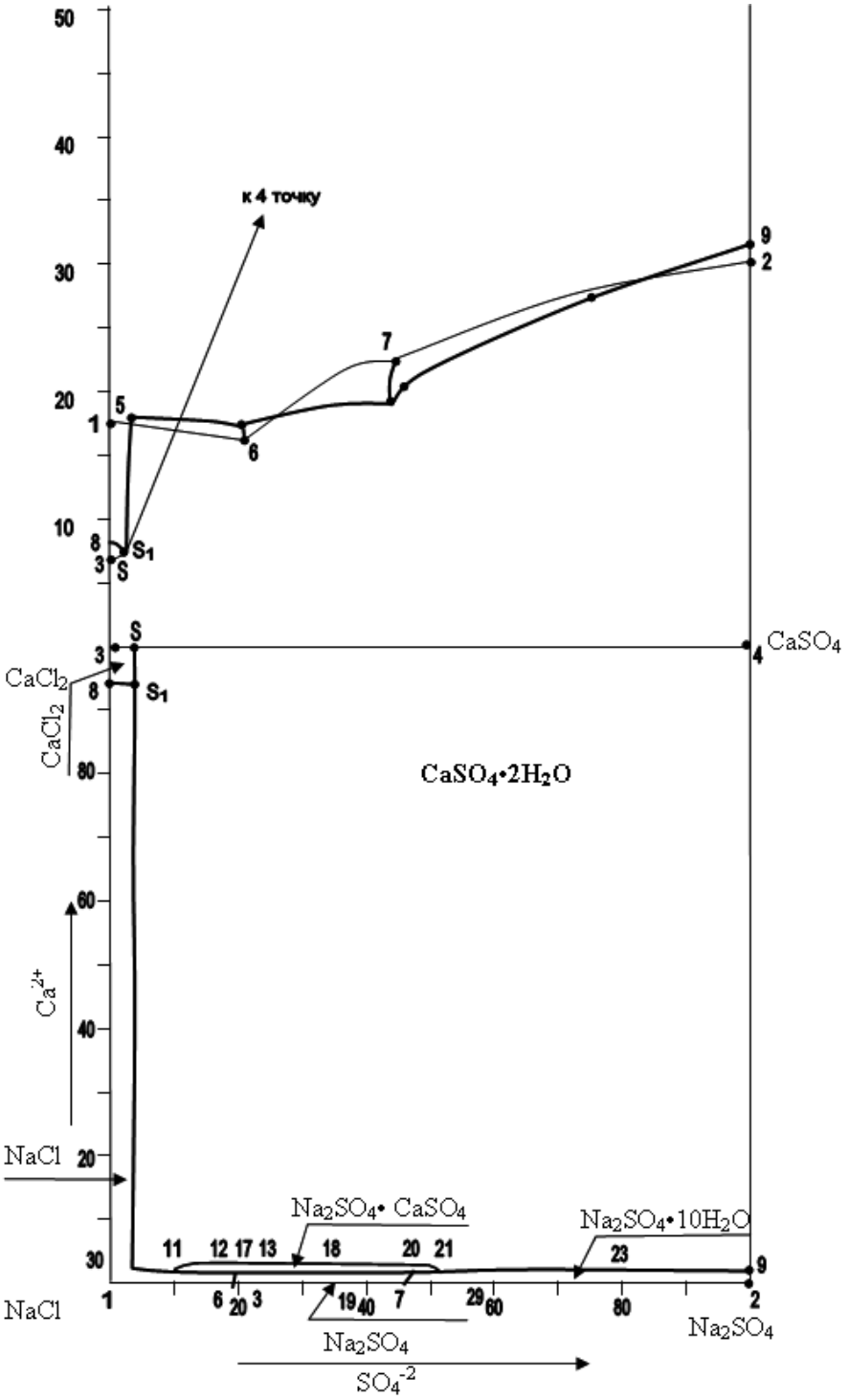

Fig.1.Diagram of the solubility of reciprocal systems 2Na+, Ca 2+//2Cl-, SO42- –H2O at 25°C

Table 2. – The influence of technological parameters on technical-analytical indicators of dissolution process

№	Technical-analytical indicators of the process	Existing technology	Developed technology		
			1	2	3
1	*2*	*3*	*4*	*5*	*6*
1	Composition of low-grade sodium chloride, mass.% NaCl	94,01	–	–	–
	н. о.	4,64	–	–	–
	SO_4^{2-}	1,15	–	–	–
	Ca^{2+}	0,49	–	–	–
	Mg^{2+}	0,115	–	–	–
	Amount of low-grade sodium chloride, g	1000	947.74	958,99	958,99

1	*2*	*3*	*4*	*5*	*6*
2	Composition of distiller fluid, mass% NaCl	5,67	–	–	–
	n. r.	–	–	–	–
	SO_4^{2-}		–	–	–
	$CaCl_2$	9,57	–	–	–
	Mg^{2+}	0,027	–	–	–
3	Additive of distiller fluid, g	–	394,36	237,19	237,19
4	Amount of circulating water, g	2559	2164,64	2321,81	2321,8
	Ratio of ions in the suspension, formed at the dissolution of SO_4^{2-}/Ca^{2+}	2,347	0,597	0,86	0,86
6	Composition of crude brine after separation i. r. and produced sulphate calcium from suspension, mass.%: NaCl	26.41	26,15	26,20	26,18
	i. r.	0,13	0,14	0,13	0,15
	SO_4^{2-}	0.32	0,155	0,20	0,23
	Ca^{2+}	0.14	0,44	0.29	0,30
	Mg^{2+}	0.03	0.03	0,04	0,041
7	Temperature of dissolution, °C	44	44	43	25
8	Ratio of ions:				
	SO_4^{2-}/Ca^{2+}	2,856	0,354	0,689	0,74
	Mg^{2+}/Ca^{2+}	0,21	0.066	0.138	0,14
9	Mass of residue, g	139,2	201,0	198,0	196,0
10	Mass of clarified solution, g	3419,8	3358	3320,0	3318,0

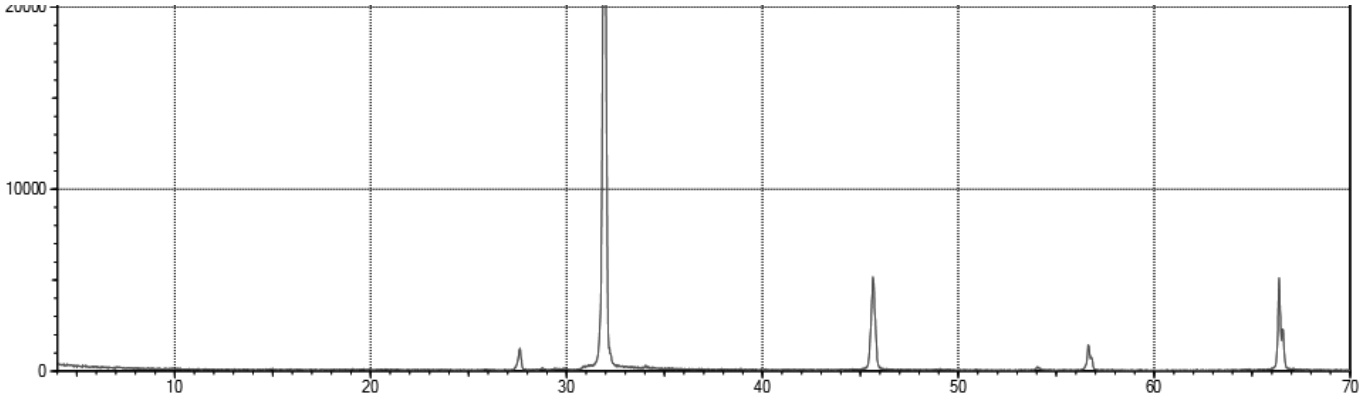

Figure.2 X-rayogram of samples. Sodium chloride from deposits of Karaumbet

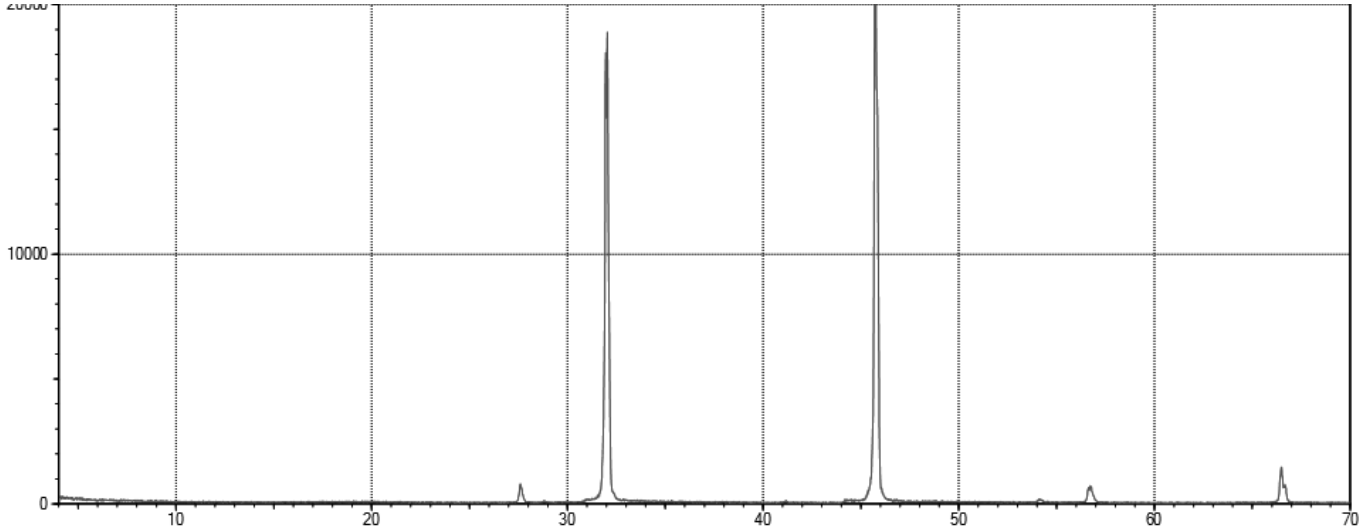

Figure.2 X-rayogram of samples. Sodium chloride from deposits of Barsakelmes

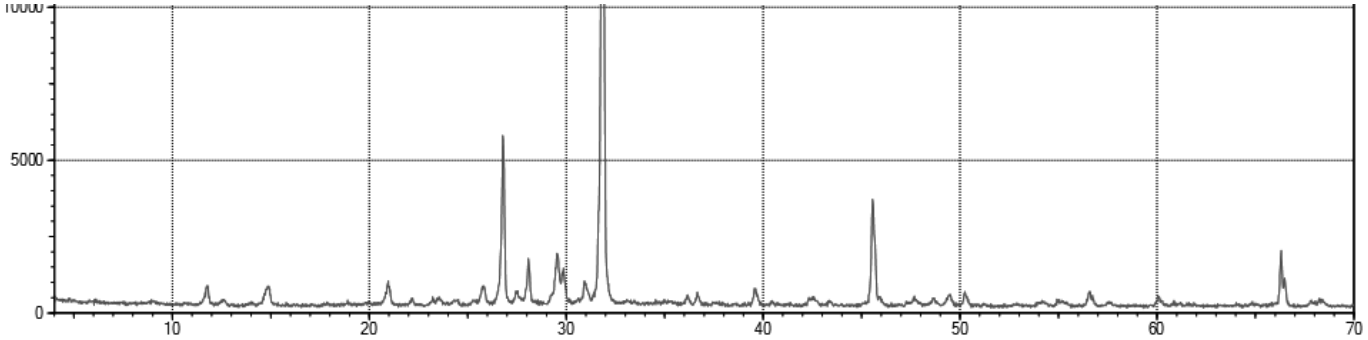

Figure.2 X-rayogram of samples. Insoluble part after dissolution of salt

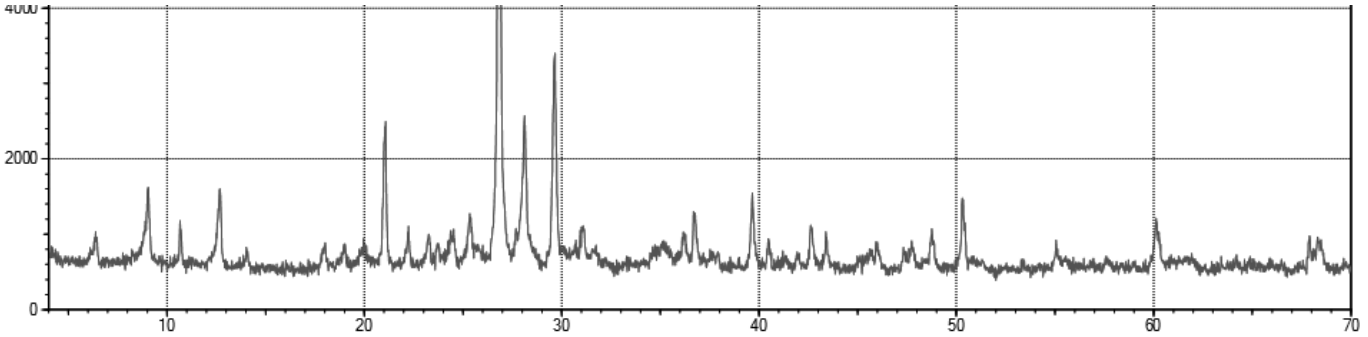

Figure.2 X-rayogram of samples. Insoluble part after the purification of crude brine from magnesium and calcium ions

In order to determine the salt composition of residue, produced by the dissolution of low-grade sulphate containing sodium chloride and its purification from ions of magnesium and calcium, chemical [11] and physico-chemical methods of analysis have been used [13–17]. The results of researches show that low-grade sodium chloride mainly consists of NaCl, and certain amount of sulfate calcium and muds (figure 2, curves 1 and 2). The residue, generating by the dissolution of salt mainly consists of calcium sulphate, NaCl and muds (curve 3). The residue, generating at the purification of crude brine from magnesium and calcium ions consists of carbonates of calcium and magnesium (dolomite) and magnesium hydroxide (curve 4).

Based on the above-mentioned investigations we can conclude that the suggested method of the purification of low-grade sodium chloride can be positively in general and in the production of soda ash:

– the efficiency of the usage of initial components is increased in the production of soda ash;

– distiller fluid of 5–10%, which is waste of sodium production, is used with the increasing of the usage coefficient of sodium chloride to 0,5–2,0% and decreasing of the consumption of water and lime to 3–8%.

References:

1. А. с. 643545 (СССР). Способ очистки хлорида натрия//Купличенко М. Е., Крашенинников Г. С, Муравьева О. И., Науменко А. И., Шемерянкин Б. В.- Заявл. 11.05.76. № 2358955/23–26; Опубл. 25.01.79. Бюл.№ 3. М.Кл.2 С 01 D 3/14.
2. Постоянный технологический регламент. УП «Кунградский содовый завод». Склад твердой соли и отделение очистки рассола производства кальцинированной соды. 2014 г. – 66 с.
3. Бодалева Н. В., Ленешков И. Н. Исследование растворимости в системе K_2SO_4-$MgSO_4$-$CaSO_4$-H_2O при 55 С-ЖНХ. т. 1, 1956, – № 5. С. 995–1007.
4. Набиев М. Н., Осичкина Р. Г., Тухтаев С. Сульфат калия с микроэлементами. Ташкент. Изд. ФАН. 1988. – 156 с.
5. Пельш А. Д. Квадратная диаграмма для изображения пятерной системы Na, K, Mg/Cl, SO_4 +H_2O вып. 27. Л: ВНИИГ, 1953, С. 84–112.
6. Здановский А. Б., Ляховская Е. И., Шлеймович Р. Э. Справочник экспериментальных данных по растворимости многокомпонентных водно-солевых систем. Том 1. Трехкомпонентные системы. Изд. «Хим литература». – М. – Л.: – 1953. – 670 с.
7. Бергман А. Г., Лужная Н. П. Физико-химические основы изучения и использования соляных месторождений хлорид-сульфатного типа. – М.: 1951. – Изд. Ан СССР. – 228 с.

8. Киргинцев и др. Растворимость неорганических веществ в воде. – Л.: Химия, 1972.-248 с.
9. Крашенинников С. А. Технология соды. – М.: Химия, 1988. – 304 с.
10. Зайцев И. Д., Ткач Г. Л., Стоев Н. Д. Производство соды. – М.: Химия, 1986. – 312 с.
11. Полуэктов Н. С. Методы анализа по фотометрии пламени. – Л.: Химия, 1967. – 307 с.
12. Шварценбах Г., Флашка Г. Комплексонометрическое титрование. – М.: Химия, 1970. – 360 с.
13. Берг Л. Г. Введение в термографию. – М.: Наука, 1969. – 368 с.
14. Кесслер И. Методы инфракрасной спектроскопии в химическом анализе. – М.: Мир, 1969. – 287 с.
15. Ковба Л. М., Трунов В. К. Рентгенофазовый анализ. – М.: МГУ, 1969. – 160 с.
16. Гиллер Я. Л. Таблицы межплоскостных расстояний. В 2-х т. – М.: Недра, 1966. – 330 с.
17. Недома И. Расшифровка рентгенограмм порошков. – М.: Металлургия, 1975. – 423 с.
18. Американская картотека ASTM. Diffraction Data cards and Alphabetical and Group Numerical Index of X-Ray Diffraction Data./Изд-во Американского общества по испытанию материалов. Нью-Йорк, 1973.
19. Миркин Л. И. Справочник по рентгеноструктурному анализу поликристаллов. – М,1991. – 863 с.

Mamedov Shakir Ahmad, PhD,
Azerbaijan University of Architecture and Construction,
Department Test and seismic stability of construction,
Azerbaijan, Baku,
E-mail: shakir-mamedov@rambler.ru

Hasanova Tukezban Jafar, PhD,
Azerbaijan University of Architecture and Construction,
Department Test and seismic stability of construction,
Azerbaijan, Baku,
E-mail: atika2014@rambler.ru

Imamalieva Jamila Nusrat, PhD,
Azerbaijan University of Architecture and Construction,
Department Test and seismic stability of construction,
Azerbaijan, Baku,
E-mail: ncamila@rambler.ru

Reserch of movement of the viscous elastic fixed vertically located cylinder in liquid with the free surface under the influence of the seismic waves

Abstract: The problem about movement of the rigid cylinder keeping vertical position under the influence of running superficial waves in a liquid is considered. The indignation of a falling wave caused by presence of the cylinder which moves is thus considered. Special decomposition on a falling harmonious wave is used. The problem dares an operational method. For a finding of the original the decision, considering that the image denominator represents tabular function, Voltaire's integrated equation of the first sort which dares a numerical method is used.

Cylinder movement in the continuous environment under the influence of waves is considered in work [1]. Problems are solved by an operational method, thus originals of required functions are looked for by numerical definition of poles of combinations of transcendental functions and calculation of not own integrals.

Using specificity of a task below, decisions are under construction the numerical solution of the integrated equation of Volter of the first sort that doesn't create computing problems of the complex roots of transcendental functions [2; 3] connected with search.

Keywords: cylinder, liquid, wave, movement, surface.

1. Problem definition

It is supposed that the rigid circular cylinder located in liquids with a free surface towers over a surface of liquid and can move in the horizontal direction. Movement of liquids it is considered from the point of view of the theory of long waves [4].

The equation of movement of the cylinder looks like

$$m\frac{d^2}{dt^2} = P - \frac{d\varepsilon}{dt}, \qquad (1)$$

where m — the mass of the cylinder, ξ — horizontal movement, P — effort on the cylinder from liquid.

Pressure of liquid upon the cylinder [4] is equal in a common ground

$$p_* = \rho g(\zeta - z) \qquad (2)$$

where ρ — density of liquid, g — acceleration of a free fall, ζ — a deviation of a surface of liquid from initial situation, z — depth.

The equation of movement of liquid looks like

$$a^2\Delta\zeta = \frac{d^2\zeta}{dt^2} \qquad (3)$$

where h — liquid depth, Δ — Laplace's operator.

Force having per unit length of a core is equal

$$q = -r_0\int_0^{2\pi} p\cos\theta d\theta \qquad (4)$$

where θ — a polar corner, r_c — cylinder radius. Having substituted pressure expression from (2) in (4) we will receive

$$q = -\rho_0 g r_0\int_0^{2\pi}(\zeta - z)\cos\theta d\theta \qquad (5)$$

Size can be presented in a look

$$\xi = \sum\xi_\nu cos\nu \qquad (\nu = 1,2\ldots) \qquad (6)$$

Having substituted (6) in (5), we will receive

$$q = -\rho g r_0\zeta_1\left(\int_0^{2\pi}\cos^2\theta\, d\theta - z\int_0^{2\pi}\cos\theta\, d\theta\right);$$

$$\int_0^{2\pi} coscos\nu d = 0 \qquad at\ \nu \neq 1,$$

or $q = -\rho g\zeta_1\pi r_0$ (7)

Boundary condition is [4]

$$\left.\frac{\partial\zeta}{\partial r}\right|_{r=r_0} = -\frac{1}{g}\frac{\partial\upsilon_n}{\partial t} \qquad (8)$$

where υ_n — a projection of speed of liquid to a normal to a cylinder surface.

Considering (6), a condition (8) it is led to a look:

$$\frac{\partial\zeta_1}{\partial r} = -\frac{1}{g}\frac{\partial\upsilon_x}{\partial t} \qquad (9)$$

$$\upsilon_n = \upsilon_x\cos\theta$$

where υ_x — cylinder speed $\left(\upsilon_x|_{r=r_0} = \frac{d\xi}{dt}\right)$

Change of a surface of liquid consists of two parts: result of a falling harmonious wave and the indignation caused by presence of the cylinder which, thus, moves, i. e.

$$\zeta = \zeta^p + \zeta^* \qquad (10)$$

$$\zeta^p = bH(t)\sin(kx - \omega t)$$

where k — wave number, ω — frequency.

Indignation of a surface of liquid is defined by the wave equation (3) which decision in Laplace-Carson's images looks like:

$$\zeta^* = \sum_{i=0}^{\infty} D_i K_i\left(\frac{pr}{a}\right)\cos i\theta \qquad (11)$$

where K_i — McDonald's function i — about.

Surface deviation on a harmonious wave considering that it is possible to present in a look:

$$\zeta^p = bH(t)(\sin kx\cos\omega t - \cos kx\sin\omega t) =$$

$$= bH(t)\{2[J_1(kr)\cos\phi - J_3(kr)\cos 3\phi + J_5(kr)\cos 5\phi - \ldots]\cos\omega t + \qquad (12)$$

$$+[J_0(kr) - 2J_2(kr)\cos 2\phi + 2J_4(kr)\cos 4\phi - \ldots]\sin\omega t\}$$

where J_n — Bessel's function.

Having substituted (12) previously having transformed according to Laplace — to Carson in (9), taking into account (6) we will receive:

$$kb\left\{2\left[J_1'(kr_0)\cos\phi - J_3'(kr_0)\cos 3\phi + J_5'(kr_0)\cos 5\phi - \ldots\right]\frac{p^2}{p^2+\omega^2} + \ldots\right.$$

$$\left. + \left[J_0'(kr_0) - 2J_2'(kr)\cos 2\phi + 2J_4'(kr)\cos 4\phi - \ldots\right]\frac{\omega p}{p^2+\omega^2}\right\} + \qquad (13)$$

$$+\frac{p}{a}\left[D_0K_0'\left(\frac{pr_0}{a}\right) + D_1K_1'\left(\frac{pr_0}{a}\right)\cos\phi + D_2K_2'\left(\frac{pr_0}{a}\right)\cos 2\phi + \ldots\right] = -\frac{p^2}{g}\bar{\xi}\cos\phi$$

Equating coefficients at in (13) it is possible to write (for):

$$-\frac{p^2}{g}\bar{\xi} = 2bkJ_1'(kr_0)\frac{p^2}{p^2+\omega^2} + \frac{p}{a}D_1K_1'\left(\frac{pr_0}{a}\right) \qquad (14)$$

If cylinder length l_1, force $P = ql$. On the cylinder force of a wave dispersing from it, i. e. acts on length l:

$$\bar{P} = -\rho g\pi r_0\cdot D_1K_1\left(\frac{pr_0}{a}\right)\cdot l \qquad (15)$$

Having substituted (15) in the movement (1) equation in images, we will receive:

$$\bar{m}\,p^2\bar{\xi} = -\rho g\pi r_0 D_1 k\left(\frac{pr_0}{a}\right) - c\bar{\xi} - \mu p\bar{\xi} \qquad (16)$$

Having excluded from (14) and (16), we will receive:

$$-p^2\rho\pi r_0 l K_1\bar{\xi} + \frac{\bar{m}}{a}p^3 K_1\bar{\xi} = 2bk\rho g\pi r_0 l K_1 J_1'\frac{p^2}{p^2+\omega^2} - \\ -\frac{c}{a}pK_1'\bar{\xi} - \frac{\mu}{a}p^2K_1'\bar{\xi},$$

Whence:

$$\bar{\xi} = \frac{\rho K J_1'(Kr_0)K_1\left(\frac{pr_0}{a}\right)\pi r_0 l}{\frac{c}{a}pK_1'\left(\frac{pr_0}{a}\right) + \frac{\mu}{a}K'\left(\frac{pr_0}{a}\right) - \rho r_0 l K_1\left(\frac{pr_0}{a}\right) + \frac{\bar{m}}{a}pK'\left(\frac{pr}{a}\right)} \cdot \frac{2bg}{p^2+\omega^2} \qquad (17)$$

Having increased numerator and a denominator in (17) by exp (pro/a), we will define the original of a denominator of the first factor:

$$z = \frac{cr_0}{2a^2}\left\{(1+\theta)arch(1+\theta) - \sqrt{(1+\theta)-1} + \frac{1}{3}\sqrt{\left[(1+\theta)-1\right]}\right\} - \rho\pi r_0 l\sqrt{(1+\theta)^2-1} - \\ - \frac{\mu}{2a}\left[(1+\theta)\sqrt{(1+\theta)^2-1} + arch(1+\theta)\right] - \frac{m}{r}\frac{(1+\theta)^2}{\sqrt{(1+\theta)^2-1}};\ \left(\theta = \frac{at}{r_0} - 1\right) \qquad (18)$$

Having entered designation $\bar{S} = \dfrac{exp\left(\frac{pr_0}{a}\right)K_1\left(\frac{pr_0}{a}\right)}{z(p)}$

According to Borel's theorem we have:

$$\frac{d}{dt}\int_0^t S(t-\tau)z(\tau)d = \sqrt{\left(\frac{at}{r_0}+1\right)^2 - 1}$$

or $\int_0^\theta S(\theta-\tau)z(\tau)d\tau = Q,$ (19)

where

$$Q = \frac{1}{2}\left[(1+\theta)\sqrt{(1+\theta)^2-1} - ln\left(1+\theta+\sqrt{(1+\theta)^2-1}\right)\right]$$

For the solution of the integrated equation (19) area of integration breaks into n of small sites of $\Delta\theta$ for the purpose of approximation of subintegral functions. Considering that on a piece $0 < \theta \le \Delta 0$ the fractional member in (18) bike in comparison with the others, we have:

$$z \approx \frac{\beta}{\sqrt{2}},\ \left(\beta = \frac{m}{r_0}\right) \qquad (20)$$

On the piece end

$$z\big| = z_1\frac{\beta}{\sqrt{2\Delta\theta}} \qquad (21)$$

From (20) and (21) follows

$$z = z_1\sqrt{\frac{\Delta\theta}{\theta}} \qquad (22)$$

Further we will define S by means of (9), from where considering that at z definition, the numerator and a denominator in (17) were increased by exp (pro/a), let's receive:

$$\bar{S}\big|_{t\sim 0} \approx -\frac{ba}{r\beta p}$$

Or

$$\bar{S}\big|_{t\sim 0} \approx -\frac{b}{\beta}$$

Т. к. $K_1\left(\frac{pr}{a}\right) \approx \sqrt{\frac{\pi a}{2pr_0}}\,e^{-\frac{pr_0}{a}},\ \frac{1}{\sqrt{\tau}} \to \sqrt{\pi p_1}$ (23)

$$z = \frac{\beta}{\sqrt{2\theta}};\qquad \bar{z} = \sqrt{\frac{\pi rp}{2a}};\quad \bar{S}\cdot\bar{z} = \sqrt{\frac{\pi a}{2pr}}$$

From (23) and (26) follows:

$$S\big|_{t\sim 0} \approx -\frac{b\beta}{2z^2} \qquad (24)$$

On the piece end $\theta_1 = \Delta\theta$ из (23)

$$S_1 = -\frac{b}{\beta}\Delta\theta \qquad (25)$$

$$S_1 = -\frac{b}{\beta}\frac{(2+\beta)^2}{2z_1^2} \qquad (26)$$

$$S_1 = \frac{2}{z_1^2}$$

For periods the integral in (20) is calculated by linear interpolation of functions *S* and *z* on each interval, except the first for *z* and the last for *S*.

Thus, on the first interval:

$$0 \le \theta \le \Delta\theta,\quad z = z_1\sqrt{\frac{\Delta\theta}{\theta}}$$

$$S = (S_{n-1} - S_n)\frac{\theta}{\Delta\theta} + S_n$$

and therefore:

$$\int_0^{\Delta\theta} S(\Delta\theta-\theta)z(\theta)d\theta = \\ = z_1\sqrt{\Delta\theta}\int_0^{\Delta\theta}\left[(S_{n-1}-S_n)\frac{\theta}{\Delta\theta} + S_n\right]\frac{d\theta}{\sqrt{\theta}} = \qquad (27)$$

$$= \frac{2}{3}z_1\Delta\theta(2S_n + S_{n-1})$$

Respectively on a piece $(n-1)\Delta\theta \le \theta \le n\Delta\theta$ will be

$$z=\left(z_n-z_{n-1}\right)\frac{\theta}{\Delta\theta}+nz_{n-1}-\left(n-1\right)z_n,$$

$$S=S_1\left(n-\frac{\theta}{\Delta\theta}\right)$$

In this case:

$$\int\limits_{(n-1)\Delta\theta}^{n\Delta\theta}S\left(n\Delta\theta-\theta\right)z\left(\theta\right)d\theta=S_1\int\limits_{(n-1)\Delta\theta}^{n\Delta\theta}\left(n-\frac{\theta}{\Delta\theta}\right)\left[\left(z_n-z_{n-1}\right)\frac{\theta}{\Delta\theta}+nz_{n-1}-\left(n-1\right)z_n\right]d\theta=$$

$$=S_1\int\limits_{(n-1)\Delta\theta}^{n\Delta\theta}\left\{\left(z_n-z_{n-1}\right)\left(n-\frac{\theta}{\Delta\theta}\right)\frac{\theta}{\Delta\theta}+\left(n-\frac{\theta}{\Delta\theta}\right)\left[nz_{n-1}-\left(n-1\right)z_n\right]\right\}d\theta=$$

$$=S_1\int\limits_{(n-1)\Delta\theta}^{n\Delta\theta}\left\{\left(z_n-z_{n-1}\right)n\frac{\theta}{\Delta\theta}-\left(z_n-z_{n-1}\right)\frac{\theta^2}{\Delta\theta}+n\left[nz_{n-1}-\left(n-1\right)z_n\right]-\left[nz_{n-1}-\left(n-1\right)z_n\right]\frac{\theta}{\Delta\theta}\right\}d\theta=$$

$$=\frac{z_n-z_{n-1}}{\Delta\theta}n\frac{\theta^2}{2}-\frac{z_n-z_{n-1}}{\Delta\theta^2}\frac{\theta^3}{3}+\left[nz_{n-1}-\left(n-1\right)z_n\right]n\theta-\frac{nz_{n-1}-\left(n-1\right)z_n}{\Delta\theta}\cdot\frac{\theta^2}{2}= \tag{28}$$

$$=\left\{\frac{1}{2}n\left(z_n-z_{n-1}\right)\left(2n-1\right)-\frac{1}{3}\left(z_n-z_{n-1}\right)\left(3n^2-3n+1\right)+n\left[nz_{n-1}-\left(n-1\right)z_n\right]-\frac{1}{2}\left[nz_{n-1}-\left(n-1\right)z_n\right]\right\}\Delta\theta=$$

$$=\frac{1}{3}\left(2z_n+z_{n-1}\right)S_1\Delta\theta.$$

On the others i-intervals

$$S=\left(S_{n-i}-S_{n-i+1}\right)\frac{\theta}{\Delta\theta}+iS_{n-i+1}-\left(i-1\right)S_{n-1}$$

$$z=\left(z_i-z_{i-1}\right)\frac{\theta}{\Delta\theta}+iz_{i-1}-\left(i-1\right)z_i.$$

Then:

$$\int\limits_{(i-1)\Delta\theta}^{i\Delta\theta}S\left(n\Delta\theta-\theta\right)z\left(\theta\right)d\theta=\int\limits_{(i-1)\Delta\theta}^{i\Delta\theta}\left[\left(S_{n-i}-S_{n-i+1}\right)\frac{\theta}{\Delta\theta}+iS_{n-i+1}-\left(i-1\right)S_{n-i}\right]\cdot\left[\left(z_i-z_{i-1}\right)\frac{\theta}{\Delta\theta}+iz_{i-1}-\left(i-1\right)z_i\right]d\theta=$$

$$=\int\limits_{(i-1)\Delta\theta}^{i\Delta\theta}\left\{\left(S_{n-i}-S_{n-i+1}\right)\left(z_i-z_{i-1}\right)\frac{\theta^2}{\Delta\theta^2}+\left(S_{n-i}-S_{n-i+1}\right)\left[iz_{i-1}-\left(i-1\right)z_i\right]\frac{\theta}{\Delta\theta}+\left[iS_{n-i+1}-\left(i-1\right)S_{n-i}\right]\left(z_i-z_{i-1}\right)\frac{\theta}{\Delta\theta}+\right.$$

$$\left.+\left[iS_{n-i+1}-\left(i-1\right)S_{n-i}\right]\left[iz_{i-1}-\left(i-1\right)z_i\right]\right\}d\theta=\left(S_{n-i}-S_{n-i+1}\right)\left(z_i-z_{i-1}\right)\left[i^3-\left(i-1\right)^3\right]\frac{\Delta\theta}{3}+ \tag{29}$$

$$+\left\{\left(S_{n-i}-S_{n-i+1}\right)\left(iz_{i-1}-\left(i-1\right)z_i\right)+\left[iS_{n-i+1}-\left(i-1\right)S_{n-i}\right]\left(z_i-z_{i-1}\right)\right\}\left[i^2-\left(i-1\right)^2\right]\frac{\Delta\theta}{2}+$$

$$+\left[iS_{n-i+1}-\left(i-1\right)S_{n-i}\right]\left[iz_{i-1}-\left(i-1\right)z_i\right]\Delta\theta.$$

Putting integrals (27), (28) and (29) we will lead the integrated equation (20) to a look:

$$\frac{2}{3}\left(2S_n+S_{n-1}\right)z_1+\sum+\frac{1}{3}\left(2z_n+z_{n-1}\right)S_1=\frac{Q}{\Delta\theta} \tag{30}$$

Here:

$$\sum=\sum_{i=2}^{n-1}\frac{1}{3}\left(S_{n-i}-S_{n-i+1}\right)\left(z_i-z_{i-1}\right)\left[i^3-\left(i-1\right)^3\right]+$$

$$+\frac{1}{2}\left\{\left(S_{n-i}-S_{n-i+1}\right)\left[iz_{i-1}-\left(i-1\right)z_i\right]+\left[iS_{n-i+1}-\left(i-1\right)S_{n-i}\right]\right\}\times \tag{31}$$

$$\times\left[i^2-\left(i-1\right)^2\right]+\left[iS_{n-i+1}-\left(i-1\right)S_n\right]\left[iz_{i-1}-\left(i-1\right)z_i\right]$$

Expression (31) can be transformed as follows

$$\left(S_{n-1}-S_{n-i+1}\right)\left\{\left(z_i-z_{i-1}\right)\left(i^2-i+\frac{1}{3}\right)+\left[iz_{i-1}-(i-1)z_i\right]\left(i-\frac{1}{2}\right)\right\}+$$

$$+\left[iS_{n-i+1}-(i-1)S_{n-1}\right]\left\{\left(z_i-z_{i-1}\right)\left(i-\frac{1}{2}\right)+\left[iz_{i-1}-(i-1)z_i\right]\right\}=$$

$$=\left(S_{n-i}-S_{n-i+1}\right)\left[i^2z_i-iz_i+\frac{1}{3}z_i-i^2z_{i-1}+iz_{i-1}-\left(\frac{1}{3}\right)z_{i-1}+i^2z_{i-1}-\left(\frac{1}{2}\right)iz_{i-1}-\right.$$

$$\left.-i(i-1)z_i+\left(\frac{1}{2}\right)(i-1)z_i\right]+\left[iS_{n-i+1}-(i-1)S_{n-i}\right]\left[iz_i-\left(\frac{1}{2}\right)z_i-iz_{i-1}+\left(\frac{1}{2}\right)z_{i-1}+iz_{i-1}-(i-1)z_i\right]=$$

$$=\left(S_{n-i}-S_{n-i+1}\right)\left(i^2-i+\frac{1}{3}-i^2+i+\left(\frac{1}{2}\right)i-\frac{1}{2}\right)z_i+\left(-i^2-i-\frac{1}{3}+i^2-\left(\frac{1}{2}\right)i\right)z_{i-1}]+$$

$$+\left[iS_{n-i+1}-(i-1)S_{n-1}\right]\left[iz_i-\left(\frac{1}{2}\right)z_i-iz_{i-1}+\left(\frac{1}{2}\right)z_{i-1}+iz_{i-1}-iz_i+z_i\right]=\left[\left(\frac{1}{2}i-\frac{1}{6}\right)z_i+\left(\frac{1}{2}i-\frac{1}{3}\right)z_{i-1}\right]\times$$

$$\times\left(S_{n-i}-S_{n-i+1}\right)+\left(\frac{1}{2}z_i+\frac{1}{2}z_{i-1}\right)\left[iS_{n-i+1}-(i-1)S_{n-i}\right]=\left(S_{n-i}-S_{n-i+1}\right)\left[\left(\frac{1}{2}i-\frac{1}{6}\right)z_i+\right.$$

$$\left.+\left(\frac{1}{2}i-\frac{1}{3}\right)z_{i-1}\right]+\left[iS_{n-i+1}-(i-1)S_{n-i}\right]\frac{1}{2}\left(z_i+z_{i-1}\right)=S_{n-i}\left[\left(\frac{1}{2}i-\frac{1}{6}\right)z_i+\left(\frac{1}{2}i-\frac{1}{3}\right)z_{i-1}-\right.$$

$$\left.-(i-1)\frac{1}{2}\left(z_i+z_{i-1}\right)\right]+S_{n-i+1}\left[\frac{1}{2}i\left(z_i+z_{i-1}\right)-\left(\frac{1}{2}i-\frac{1}{6}\right)z_i-\left(\frac{1}{2}i-\frac{1}{3}\right)z_{i-1}\right]=$$

$$=S_{n-i}\left(\frac{1}{3}z_i+\frac{1}{6}z_{i-1}\right)+S_{n-i+1}\left(\frac{1}{6}z_i+\frac{1}{3}z_{i-1}\right)=\frac{1}{3}S_{n-i}\left(z_i+\frac{1}{2}z_{i-1}\right)+\frac{1}{3}S_{n-i+1}\left(\frac{1}{2}z_i+z_{i-1}\right).$$

Finally:

$$\sum=\frac{1}{3}\sum_{i=2}^{n-1}\left[\left(z_i+\frac{1}{2}z_{i-1}\right)S_{n-1}+\left(\frac{1}{2}z_i+z_{i-1}\right)S_{n-i+1}\right] \quad (32)$$

The formula (30) taking into account (32) represents a recurrent formula for definition S_n.

From (17), considering that the original:

$$\frac{p}{p^2+\omega^2}\div\frac{\sin\omega t}{\omega}$$

according to Borel's theorem it is possible to define movement:

$$\xi=2\frac{KJ_1'}{\omega}\int_0^{\theta}S(\theta)\sin(\theta-\tau)d\tau \quad (33)$$

In dimensionless sizes:

$$\chi=\frac{\omega\xi}{2kbgJ_1'}=\int_0^{\theta}S(\theta)\sin(\theta-\tau)d\tau$$

Replacing integral with approximately final sum it is had:

$$\chi=\Delta\theta\sum_{i=1}^{n}S_i\sin\left[(n-i)\Delta\theta\right] \quad (34)$$

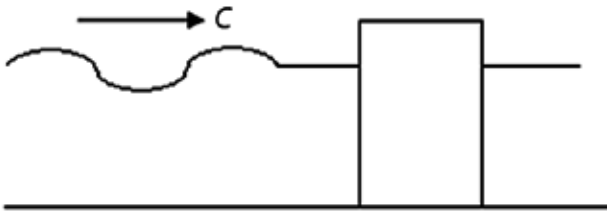

Figure 1

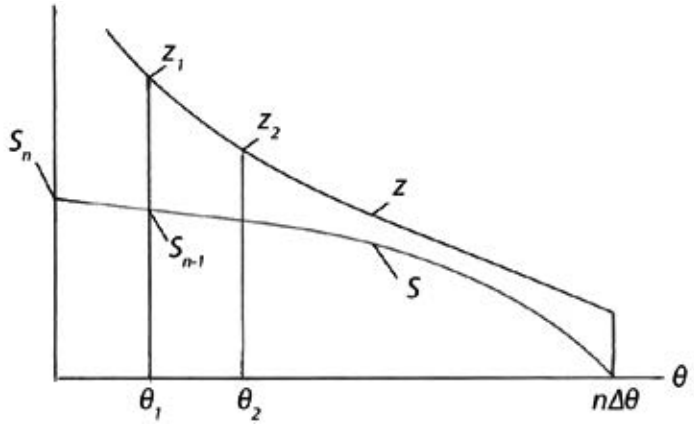

Figure 2

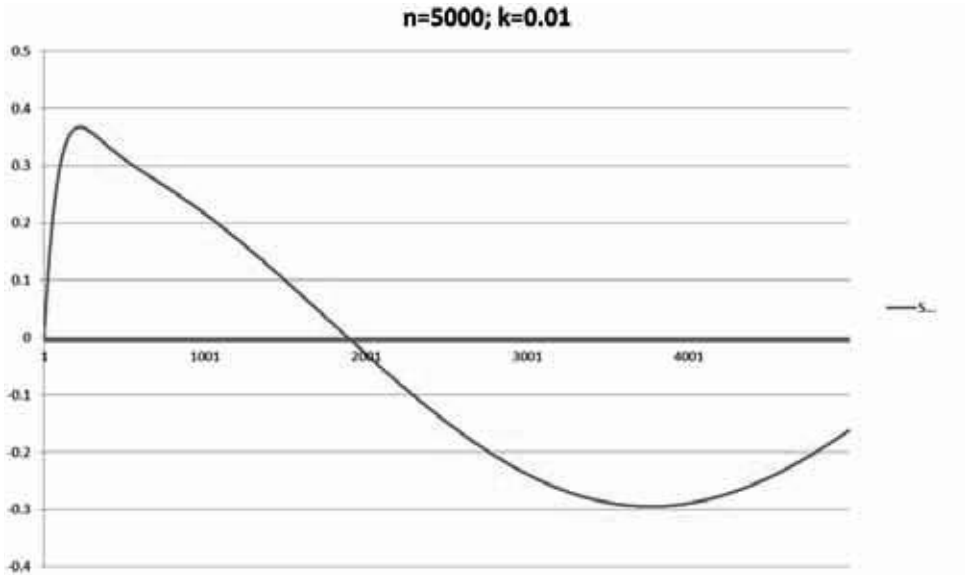

Figure 3

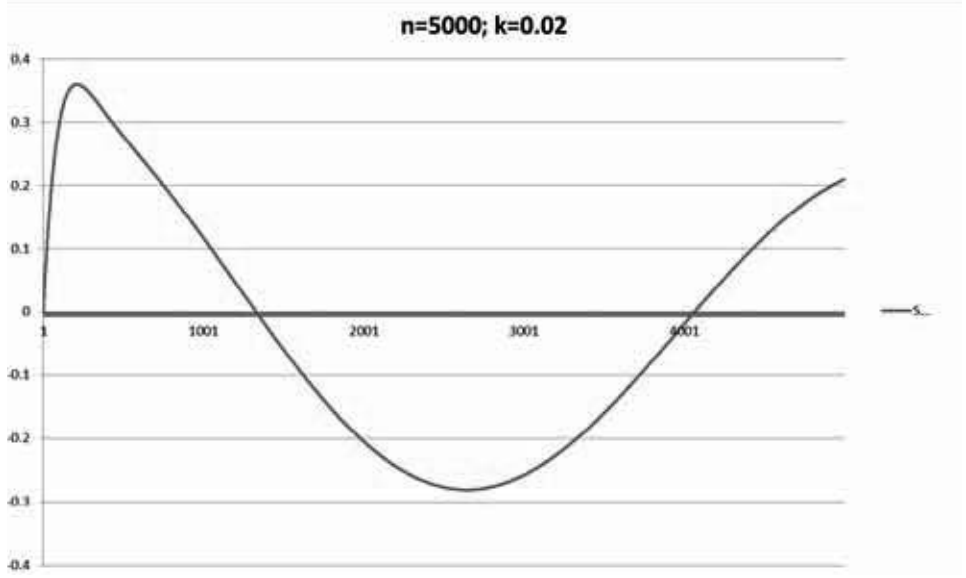

Figure 4

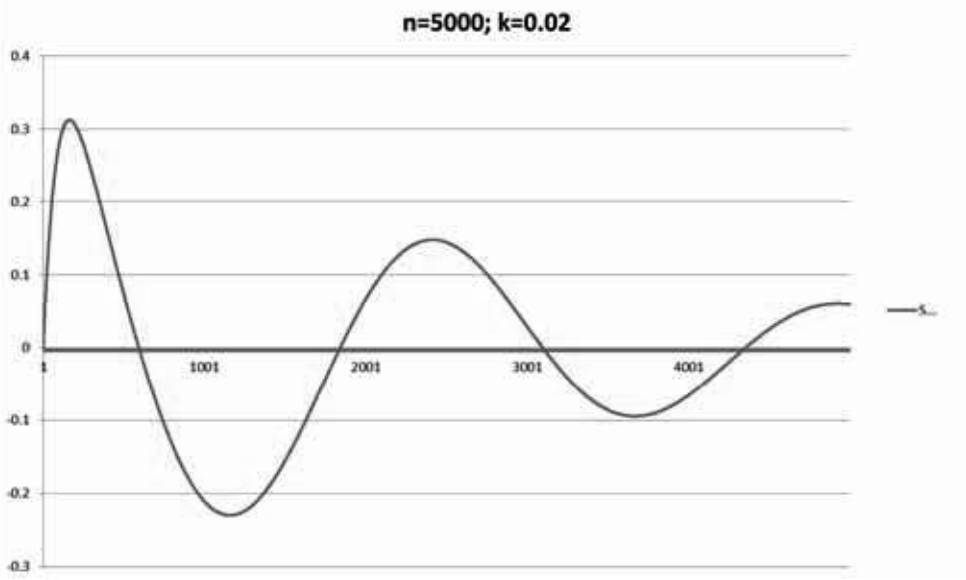

Figure 5

In figure 3 schedule S (θ) is submitted at β = 4, and in fig. 4 the schedule of dependence of movement from time is submitted: oscillations are imposed on cylinder oscillations with the big period answering to elastic fixing with the smaller period, caused by the frequency of waves in liquid.

References:

1. Forrestol M. Zh., Alzkheymer B. E. Unsteady movement of the rigid cylinder under the influence of elastic and acoustic waves. Applied mechanics. Series E, ASME, 1968, P. 278–283.
2. Kubenko V. D., Panasyuk N. N. Action of non-stationary waves on cylindrical bodies in compressed liquid. Applied mechanics, 1973, т. 9, century 12. P. 77–82.
3. Agalarova T. J. Interaction of an acoustic wave with an oscillator. The collection of scientific works on mechanics, No. 7, – Baku, 1997. P. 181–184.
4. Kochin N. E., Kibel I. A., Rose N. C. Theoretical hydromechanics. Prod. technic. – a teor. lit., – Moscow. 1955. P. 509–513.
5. Ditkin V. A., Prudnikov A. P. Directory on operational calculation. The higher school, – M. 1965.

Murvatov Faxraddin Tadji,
Scientific research institute
"Geotechnological Problems of Oil Gas and Chemistry"
Republic of Azerbaijan, Baku
Leading research fellow
E-mail: rahimova_mahluqa@mail.ru

Application of the influence of nanostructural coordination polymers based composite solution on well-bottom zone (WBZ)

Abstract: In the article study and application results of influence measure carried out in WBZ of well N111 of the South-East Sadan oil-gas area of Siyazan monoclinal oil field by 3% layer water composition of 1% mixture of BF-1 and BF reagents have been analyzed and use of the reagents in heavily extracted oils fields has been recommended to increase the production efficiency.

Keywords: rubber, permeability, nanostructural coordination polymer based composite fluid, WBZ influence.

Nowadays negative tendencies as worsening of hydraulic condition in the old oil fields, deteriorating of oil reserves structure, formation of great number of heavily extracted reserves, complication of exploitation condition of the wells, increase of interval between repairs and wells with little production, increase of geological production, technological and etc. risks are observed. The main part of hydrocarbon reserves of oil deposits consists of oils having high viscosity, anomal property, and asphalten-resin-paraffin (ARP) containing compositions. For speeding up the flow of such oils into the well, the well bottom zone is influenced by chemical, thermochemical, thermal, microfoam system and other methods [1–4]. But in many cases these methods are not efficient and create problems with unknown results. For adopting of such hydrocarbons use of more complicated technologies brings to the increase of various risks. By the carried out analyses it has been determined using traditional oil extracting methods in the development 66–58% of oil reserves can remain in the earth [5–7].

Let's mention that in Siyazan monoclinal oil deposits (SMOD) simultaneous exploitation of several reservoirs with various regimes, pressure, productivity and volume filtration characteristics is followed by incompatibilities. In such case as a result of strong flow from various characteristic formations complex to the well, artificial opportunities for the movement of water with oil and gas appear. Natural isolation of reservoirs is gradually disturbed, their content and properties worsen in the contact with layer fluids having various temperature, pressure, lithological — hydrogeological, oil-gas properties, reservoir oils become heavier, the structure changes and overturns to heavily extracted one.

It also brings to sharp weakening of reservoir system. Thus, heavy hydrocarbons in the content of oil crystallizing first settle to the well bottom zone and then gradually spread into the far well bottom reservoirs. As a result of high viscosity, freezing temperature, anomal rheological behavior extraction and transportation of such oils create serious problems.

For intensifying of such oils extraction, applied influence on WBZ including methods of influence by chloride acid have little efficiency but in many cases they are efficienless. Ecological risks significantly increase and bring harm to the enterprises from economic point. Thus from abovementioned causes connected with settling of hydrocarbons including resin substance into the well bottom zone while influencing WBZ by HCl acid, influence of the acid becomes significantly limited and influence efficiency reduces in minimum.

Connected with the created reality and sharp technical, technological situation, unical, specific geologico-geophysical and exploitation condition in SMOD for bringing of new elements into existing development system in the field, completion of residue oil reserves, substantiation of more innovative methods and technologies, application and continuation of development must be considered the most urgent problem.

For this purpose, laboratory investigations on nanostructural coordination polymer based reagents have been carried out in Siyazan oil on the basis of various principles and significant results have been obtained.

On 01.06.2015 300 ml volume oil sample was taken from producing well № 111 in the south-east Saadan oil-gas deposit and added some volume of 1.0% composite of nanostructural coordination polymer based BF-1 and BF-2 reagents alkalized in diesel fraction waste (ADFW) and viscosity change was observed (at 20°C). The results of the observation were given in table 1.

Table 1. – Change of oil viscosity by 0,1% composite additives of BF-1 and BF-2 reagents in ADFW

№	Additive volume, ml	Oil viscosity, 9 sSt
1	0,0	14,6
2	20,0	11,0
3	40,0	9,4
4	60,0	7,4
5	80,0	5,9
6	100,0	5,2
7	120,0	4,4

As it is seen from table 1 oil viscosity significantly reduces when additives are added (to 70%). For studying the influence of the additive on other indices, physico-chemical analysis of oil has been carried out before and after the additive is added. The results of the analysis are given in table 2.

Table 2. – Change of oil indices (in 120 ml. volume) with 1.0% composite additives of BF-1 and BF-2 reagents in ADFW

№	Indices	Before addition	After addition 120 ml)
1	Pure oil%	66,67	69.8
2	Special weight of oil (20°C), kg\m	891	–
3	Water separated from oil,%	0,0	16,67
4	Viscosity	14,6	4,4
5	Resin,%	40,0	26,0
6	Mechanical mixtures,%	33,33	16,66

As it is seen from table 2 by adding additive oil viscosity-reduces 70%, resin quantity 35,0%, mechanical mixtures 50%.

To learn the influence of the mixture of this layer water composite on oil viscosity, change of the viscosity of 3.0% composite prepared in layer water and added into 300 ml volume oil sample taken from well N111 on 03.06.2015 has been observed and its results have been given in table 3.

Table 3. – Change of oil viscosity with 3,0% layer water mixture additive of 1.0% composite of BF-1 and BF-2 reagents in ADFW

№	Additive volume, ml	Oil viscosity, 9 sSt
1	0,0	12,6
2	20,0	12,2
3	40,0	11,2
4	60,0	9,2
5	80,0	8,0
6	100,0	6,7
7	120,0	5,2
8	140,0	4,8
9	160,0	4,4

As it seen from table 3 reduce in the oil viscosity by mixture additives has been observed.

Considering positive results of the laboratory researches on 27.06.2015 influence measure on WBZ in well N111 of Siyazan field has been carried out with, 3% layer water composite of 1.0% mixture of BF-1 and BF-2 in ADFW.

For carrying out technological process one cementing unit SA-320, one nanoreagent transporting car, one liquid (water) transporting car have been used. During the measure 60 ton composite, 90 ton injecting fluid have been used.

The technological process is expressed by preparing nanocomposite, transporting to the well and injecting according to the scheme given in figure 1.The work was carried out on the following technology: raising the depth pump and keeping the hanger at 350 m, 6,0 m^3 nanoreagent has been injected into the pipe, then 1.0 ton pressure has been injected fluid out of the pipe and 8.0 ton pressure fluid behind of the pipe. After 72 hours' stop the well has been operated by lowering the hanger to the previous depth (737 m) with the help of 30mm pump. The results of the application are given in table 4.

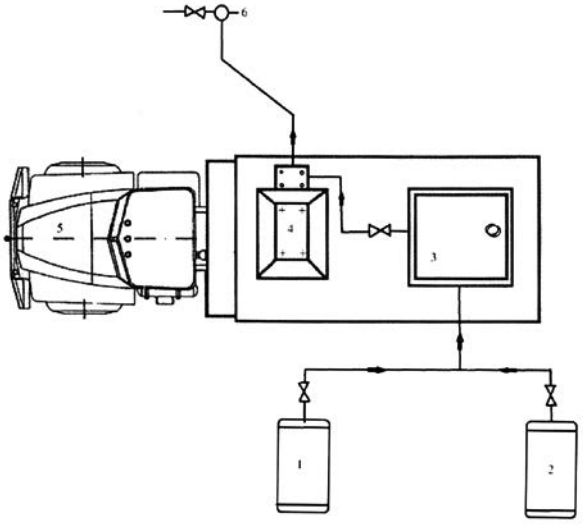

Figure 1. The scheme of the equipment location during the influence on WBZ with nanocomposite: 1–tank for mixture of BF-1 and BF-2 in ADFW. 2–tank for injecting fluid (layer water) 3–tank for nanocomposite in the unit (3.0% mixture of nanoreagent in layer water); 4–pump for injecting nanocomposite and pressure fluid; 5–unit; 6–well

Table 4.

Well №	Date of the measure	Production t/day				
		before measure		after measure		
		Oil	Water	Date	Oil	Water
111	27.06.2015	0.3	0.4	July	1.3	0
				August	1.2	0
				September	1.5	0
				October	1.5	0
				November	1.5	0
				December	1.5	0

205.3 ton additional oil has been produced from well N111 from the beginning of the measure till the end of 2015. After the first measure efficiency has been lasted. Work dynamograms of the depth pump in well N111 before and after measure has been given in figure 2.

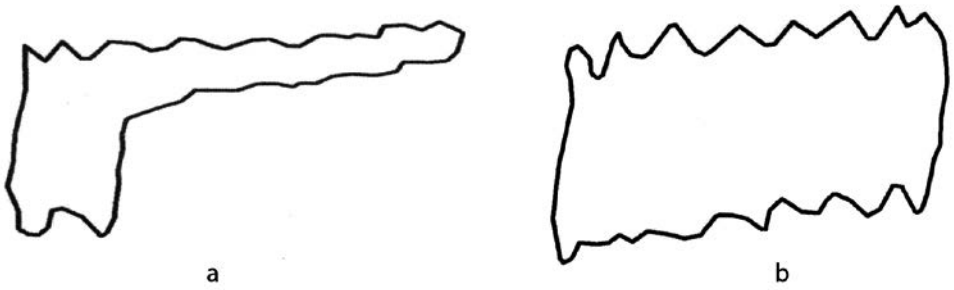

Figure 2. Work dynamograms of depth pump of well N111; a) before measure b) after measure

After the measure physico-chemical analysis of periodically taken oil samples has been carried out, their rheological properties have been studied and real results have been obtained. Analysis results are given in table 5.

Table 5. – Change of the indices of the oil taken from well N111 depending on time

№	Indices	Before measure	After measure					
		01.06.–2015	19.07.–2015	21.07.–2015	24.07.–2015	30.07.–2015	14.08.–2015	19.09.–2015	11.11.–2015
1	Pure oil,%	66,67	66,67	73,3	73,3	71,6	100	100	100
2	Specific weight of oil, kg/m^3 (20°)	891,0	890,0	890,0	890,0	890,0	890,0	891,0	891,0
3	Water separated from oil%	0	0	0	0	1,16	0	0	0
4	Rubber,%	40	16	28	20	30	34	34	36
5	Oil viscosity, sSt	14,6	7,0	6,5	5,9	4,8	10,8	10,8	10,8
6	Mechani-cal mix-tures,%	33,33	33,33	26,6	26,6	28,3	0	0	0

As it is seen from table 5 quality indices of produced oil are improving after measure.

Analysis of measure results of the influence on WBZ of well N111 carried out by 3% composition in layer water of 1% mixture of equal quantity mixtures of BF-1 and BF-2 reagents based on nanostructural coordination polymers show that the composite can be applied and it will be very useful for increasing production efficiency in heavy oil fields with high viscosity.

References:

1. Hasanov A. A., Ibrahimov H.M, Efendiyev Z. S., Shamilov V. M., Hasanov I. Z. Extraction methods of oil residues from long used fields of Azerbaijan//Azerbaijan oil industry N5, 2015. P. 37–43.
2. Arens V. J. Geotechnical methods of Minerals extraction. M. Nedra, 1986. P. 263.
3. Ibragimov G.Z and others. Use of chemical reagents for intensification of oil production – M. Nedra, 1991. P. 382.
4. Bagirov M.K and others. Increase of layer oil output by using microfoam systems – Baku, Sabah, P. 279.
5. Gumerskiy Kh.Kh., Shahverdiyev F.Kh., Mamedov Y. G., Generalization of world experience in oil deposits development//Azerbaijan oil industry N11, P. 14–29.
6. Kaminge B. K. Problem of extraction of residue oils//Oil, gas and petroleum chemistry abroad – 1991. N4, P. 16–20.
7. Shelkachev V. N. Analyses of national oil extraction in comparison with abroad//Oil industry 1991, N10. P. 32–39.

Simonyan Arsen Gevorgovich,
Yerevan State University, Postgraduate Student, the Faculty of Pharmacy and Chemistry
E-mail: sim-simov@mail.ru

Pirumyan Gevorg Petrosovich,
Yerevan State University, Doctor of Technical Science, Professor, the Faculty of Pharmacy and Chemistry,
E-mail: gevorg_pirumyan@mail.ru

Simonyan Gevorg Sarkisovich,
Yerevan State University, Candidate of Chemiical Science, Associat Professor, the Faculty of Pharmacy and Chemistry,
E-mail: gevorg.simonyan@ysu.am

Analysis of environmental status of the Kechut Artificial Reservoir and river Arpa with armenian index of water quality

Abstract: The water quality of Kechut Artificial Reservoir and river Arpa was evaluated by Armenian water guality index at first time. It was shown that from the source to the mouth of the river the values of the Armenian water guality index increases, indicating the decline in the water quality of river Arpa. It was estab-

lished that the Armenian water guality index has a linear relationship with the Water contamination index, Specific-combinatorial water quality index and Entropic water quality index and has an inverse relationship with the Canadian water quality index.

Keywords: river Arpa, Kechut Artificial Reservoir, entropy, geoecological syntropy Water quality index, Armenian water guality index.

Introduction. For evaluation of water contamination degree the comprehensive indicators are used which take possible to evaluate the contamination of water at the same time on a wide range of quality indicators. The study of ecological status of Republic Armenia Rivers is importance both for evaluation of water quality of that objects and for their further rational use. Development of water quality assessment methods using conventional indicators comprehensively taking into account various properties of surface water is an important issue. It must be noted that most developed complex characteristics of water object in one way or another connected with the existing maximum permissible concentration (MPC).

In the last years we suggest Entropic water guality index (EWQI) and Armenian water guality index (AWQI) for evaluation surface water quality [1; 2].

The aim of presented paper is evaluation of Kechut Water Reservoir and river Arpa by Armenian Water Quality Index.

Kechut Artificial Reservoir on the Arpa River, 3.5 km south of the resort town of Jermuk. Reservoir with an area of 145 hectares, the total amount — 23 million cubic meters, the average depth — 20 m, coastline length — 8.5 km [3]. Kechut Water Reservoir has one monitoring post: number 114. Arpa River originates in north-west of Artsakh Plateau, at an altitude of 3200m and flows into the Araks River, on the border of Nakhijevan and Turkey. The length of river is 126km (in Armenia 90km), basin — 2630km^2. It flows through the gorges with a big difference in altitude. Mines and waterfalls are fallen into the river near the town Jermuk. Arpa valley is wide in some parts of average flow, the river flows through Araks plain in lower flow [3]. On the Arpa River are five monitoring post: number 83–0.5 km above the city of Jermuk, number 84–0.5 km above the city of Vayk, number 85–0.5 km below the city of Vayk, number 86–0.5 km above the city of Yeghegnadzor, number 87–0.5 km below the village Areni.

Determination procedure. In hydroecological systems there can be processes both with increase, and with entropy reduction. The concept of entropy has many interpretations in various fields of human knowledge. The system interacts with the outside world as a whole**.** An open system can exchange energy, material and, which is not less important, information with environment. The system must consume information from the environment and provide information environment for act and interact with environment. Shannon was the first who related concepts of entropy and information [4]. He was suggesting that entropy is the amount of information attributable to one basic message source, generating statistically independent reports.

Entropy general equation of Shannon was been used at the first time by Mac-Artur in 1955 for evaluation of degree of structuring biogenesis [5]. In 1957, R. Margalef postulated theoretical concept that meets a variety of entropy for a random selection of species from the community [6]. As a result of these works widespread and universal recognition received index Shannon H sometimes referred to as a Shannon information index of diversity [4]:

$$H = -\sum {n_i}/{N} \log_2 \left({n_i}/{N} \right)$$

Pollution of water systems can be represented as a system of the hydro-chemical parameters (elements), the concentration of which exceeds the MPC. Then in the equation Shannon pi-probability of the number of cases of MPC excess of i-substance or water indicator of total cases of MPC – N, $P_i = n_i/N$.

The following computational algorithm is used for determination I — geoecological syntropy [7], H- Shannon entropy, EWQI and AWQI values:

1. Determines the number of cases of MPC excess of i-substance or indicator of water –*n.*

2. Estimates the total amount of cases the maximum permissible concentration $(N) - N = \sum n$.

3. Computes $\log_2 n$, $\mathrm{nlog}_2 n$, $\sum \mathrm{nlog}_2 n$.

4. Determines geoecological syntropy (I) and entropy (H): $\mathrm{H} = \log_2 N - \dfrac{\sum \mathrm{nlog}_2 n}{N}$,

5. $I = \dfrac{\sum \mathrm{nlog}_2 n}{N}$,

6. $\mathrm{H} = \log_2 N - I$.

7. Then EWQI is determined: $\mathrm{G} = {\mathrm{H}}/{\mathrm{I}}$

8. Further, the total amount multiplicity MAC exceedances is estimated (M) – $\mathrm{M} = \sum \mathrm{m}$.

9. Computes $\log_2 M$

10. Armenian Water Quality Index was obtained: $\mathrm{AIGW} = \mathrm{G} + 0.1 \log_2 M$

Results and Discussion.

It was established in the river water is regularly increased MPC of copper, vanadium, aluminum, chrom, manganese and selenium. For example, in 2009 year in the position № 85 of River Arpa NO_2^-, V, Al, Mn and Se number of MPC increasing cases is 2, 11, 11, 2, and 1 times, respectively. The amount of excess cases of MPC — N = 27, $\sum n\log_2 n = 80.06$, I = 80.06/27 =2.96, H = $\log_2 27$–2.96 = 4.75–2.96 = 1.79, EWQI = G = 1.79/2.96 = 0.604. The total amount of the multiplicity of MPC exceedances — $M = \sum m = 12.6$, $\log_2 M = 3.653$, AWQI = 0.604 + 0.3653=0.9693 (see Table 1).

Table 1. – Entropic and Armenian water quality indexes for River Arpa and Kechut Artificial Reservoir

Positions	**83**	**84**	**85**	**86**	**87**	**114**
I	3,12	3.17	2,96	3.18	3.12	3.32
H	1.52	1,22	1,79	1,57	1.63	1.0
EWQI	0.488	0,385	0.604	0,494	0,523	0.301
M=Σm	8.1	9.0	12.6	12.5	13.9	6.7
$\log_2 M$	3.016	3.168	3.653	3.642	3.795	2.742
AWQI	0.7896	0.7018	0.9693	0.8582	0.9025	0.5752

It was established that the AWQI is less than one. This indicates that the water river Arpa is not contaminated. It was shown that from the source to the mouth of the river values of the AWQI increases, indicating, the decline in the water quality of river Arpa.

Quality of River Arpa and Kechut Artificial Reservoir water also comprehensively evaluate by other indexes: Water Contamination Index (WCI), Canadian Water Quality Index (CWQI) and Specific-combinatorial Water Quality Index (SCWQI) [8–11] (see Table 2).

Table 2. – Water Quality Indexes for Arpa and Kechut Artificial Reservoir

Index	**AWQI**	**EWQI**	**WCI**	**CWQI**	**SCWQI**
83	0.7896	0.488	1.14	83.78	1.60
84	0.7018	0.385	1.16	82.04	1.51
85	0.9693	0.604	1.45	77.67	1.87
86	0.8582	0.494	1.45	79.47	1.76
87	0.9025	0.523	1.30	76.90	1.53
114	0.5750	0.301	1.22	80.68	1.9

With the help of a computer program «Origin-6" made an analysis of the linear relationship between AWQI and drugimy water quality index (WQI):

AWQI = a + b · [WQI]

For the river Arpaa good correlation.

AWQI = (0.1303 ± 0.3107) + (0.5492 ± 0.2378) · WCI, R=0.80004, N=5,

AWQI = (0.0809 ± 0.4551) + (0.4615 ± 0.2741) · SCWQI, R=0.69692, N=5,

AWQI = (0.2133 ± 0.0997) + (1.2650 ± 0.1985) · EWQI, R=0.96514, N=5,

AWQI = (3.1571 ± 0.9495) – (0.0289 ±0.0119) · CWQI, R=0.81512, N=5,

A good correlation is obtained also when the river Arpa and Kechut Water Reservoir considered together

AWQI = (–0.1095 ± 0.4916) + (0.7064 ± 0.3802) · WCI, R=0.68059, N=6,

AWQI = (3.4995 ± 1.7499) – (0.0332 ± 0.0218) · SCWQI, R=0.60529, N=6,

AWQI = (0.1846 ± 0.0548) + (1.3198 ± 0.1151) · EWQI, R=0.98511, N=6,

Analysis of obtained data indicate that AWQI has liner dependence with WCI, SCWQI, EWQI and an inverse dependence with CWQI:

Conclusion

1. For the first time using the AWQI of the river Arpa and Kechut Artificial Reservoir.

2. It was shown that from the source to the mouth of the river values of the AWQI increases, indicating, the decline in the water quality of river Arpa.

3. It was established that the AWQI is less than one. This indicates that the water river Arpa is not contaminated.

4. It was shown that the AWQI has an inverse dependence with CWQI and a linear relationship with CWQI WCI, SCWQI, EWQI

References:

1. Pirumyan G. P., Simonyan A. G. Analysis of the ecological state of Aghstev using the entropy index.//Science bulletin. – 2016. – № 1 (7), – P. 191–195.
2. Simonyan A. G. Analysis of environmental status of the river Voghji with Armenian index of water quality.//Proceedings of YSU, Series Cemistry and Biology. – 2016. – № 2, – P. 20–24.
3. Sargsyan V. O. Armenian Water. Yerevan: YSUAB,2008. – 208 p.
4. Shannon C. Works on information theory and cybernetics. – M.: IL, – 1963. – 830 p.
5. MacArthur R. M. Fluctuation of animal populations and measure of community stabiliry//Ecology. – 1955. – V.36. – № 3. – P.533–536.
6. Margalef R. Information theory in ecology//Gen. Syst. – 1958. – V.3. P. 36–71.
7. Simonyan G. S. Assessment of hydrogeological systems in the light of information theory synergistic//Proceedings of the All-Russian scientific-practical conference. Environmental safety and Nature: Science, Innovation, upravlenie. Mahachkala: ALEPH, – 2013. – P. 275–280.
8. Nikanorov A. M. Scientific basis for water quality monitoring. St. Petersburg: Gidrometeoizdat, 2005. – 577 p.
9. Temporary methodical instructions by a complex assessment of quality of surface and sea water on hydrochemical indicators, are enacted by the instruction Goskomgidromet – № 250–1163 on 09/22/86. – M.:1986. – 5 p.
10. RD 52.24.643–2002. The leading document. Methodical instructions. A method of a complex assessment of degree of impurity of a surface water on hydrochemical indicators. St. Petersburg: Gidrometeoizdat publ, 2002. – 55 p.
11. CCME Water Quality Index. Technical Report, Excerpt from Publication Ni 1299, SBN 1–896997–34–1, Winnipeg, 2001.

Sharipov Khasan T.,
Tashkent State Technical University,
Professor, Doctor of Chemical Sciences,
Deputy Chairman of the SUE
«Fan va tarakkiet"

Sharafutdinov Ulugbek Z.,
Navoi Mining and Metallurgical Combinate,
Chief of the technical control service of the MA. of the NMMC
E-mail: u0505@mail.ru

Saparov Anvarjon B.,
Navoi Mining and Metallurgical Combinate,
NMMC's chief of the process engineering department

Current state of the uranium extraction at the NMMC

Abstract: Currently of the uranium mined in NMMC is obtained by means of underground leaching in the Kyzyl-Kum open pits. This method allows to reduce the cost of uranium mining and ensure the environmentally clean production.

Keywords: uranium, underground leaching, sorption, extraction, rhenium, environmental protection.

The Basic proven, estimated and expected reserves of the uranium are concentrated at Kyzyl-Kum Province of the Uzbekistan. From 1940s there were intensified research works on the natural recourses at the territory of the Uzbekistan: have been carried out complex geologic surveying at Kyzyl-Kum and special exploration works on uranium, as well as aeroradiometric and surface geological-radiometric searches.

As a result of such exploration works there has been found out more than 70 uranium ore occurrences, this discoveries was the beginning of the development of Kyzyl-Kum region from the Uchkuduk deposits at 1952 years. Just from the base of this deposit at 1958 there has been started the construction of the Navoi Mining and

Metallurgical Combinate (NMMC) and then in 1962 for the first time in mining industry by specialists of the NMMC was discovered the innovative technology of the uranium extraction by the underground leaching method.

Determined that the uranium extraction by underground leaching method have a number of advantages in comparison with traditional method:

– Smaller power consumption;

– Lower capital and operational costs;

– Possibility of the profitable execution of the poor sandstone uranium ores;

– Insignificantly radiation influence on environment.

Today the uranium extraction at NMMC is executed only by underground leaching method. NMMC's uranium extraction structure consists of three uranium production enterprises there are.

– Northern Mining Administration: Uchkuduck, Kendik-Tube, Meylisay mined deposits;

– Mining Administration № 5: Shimoliy Bukinoy, Janubiy Bukinoy, Aulbek, Kuhnur, Istiklol, Northern Kanimex, Beshkok, Loyliken, Sugrali, Ketmonchi, Yogdu mined deposits;

– South Mining Administration: Sabirsoy, Jarkuduck mined deposits;

– and Gydrometallurgical Plant № 1 for output of the uranium oxide concentrate after sulfuric salts processing.

Uranium extraction by underground leaching at NMMC's structures executed of three differ methods using various leaching chemical agents and their combinations: acid, acid-carbonate, nonchemical treatment.

Both traditional and underground leaching methods initially accessed ore body. Uranium ore deposits have been accessed by injection and extraction wells system. Depending on filtration properties and rock ore homogeneity there are used various drilling patterns: rectilinear, hexagonal with different distance between rows and holes. Usually at NMMC's sites the holes constructed by rectilinear circuit which clasped ore shoots fully, although in comparison with hexagonal way this way is less effective. The hexagonal layout does not become common use by reason of disadvantage costs on consumables. There are developed deposits with ore depth formation up to 500 meters and more with combined mining and geological conditions due to uranium reserves depletion superposed on shallow depth. Provision of the holes qualitative constructions become much actual from which work depends extraction efficiency considering the fact that geotechnological holes are compound construction.

Well tube filters are integrant parts of the holes, which are made at the NMMC's Machinery Plant, its provides for maximal porosity with high stabile production rate of the holes. The rising of the solution from borehole on underground leaching areas has been made by electro-submersible pumping units, replaced air-lift solution rising units starting from 2000 year. Usage of the electro-submersible pumping unit s had achieved the uranium production considerably at a reduced power supply of the production process and to omit the usage of the expensive compressor units.

Implementation attempts of the electro-submersible pumping units as units lifting solution has been used in the 80-s, but due to short working life of such units and unavailability of the standard size ranges this works was stopped. Today by the NMMC's subdivisions have been gained wide experience on qualitative maintenance of the submersible pumping units, this increase interval between failures of the pumping units up to 12000 hours, by comparison in 2000–2002 years the interval between failures was 2500 hours. Currently at NMMC' subdivisions are used the submersible pumping units of the following companies: Oddesse (Germany), Grundfos (Denmark, Germany), Wilo (Germany), Impo (Turkey).

After lifting on daylight the productive solutions using pumps on the lines of process pipelines are going to sorption treatment. Uranium sorption from productive solutions is made by ion exchange resin Purolite A-606 (England), BD-706, BO-020 (China) at the ion-exchange columns. Uranium poor solution (mother solution) passed the sorption treatment has been reinforced by reagent and returned back on production sites for injection wells feed for further uranium leaching. Enriched ion exchange resin is sent to desorption column, executed by sulfuronitrate solutions. Uranium extractions from industrial reclaim is carried out by ammonia water by cascade precipitation on pH defined value. For separation from solution precipitated uranium is passed through filter-press. After filtration the yellow cake is dissolved at sulphuric acid solution until the formation of the sulphuric salts, which are intermediate product of the underground leaching process. Further sulfuric salts from subdivisions have been delivered to Hydrometallurgical Plant #1, where dissolved uranium has got extraction concentrating using organic extractant. Uranium rich organic phase is passed re-extraction by carbonate and ammonium bicarbonate mix. Obtained pulp from crystals of the ammonium-uranyl-three-carbonate after decontamination has been delivered to filtration. Further filtered crystals will be roasted until the end product formation in the form of uranium oxide concentrate. Uranium oxide concentrate, produced at NMMC is exporting

to foreign countries fully, that consistently provides NMMC for foreign currencies. In order to provide the scale-up uranium production outputs, NMMC specialists works hard on exploration and continually going into operation of the new deposits. New deposits are characterized by bigger depth of the ore formation, as was mentioned previously and higher rock carbonate content of the ore-hosting deposits. The carbonate content indicator of the old deposits is not exceed 0,6–1,0%, and at new sites carbonate content indicator is more than 2%, ran up at some sites 10–12%. In this case using of the sulphuric acid as leaching reagent is not technically and economically reasonable, whereas the communication the carbonates with sulphuric acid results in reduction of the filtration properties of the waterbearing ore-hosting bed and impossibility of the uranium extraction in future.

Today we are monitoring the reserves classified as off-balance, whereas there are available positive results of the ore development with increased carbonate content on the Aulbek deposit.

There are carried out development works on the Maylisay, Northern Kanimeh and Yogdu deposits. At the same time planned uranium extraction ratio is unchanged. Increasing of the ore body formation depth from 110 to 550 meters and mean effective power of the ore-hosting water bearing beds from 12 to 20 meters as well as reduction of the value per surface unit of the open ore bodies adversely affected on ore deposits development. The main cause is the uranium impoverishment at product solutions, as well as actual power increase of the ore-hosting water-bearing beds caused on high reagents consumption used for uranium extraction. Currently the specialists of the NMMC and Research Institutes of the Republic of Uzbekistan carried out the works on identification the most effective technical procedure for the processing of above mentioned deposits. Development of the infiltration uranium deposits by the underground leaching method had been considered as monogene at the initial period. Later has been ascertained that single elements accumulated in process solutions of the underground leaching and can be extracted as by-product. Based on market data rhenium, molybdenum and other rare-earth elements are one of the perspective by-products. At the NMMC's Mining Administration № 5 and Northern Mining Administrations is extracted rhenium as by-product from tail solutions of the geo-technological sites of the underground leaching. Special attention is given to environmental protection questions. During development by underground leaching method the key source of pollution are process solution spillages on loss-of-piping integrity, hole washing leakages, solution spillage on submersible pumping, slime and core on making holes, residual solutions in production sections as well as their spreading into water-bearing grounds and others. Herewith the main polluted objects are atmospheric air, ground, surface and mostly underground waters. Simultaneous operations monitoring for environmental conditions is the environment-related activity of the NMMC management.

This makes it possible to establish influence on atmospheric air, water reservoirs, soil covering and flora, as well as to determine qualitative and quantity characteristics of the contaminants and to monitor the compliance of the adjusted standards of the maximum permissible emissions and discharges the hazardous substances.

Soil covering protection: at desert and semiarid climate zone on blown and semi-blown sands on wind ward are build the countershafts from native soil and covered by restraining material. All process wells equipped by hatchways those excepts their leaking on overflow. Solutions flushing on cleaning and hole washing is made in special reservoirs for settling and subsequent return in holes.

Surface water protection: For protection of the water bodies there provided relevant engineering constructions as crown ditches, by-pass canals, barrages, transfers and others), excludes their pollution and providing allocation water recourses as well as safety process equipment and communication lines. In the presence of water zones at the underground leaching areas there are formed the water quality monitoring stations, which placed at three zones: internal (within the balance emplacement), peripheral (on 20 meters from internal), and regional (side with peripheral zone). Data observed on perimeter inspection holes, placed on productive water-bearing horizons, suggests that on all underground leaching zones independently of applied process layout out of 200–300 meters from ore deposit circuit the natural background edge waters remains unchanged. Radiation control is conducted by working conditions supervisory services and environment protection services, as well as sanitary-industrial laboratories, territorial and central organization of the State Committee for Health Supervision, State Committee for Ecology, State Inspection «Sanoatkontechnazorat». NMMC's many years' experience on underground leaching method confirms its high performance and environmental safety, which expands implementation area. Market conditions demand considerable relations for technical excellence of all uranium production components and their cost re-

duction. In this regard by NMMC specialists has been developed economic uranium extraction development program until 2020 year and have been implemented some measures:

– Bridging into service of the new perspective deposits;

– Modernization of the existing sulfate plant and construction of the new one;

– Construction and start-up in 2013–2016 new underground leaching deposits under North Kanimeh and Sugrali deposits;

– Reconstruction of the shop # 3 of the Hydrometallurgical plant # 1;

– Development of the program shall guarantee stable growth of the uranium production output at NMMC until 2020.

Yunusov Bokhodir,
senior teacher
chair «Informatics, automation and managements»,
Tashkent chemical institute of technology,
Tashkent, Uzbekistan
E-mail: Ulug85bek77@mail.ru

Development of Algorithm of process management of ore enrichment in fluidizated layer

Abstract: The automated installation with the device of multicell separation of loose material is developed, with algorithm of intellectual management air separation process in a fluidizated layer of the crushed particles of the different limiting sizes and offered a function chart of an automated control system by process of an air separation of loose materials in a fluidizated layer. For this purpose using Archimedes, Lyashchenko and Reynolds's criteria, algorithmization of calculation of speeds the beginning of a fluidization and an ablation of particles of different density and is carried out the sizes, the formalized equations allowed creation of computer model of process of an air separation of firm particles in a fluidizated layer with use of a package applied the MATLAB programs. Nomograms of change of speed of gas depending on density and the sizes of particles of separated loose material are received.

Keywords: mathematical model, air separation, beginning of speed fluidization, speed of ablation, algorithm of management, automated control system.

Application of methods of an air separation at enrichment of ores of rare and precious metals is caused by that use of traditional methods are accompanied by big power consumption and water.

Technological installation of an air separation offered by us in a fluidizated layer analyzed by use of the multistage system analysis [1].

For the bottom hierarchical level process of moving of particles is defined. For this purpose, considering the forces influencing a particle, possible movings of certain particles are defined. Thus, it is possible to find equilibrium speed of a stream, at which particles of a certain weight will be is in a scaled condition [2–5].

For particles of the identical size ablation from the device depends on weight (specific weight) of particles.

Calculations defined speed of an air stream for a conclusion of a particle of easy weight. The maximum limit of this speed should not reach the speed deducing particles with heavy weight.

By fluidizated consideration with use of the criterion equations, is defined possibilities of creation of a fluidizated layer and questions of determination of speed of ablation of particles.

Considering disorder of the sizes of particles, defined equivalent diameter of a particle. Knowing equivalent diameter, it is possible to define speed of the beginning of a fluidizated and to pass to definition of criterion of Archimedes. Then, it is possible to define Reynolds's criterion for a fluidizated layer.

Reynolds's criterion for a particle is defined by the classical equation according to which it is possible to define speed of a fluidizated or speed of a ablation of particles.

If speed is known, it is possible to define a consumption of gas.

Thus, it is possible to define speed or a consumption of gas for providing a fluidization.

On the basis of such algorithm the computer model of process of a air separation of firm particles in a fluidizated layer with use of a package applied the MATLAB programs (the Fig. 1 is made.). By means of computer model speed or the consumption of gas (air) providing a fluidizated or speed of ablation of particles is defined.

It is possible to define ablation limits, both heavy particles, and easy particles. If these diameters do not satisfy the put requirements, options change of an expense and speed of gas depending on diameter of particles then are considered. Choosing diameter of particles and its limits of change, it is possible to find the solution of separation of a loose material with various density.

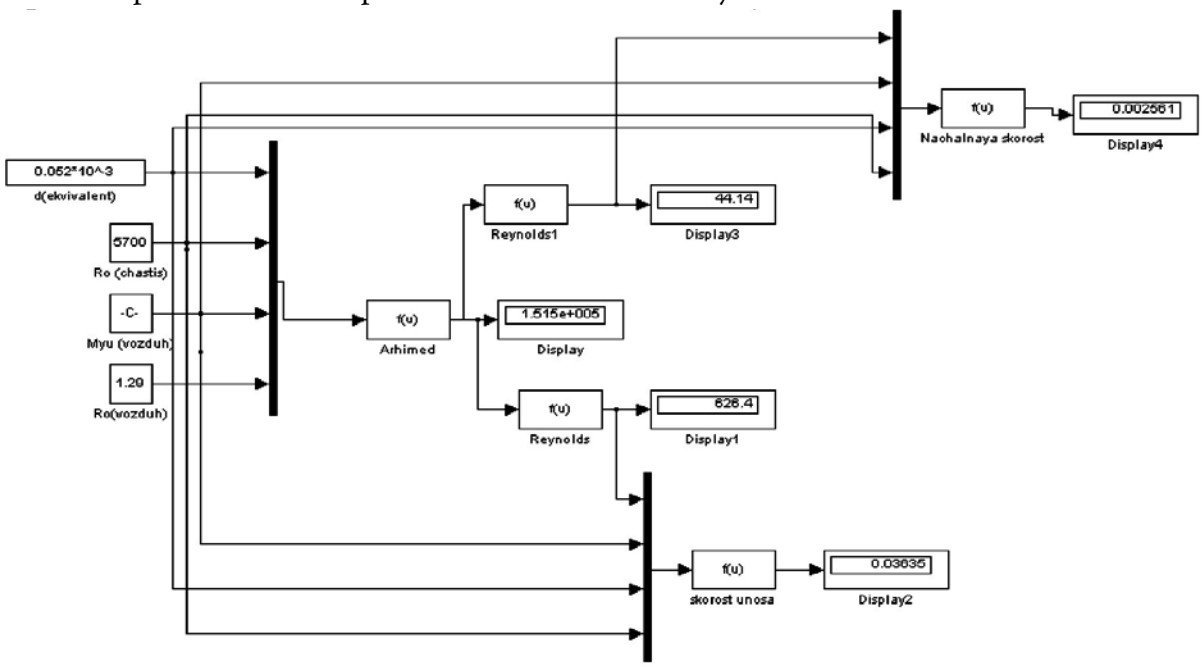

Fig. 1. Computer model for calculation of speeds of a ablation and the fluidizated beginning depending on diameter and a type of particles.

On figure 2. The dependences of speed ablation begins from diameter and a type of particles are given.

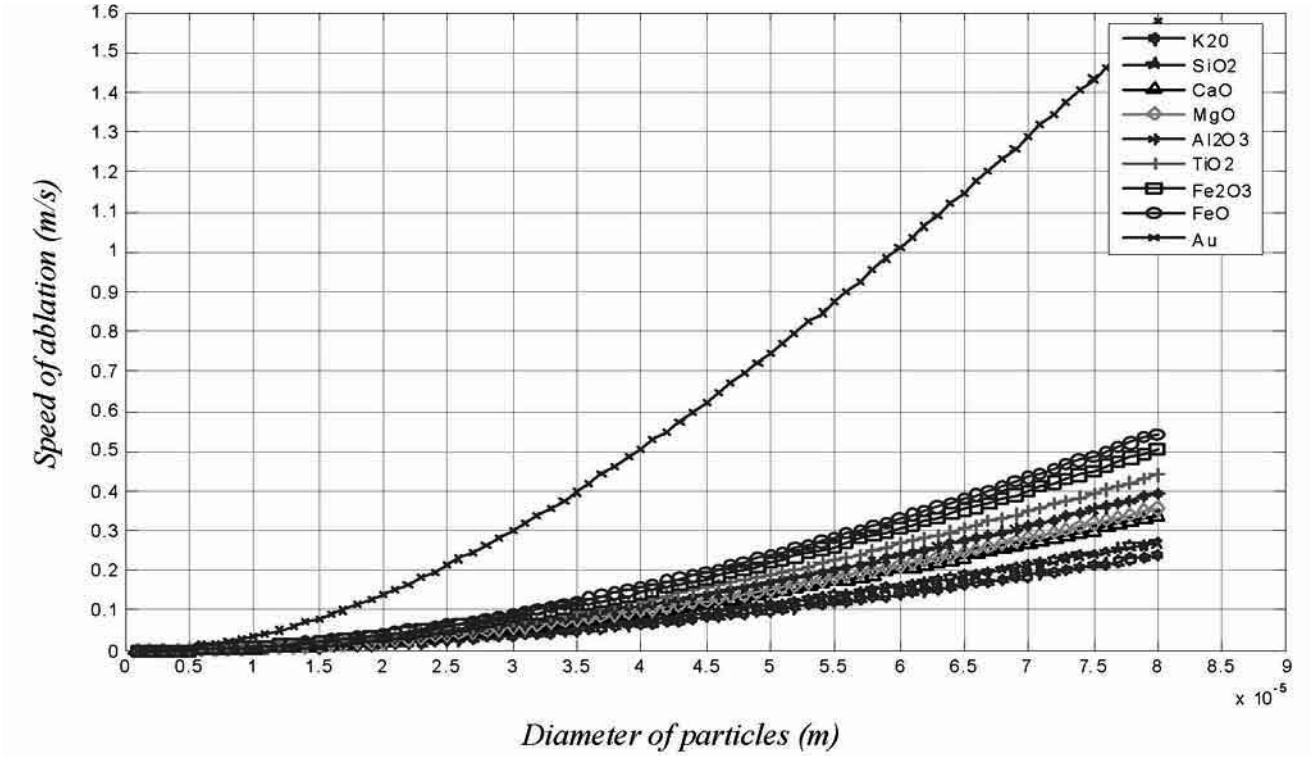

Fig. 2. Dependence of speed of ablation from diameter and a type of particles

From schedules (fig. 2) it is possible to define speed of air at which the components being in a mix, with certain sizes of particles in the device with a fluidizated layer, will be in a suspension.

The analysis of schedules shows that for the chosen test of ore, with reduction of the sizes of particles (0.001÷0.020 мм), the limiting sizes of the particles, providing a good separation decreases to two, at most till three sizes of particles. With reduction of the limiting sizes of the particles, each test is necessary for passing through installation with the fluidizated layer, adjusted on these limiting sizes. In this regard, the air separation of particles with the smaller sizes will need bigger number of devices with a fluidizated layer. At the big sizes of particles (0.060÷0.080 мм), the limiting sizes of the particles, providing a good separating increase till seven and nine sizes of particles. On the other hand, at smaller diameters of particles of influence of the maintenance of an enriched material on particle density it is more than at big diameters of particles. Therefore, we recommend to carry out enrichment of a loose material in a range of the crushed particles 0.030÷0.050 мм where the limiting sizes of particles providing a good separations are in limits of five and six sizes of particles. Thus, ore enrichment in this range will need four installations with a fluidizated layer.

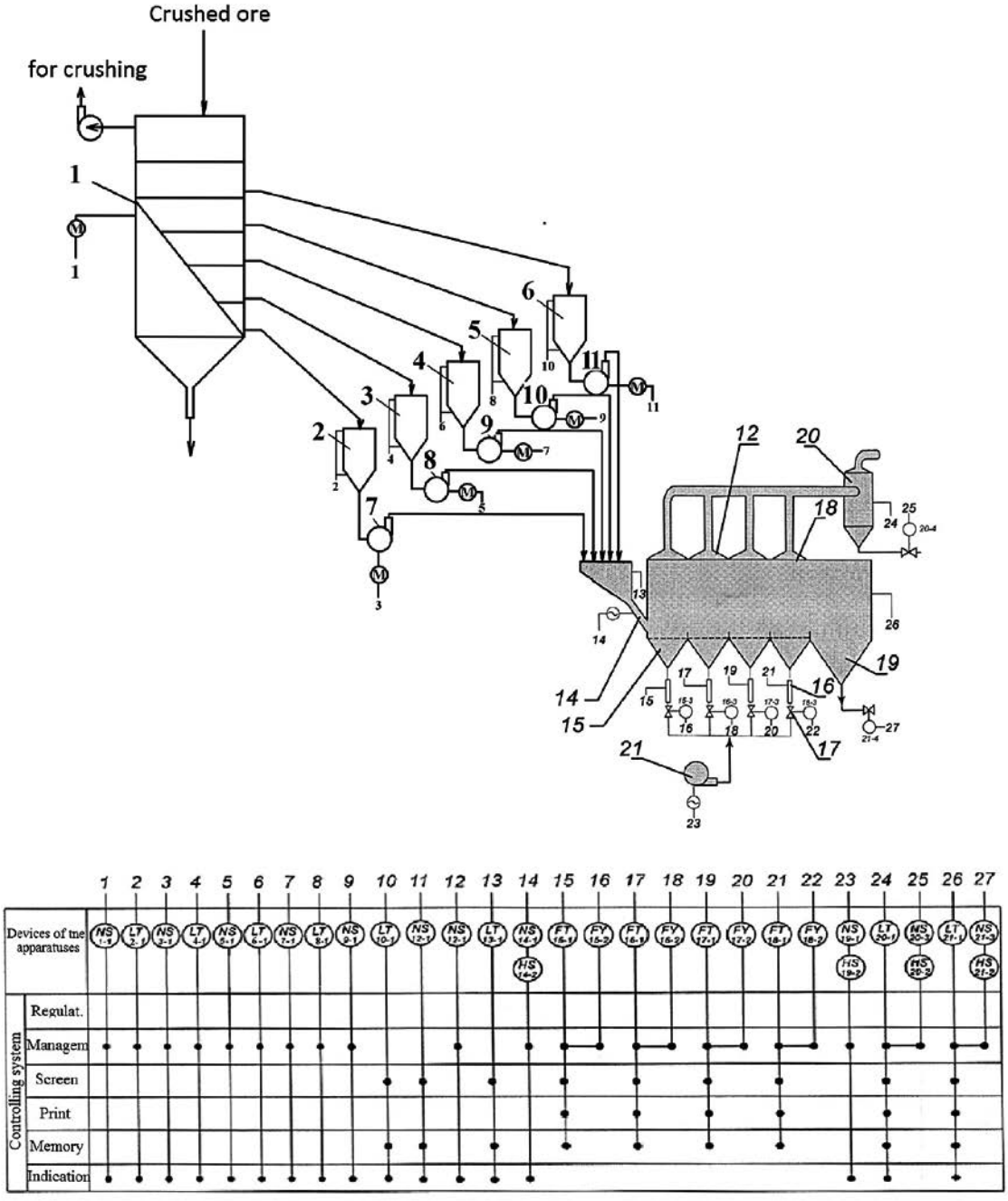

Fig. 3. A function chart of an automated control system for process of an air separating of loose materials in a fluidizated layer

Computer models air separation particles in a fluidizated layer, both for a periodic mode, and for a continuous operating mode of the device are formalized. The design procedure of air separation of particles in a continuous operating mode of the device is developed.

On the basis of the carried-out analysis and calculation installation with the device multicell separation of a loose material is developed. This device has the extended case of corridor type which on length is divided into the squares, each square has separate air intakes with the set expense and each square has a partition for maintenance of a fluidizated layer.

The offered technological scheme of preliminary enrichment with use of installation of separation is provided in a fluidizated layer on rice 3. For separation in a fluidizated layer ore is crushed previously by means of a grid-iron roar, a rotor inertial crusher, an loading elevator, an inertial roar, a crusher of the combined shock action and a centrifugal mill of counter blow. The crushed ore moves in system 1, established consistently, for separation on the sizes of particles on sets 50, 44, 39, 34 and 30 microns. The exit with everyone sieves goes to separate bunkers 2–6 and gravel pumps 7–11, moves in the loading bunker 13 of installation of a multistage air separation in a fluidizated layer 12. Installation works as follows:

From one of capacities 2–6 through a feeder the 14th material arrives in the first section of a air separator where under the influence of the air submitted from under grids 15, the boiling layer and easy components is formed are carried away by air in a cyclone 20, and the ore rest, because of a fluidizated to pass through a partition 18 to the following step of a separation.

Air moves in separate sections of a separator. In process of transition of ore to the following step, ore is more and more released from easy components. From the last step the rest of ore arrives in the collection of heavy components 19 and from there the enriched ore is loaded into containers.

Considering higher to carry out the provided recommendations enrichment of a loose material in a range of the crushed particles 0.030÷0.050 мм, from nomograms, the limiting sizes of particles providing a good separation (0.030÷0.034, 0.035÷0.039, 0.040÷0.044 and 0.045÷0.050 мм) were defined. Exits from each of these sieve go to separate capacities 2–6. The crushed ore of the next sizes gathering in various capacities is exposed to process of an air separation: A) particles in the size less than 30 microns (capacity 2); B) particles in the size of 30–34 microns (capacity 3); C) particles in the size of 35–39 microns (capacity 4); D) particles in the size of 40–44 microns (capacity 5); F) particles in the size of 45–50 microns (capacity 6). It is necessary to provide a process continuity for what gravel pumps different fractions move serially in the loading bunker and from there in the first section of an air separation. In process of a dumping of a loose material in the bunker, there is a switching on other bunker and each time a consumption of air submitted to a air separation changes depending on the sizes of particles.

We offered the automation scheme in which switching for new speeds (expenses) of air depending on the sizes of particles is carried out by an automated control system (fig. 3) for what algorithms of management of giving in the loading bunker of particles of the different sizes (fig. 4) are developed.

Algorithm of management of air separation process in a fluidizated layer is as follows:

In this system there are bunkers for five fractions of a loose material, each of which are supplied with primary converters of level with analog that target signal. Usually, capacities are filled not evenly. At separation of the crushed ore with the help sieve some capacities are filled quicker, and some slowly. For management of such processes use adaptive control systems. Process an air separation begins supply of the crushed ore with the bunker in which level of a loose material has the maximum value. Signals from primary converters continuously appears in the controller. After a dumping of this bunker, the controller carries out shutdown of its capacity pump, comparison of levels in all other capacities further is carried out, the capacity pump turns on where level has the maximum value and a loose material from this capacity moves in the loading bunker. The controller switches the consumption of air corresponding to the new size of particles.

Each time when level of a loose material reaches the bottom level, is disconnected the bunker pump from which the loose material is selected and the bunker pump starts to work where level has the maximum value and a consumption of air is switched according to the limiting sizes of particles in this bunker.

In case in any bunker level reaches maximum-permissible maximum value, the bunker pump with which is disconnected the loose material is selected and the bunker pump starts to work where level reached extremely maximum value and a consumption of an air is switched according to the limiting sizes of particles in this bunker.

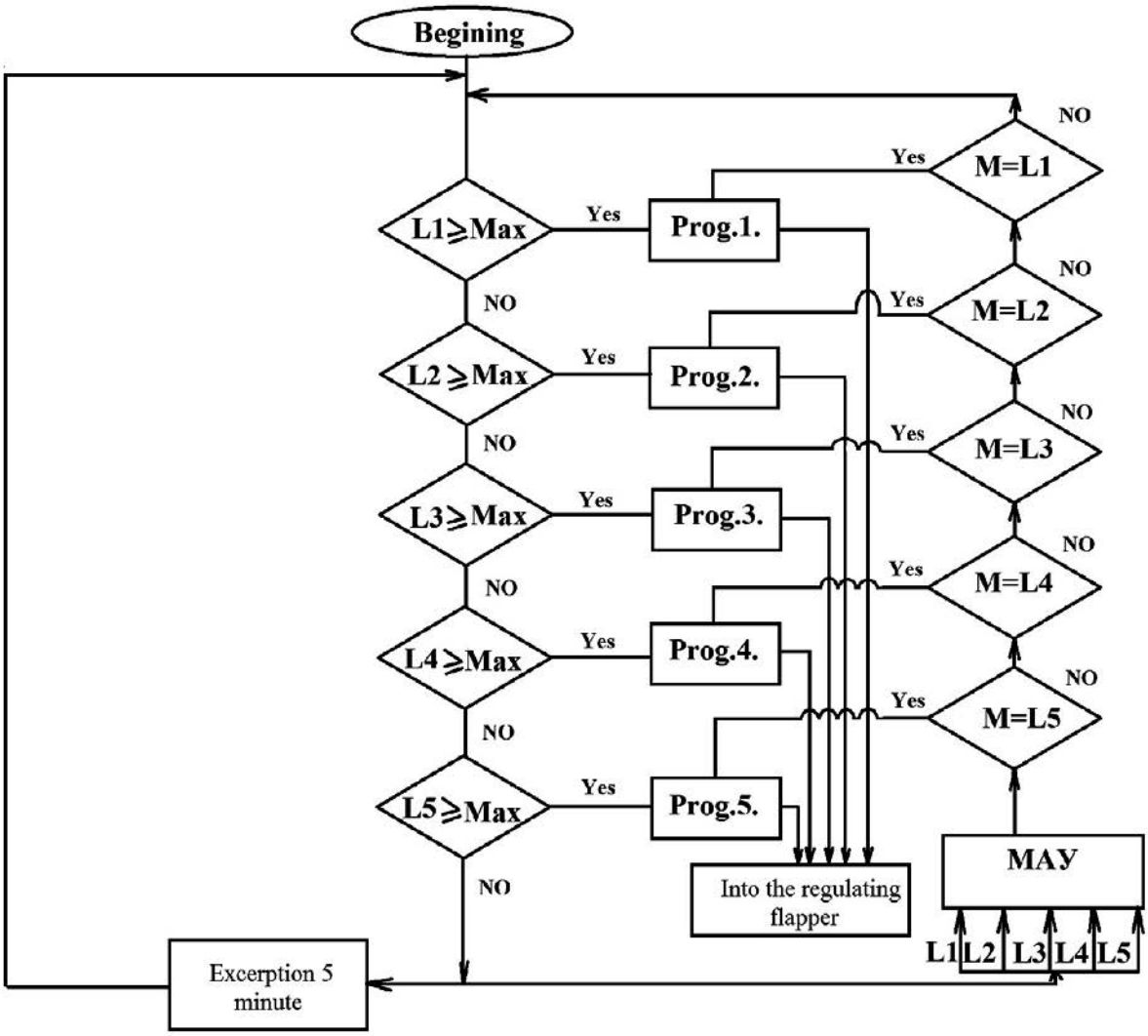

Fig. 4. Algorithm of management of an automated control system for an air separation process in a fluidizated layer

References:

1. Yusupbekov N. R., Igamberdiev H. Z., Bazarov M. B. Modeling and control of industrial-technological systems with parametrical indeterminacies of interval type. II. Interval estimations of parameters of models of operated plants//The chemical process engineering. Control and Management. – Tashkent, 2008. – No. 4. – P. 74–78.
2. Yusupbekov N. R., Nurmukhamedov H. S., Zokirov S. G. Main processes and devices of chemical technology – Tashkent, Teacher, 2003. – 557 B.
3. Formalization of mathematical model of process of air separation of loose materials/D. T. Karabaev, B. I., Yunusov, A. A., Artikov./Sixth, World Conference on Intelligent Systems for Industrial Automation. – Tashkent, Uzbekistan November 25–27, 2010.
4. Pneumoseparation process computer modeling of the crushed ore in a fluidizated layer/B. I. Yunusov., D. T. Karabaev A. A. Artikov./Seven, World Conference on Intelligent Systems for Industrial Automation. – Tashkent, Uzbekistan November 25–27, 2012.
5. Determination of speeds of fluidizated separation of loose materials./Yunusov B. I., Karabayev D. T., Artikov A. A./ТашГТУ, Chemical technology. Control and Management. 2/2011.

Yunusov Bokhodir,
senior teacher chair
«Informatics, automation and managements»,
Tashkent chemical institute of technology,
Tashkent, Uzbekistan
E-mail: Ulug85bek77@mail.ru

Theorethical bases of process of an air separation of loose materials in a fluidizated layer

Abstract: In this work on the basis of the multistage system analysis the computer model of process of an air separation of loose materials in a fluidizated layer is constructed. The recommended technique allows to investigate separation conditions in a fluidizated layer of easy and heavy components of loose materials.

By consideration of the criterial equations of Archimedes and Reynolds, options of creation of a fluidizated layer and questions of determination of speed of ablation of particles are defined. The interrelation of distribution of density of a separated material from diameter of particles that allowed to define a air separation zone with use of a fluidizated layer is defined.

On computer model calculations of an air separation of a loose material with various density are made.

Keywords: multistage system analysis, mathematical model, computer model, air separation, speed fluidization beginning, speed of ablation.

Process of enrichment of non-ferrous ores, precious and rare metals, is an important link in production of metals. The researches which have been carried out in recent years showed on possibility of realization of more economic and simple way of air separation of loose materials [1; 2].

Emergence of computer programs allowed to carry out exact modeling of technological process of an air separation, to reveal the narrow ranges of modes providing the best separation of a material. It is known that ore consists of joints of a set of minerals which have various density. By research of process of an air separation of loose materials on its mathematical model it is possible to define the dependences reflecting nature of change of the sizes of particles at various design data of a separator, to determine consistent patterns of change of target concentration of useful components as a part of ore depending on the geometrical sizes and density of particles, and also the constructive sizes of the device [3–5].

Development of theoretical bases of an air separation allowed to investigate process of an air separation of loose materials on its mathematical model and to define regularities of change of target concentration of useful components as a part of ore depending on the geometrical sizes and density of particles, and also the constructive sizes of the device.

Installation of a fluidizated separating (Fig. 1.) consists of the following several elements: the compressor 1, the needle gate 2, rotameter 3, the device of a fluidization 6, cyclones 8 and collections for the besieged materials 9. In the bottom flange 5 the grid previously is established. The capacity of an air separation is connected to the cyclones 8, serving for catching of easy components of ore.

Installation works as follows: test of a separated material, load into the device of a fluidization and then the upper flange 5 is densely closed with the help of rubber laying, bolts and nuts (4 and 7). At the closed needle gate 2 the compressor 1 turns on and slowly opening by means of the gate 2 air in the device of a fluidization 6, the consumption of air on parameter 3, the beginning of a fluidizated corresponding to speed for particles with certain sizes and density of particles is established.

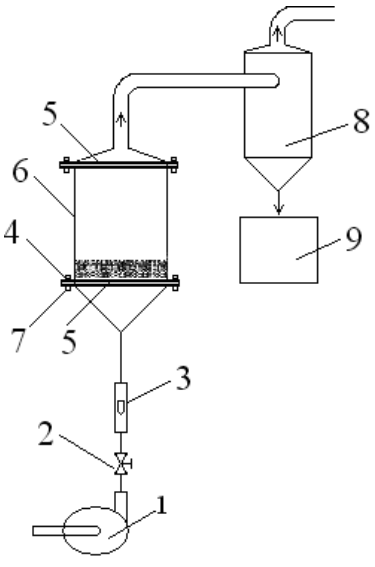

Fig. 1. Scheme of an air separation of loose materials

The material under the influence of air is given in a condition of a boiling layer. From a boiling layer consistently are carried away in cyclones 8, easy components, and in a fluidizated layer there are heavy components.

The main device here is the device with a fluidizated layer. If at the first stage of the multistage system analysis the system is dismembered on the elements considered above, and the device with a fluidizated layer also is dismembered on a number of elements: gas supply, grid, zone of a fluidization and ablation zone. The zone of a fluidization is divided into two components: gas and firm phases. In turn, the firm phase consists of particles of the first, the second, the third etc. components (fig. 2).

Let's consider, what parameters are entrance, and what parameters define a condition of elements of installation, i. e. are target parameters.

Input parameters of object are: an expense of a firm material, concentration of a loose material, the sizes of firm particles, a consumption of gas, pressure in the device, concentration of studied components on an entrance. Target parameters: an expense of the enriched material, concentration of a component in the enriched material, a consumption of gas, concentration of studied components in gas.

In precisely the same way it is possible to define input and target parameters for each element of installation. Let's say for the compressor an input parameter is energy, and days off — an expense and pressure of gas.

Input parameters of a fluidizated layer are: expense of a firm loose material, concentration of a loose material, sizes of a loose material. Target parameters is the expense of the enriched material.

Entrance parameters of gas phase of a fluidizated layer: consumption of gas, concentration of a valuable component. Target parameters: consumption of gas, concentration of a valuable component and pressure.

The firm phase of a fluidizated layer is characterized: expense of a firm phase, concentration of a valuable component, in diameter of particles. As target parameters here act: an expense of the enriched material, concentration of a valuable component in the enriched material, an expense of the easy component which is carrying away with gas.

When modeling by input parameters of particles are: consumption of gas, speed of gas, density of particles and diameter. Target parameter of object is speed of particles [3].

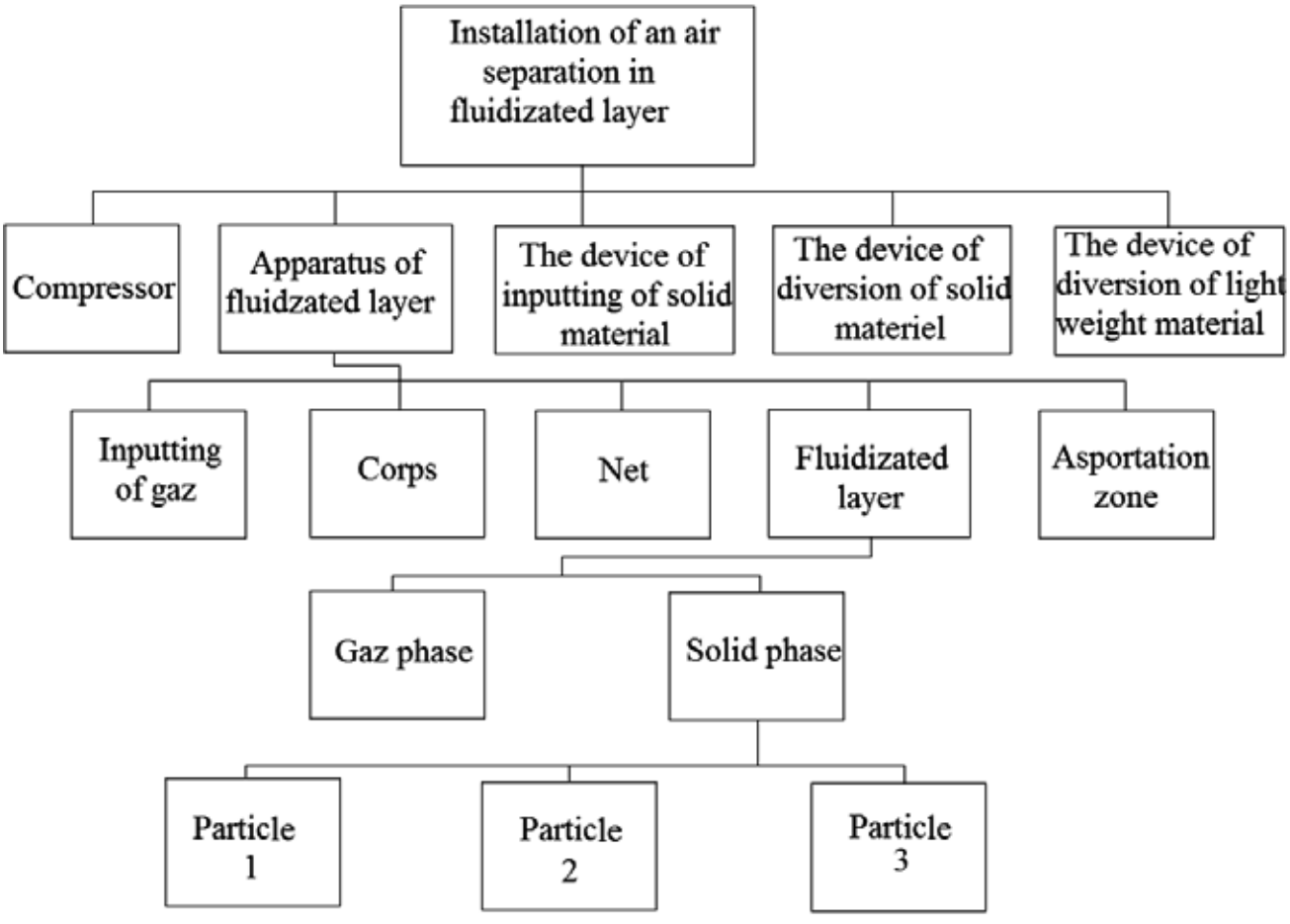

Fig. 2. Components and knots of installation of an air separating of loose materials in a fluidizated layer

Thus, having considered consistently all phenomena and the effects which are taking place in studied installation, it is possible to make mathematical model of process of an air separating of particles of a loose material in a fluidizated layer.

If to present that each particle of the crushed material has a sphere form, with the identical sizes, but different masses, the task consists in removal by means of an air stream of easy particles from a mix.

Each particle is influenced by the following two forces:

Force of weight of the spherical particle, operating with top down is equal:

$$F_1 = m_p * g \quad (1)$$

where m_p — mass of a particle, g — acceleration of a free fall.

The force created by an air stream, lifting a particle from below up is equal:

$$F_2 = \lambda * S * P_a * \frac{W^2}{2} \quad (2)$$

Where, λ — the factor expressing a turbulent or laminar mode, W — speed air a stream, P_a — density of air, S — the area of a spherical particle which the stream affects.

If the forces operating on particles, are equal each other, particles are in balance. Mathematical expression of this condition looks as follows:

$$F_1 = F_2$$

$$m_p g = \lambda * S * P_a * \frac{W^2}{2} \quad (3)$$

Where m_p — it is possible to replace mass of a particle m_p with the following equation:

$$m_p = p_p * V_p \quad (4)$$

Where P_p particle density, V_p — particle volume.

It was accepted that the particle has a form of a sphere and, considering that the volume of a particle is equal:

$$V_0 = \frac{4}{3}\pi * r^3 = \frac{1}{6}\pi * d^3 \quad (5)$$

And having substituted value V_p in the equation (4), and the received expression in the equation (3), we find:

$$\rho_p \frac{1}{6}\pi * d^3 * g = \lambda * \pi \frac{d^2}{4} * p_a * \frac{W^2}{2} \quad (6)$$

Solving this equation of rather equilibrium speed W, it is possible to receive the well-known equation [6]:

$$w = \sqrt{\frac{4}{3} * \frac{p_p * d_p * g}{\lambda * p_a}} \quad (7)$$

The form of particles of real disperse materials usually differs from the spherical. Such difference at mathematical modeling of technological processes is considered by means of geometrical factor of a form.

The maximum limit of this speed should not reach the speed deducing particles with heavy weight, i. e.

$$w_l < w < w_s$$

Thus, having calculated speed for the established border it is possible to carry out an air separation process.

Essential indicator of process of an air separation of ores of non-ferrous metals at enrichment is the office of heavy particles from a stream. It is reached by change of speed of a stream. Therefore it is necessary to know, at what speeds particles of heavy fraction are besieged. It depends on diameter of particles and their density.

At smooth increase in speed of a stream from 0 to some first critical value there is a usual process of filtering at which firm particles are not mobile.

To transition from a filtration mode to a mode of a fluidization there corresponds critical speed of a fluidization of W_{fl} called in the speed of the beginning of a fluidization. At the moment of the fluidization beginning the weight of the granular material falling on unit of area of cross-section section of the device, is counterbalanced by force of hydraulic resistance of a layer.

Since speed of the beginning of a fluidization and above, pressure difference in a layer $\varnothing P_l$ keeps almost constant value. This results from the fact that with growth of speed of the fluidization agent contact between particles decreases, and they receive a great opportunity for chaotic hashing in all directions. The average distance between particles thus increases, that is the fenestration of a layer ε and, therefore, its height of h increases ε.

For determination of the size W_{fl} there is rather large number of semi-empirical and theoretical dependences. At a formula conclusion the fenestration of a layer of motionless spherical particles can be accepted equal 0,4.

The top border of a fluidization condition corresponds to speed of a free ablation of single particles. It is obvious that at the speed of a stream surpassing speed of a ablation, $W_a > W_f$, will be there is an ablation of particles from a layer of a granular material.

On the other hand it is possible to consider classical methods of formalization of descriptions for calculation of process of an air separation of a loose material in a fluidizated layer

Processes of interaction of a gas phase with particles of a firm phase have special value. Considering disorder of the sizes of particles, the concept of equivalent diameter of particles is entered. It is supposed that particles have various values of diameters, changing from the minimum value of diameter to the maximum value. Proceeding from a percentage ratio of the sizes of the particles, equivalent diameter decides on the help of the equation

$$d_e = \frac{100}{\sum \frac{x_i}{d_i}} \quad (8)$$

If equivalent diameter is known, for determination of speed of the beginning of a fluidization it is necessary to determine Archimedes criteria by the equation:

$$Ar = \frac{d_E^2 * p^2 * g}{\mu^2} * \frac{p_s - p}{p} \quad (9)$$

Knowing Archimedes criterion, it is possible to define Reynolds's criterion for a fluidizated layer.

$$Re_{fl} = \frac{Ar}{1400 + 5.22\sqrt{Ar}} \quad (10)$$

It is also known that Reynolds's criterion for a particle is defined by the classical equation on which it is possible to determine speed of a fluidization of gas by the equation:

$$Re = \frac{w_{fl} * d * p}{\mu} \qquad w_{fl} = \frac{Re * \mu}{d * p} \quad (11)$$

Also settlement equation of criterion of Reynolds for a case of an ablation of particles is known:

$$Re_f = \frac{Ar}{18 + 0.575\sqrt{Ar}} \quad (12)$$

Taking into account the equation (12), according to the classical equation of criterion of Reynolds, it will be possible to define speed an ablation of particles, that is speed of ablation of a particle.

$$w_f = \frac{Re_f * \mu}{d * p} \quad (13)$$

This equation gives the chance to define speed and a consumption of gas for providing a fluidization, or ablation of particles. Varying diameters of particles it is possible to define a consumption of gas for material separation with various density.

Using the known equations of calculation of criteria of Archimedes, Lyashchenko and Reynolds the equations for calculation of speeds the fluidization and ablation beginning for particles of different density and are chosen the sizes and on their basis the computer model of process of an air separation of firm particles in a fluidizated layer, with use of a package of the MATLAB program (the Fig. 3 is constructed.).

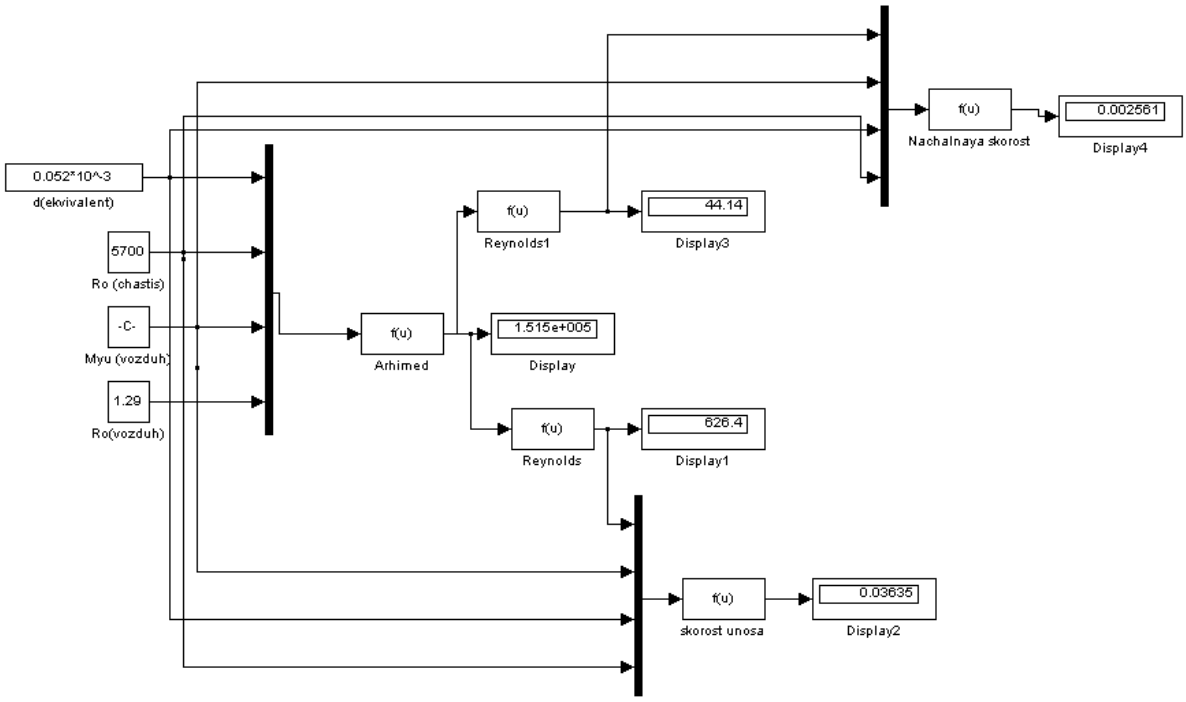

Fig. 3. Computer model of process of an air separation of firm particles in a fluidizated layer.

Calculations of speeds depending on diameter and density of particles carried out the fluidization and ablation beginning for minerals of SiO_2, Al_2O_3, K_2O, CaO, MgO, TiO_2, FeO and Fe_2O_3 being in ore. In the crushed ore each particle too consists of joints of minerals. In particles it is more than one mineral and it is less than other minerals. Therefore, the particles containing heavy components will be heavier. With reduction of the sizes of particles, influence of minerals of heavy components on all of a particle will be more.

On computer model (fig. 3) changes of speeds the fluidization beginning (fig. 4) and ablation (table 2) depending on the size of particles of a separated loose material and density are calculated.

The analysis of the received results shows that at the big sizes of particles 0.060÷0.080 мм, the limiting sizes

of particles providing a good separating increase till seven and nine sizes of particles. It is possible to note that for ore enrichment with the sizes of particles in a range 0.010÷0.030 мм, the limiting sizes of particles providing a good separation are in limits of one, two and three sizes of particles. On the other hand, at smaller diameters of particles of influence of the maintenance of an enriched material (heavy components) on particle density it is more than at big diameters of particles.

On computer model calculations of speeds the fluidization and ablation beginning depending on diameter are made and density of particles for ore test which structure is presented in table 1.

Considering it, we recommend to carry out ore enrichment in a range of the crushed particles from 0.030 мм till 0.050 мм (fig. 5) where the limiting sizes of particles providing a good separation are in limits from 0.030 мм till 0.034 мм, from 0.034 мм till 0.039 мм, from 0.039 мм till 0.044 мм and from 0.044 мм till 0.050 мм. Thus, ore enrichment in this range will need four installations with a fluidizated layer.

Table 1.

№	Component	Mass fraction of %	DensityKg/m^3	№	Component	Mass fraction of %	Density Kg/m^3
1.	Al_2O_3	13,31	3990	8.	K_2O	3,97	2320
2.	SiO_2	67,52	2650	9.	Na_2O	0,14	2390
3.	TiO_2	0,41	4505	10	CaO	1,55	3370
4.	Fe_2O_3	4,49	5240	11	P_2O_5	0,19	2390
5.	MgO	0,60	3580	12	$S_{общ}$	3,45	
6.	MnO	0,06	5460	13	H_2O	0,42	
7.	FeO	1,62	5700	14	п. п.п	2,52	

Dependence of speed of ablation on diameter and type of particles

Table 2.

Diameter of particles	Speed of ablation depending on diameter and a type of particles								
	Au	FeO	Fe_2O_3	TiO_2	Al_2O_3	MgO	CaO	SiO_2	K_20
0.000030	0.301	0.092	0.085	0.073	0.065	0.058	0.055	0.044	0.038
0.000031	0.319	0.098	0.090	0.078	0.069	0.062	0.059	0.046	0.041
0.000032	0.339	0.104	0.096	0.083	0.073	0.066	0.062	0.049	0.043
0.000033	0.358	0.110	0.102	0.088	0.078	0.070	0.066	0.052	0.046
0.000034	0.378	0.117	0.107	0.093	0.083	0.074	0.070	0.055	0.049
0.000035	0.398	0.123	0.114	0.098	0.087	0.079	0.074	0.059	0.051
0.000036	0.419	0.130	0.120	0.103	0.092	0.083	0.078	0.062	0.054
0.000037	0.440	0.137	0.126	0.109	0.097	0.087	0.082	0.065	0.057
0.000038	0.462	0.144	0.133	0.115	0.102	0.092	0.087	0.069	0.060
0.000039	0.484	0.151	0.139	0.120	0.107	0.096	0.091	0.072	0.063
0.000040	0.506	0.158	0.146	0.126	0.112	0.101	0.095	0.076	0.067
0.000041	0.528	0.166	0.153	0.132	0.118	0.106	0.100	0.079	0.070
0.000042	0.551	0.173	0.160	0.138	0.123	0.111	0.105	0.083	0.073
0.000043	0.575	0.181	0.167	0.145	0.129	0.116	0.109	0.087	0.076
0.000044	0.598	0.189	0.174	0.151	0.134	0.121	0.114	0.091	0.080
0.000045	0.622	0.197	0.182	0.157	0.140	0.126	0.119	0.095	0.083
0.000046	0.646	0.205	0.189	0.164	0.146	0.132	0.124	0.099	0.087
0.000047	0.670	0.213	0.197	0.171	0.152	0.137	0.129	0.103	0.090
0.000048	0.695	0.226	0.205	0.177	0.158	0.143	0.135	0.107	0.094
0.000049	0.720	0.230	0.213	0.184	0.164	0.148	0.140	0.111	0.098
0.000050	0.745	0.239	0.221	0.191	0.170	0.154	0.145	0.115	0.102

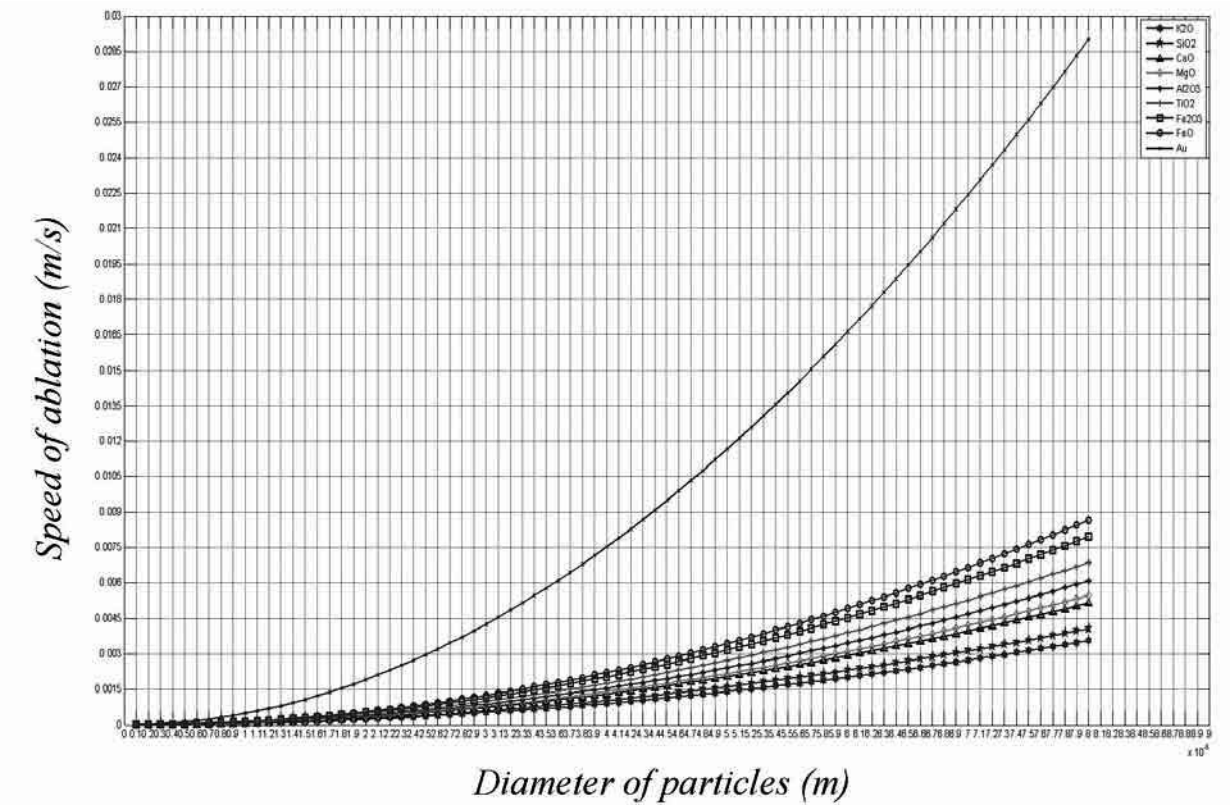

Fig. 4. Dependence of speed of the beginning fluidization from diameter and a type of particles

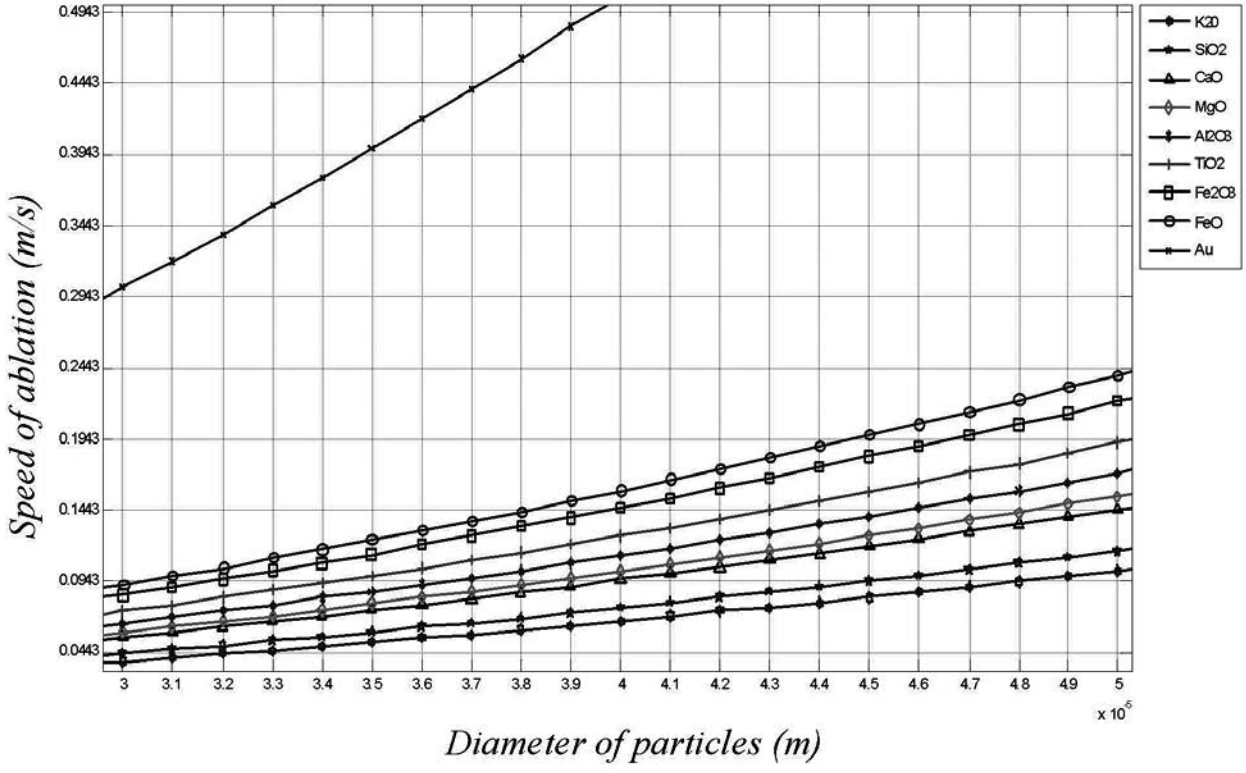

Fig. 5. Dependence of speed of ablation from diameter and a type of particles

The technological scheme on processing of ores according to the scheme of preliminary enrichment and separation in a psevdoozhizhenny layer is offered.

Crushed till certain sizes and the ore sifted on sets, in limits from 0.030 мм till 0.034 мм, from 0.034 мм till 0.039 мм, from 0.039 мм till 0.044 мм and from 0.044 мм till 0.050 мм, moves in four separate capacities. Further, sandy pumps, the loose material moves in separate installations of a multistage air separation in a fluidizated layer where there is a separation of a loose material.

References:

1. Lebedev I. F. Research of processes of division of minerals of various density in an air-sand stream and development of new devices of an air separation the dissertation Author's abstract on competition of a scientific degree of Candidate of Technical Sciences. – M. – 2008.
2. Matveev A. I., Vinokurov V. P., Fedorov V. M. Prospects of application of modular mobile ore enrichment installations. – Yakutsk: Publishing house of YaNTs of the Siberian Branch of the Russian Academy of Science, 1997. – 120 p.
3. The system analysis of a pnevmoseparirovaniye of loose materials in fluidizated layer/Yunusov B. I., Karabayev D. T., Artikov A. A./ТашГТУ, Chemical technology. Control and management. 2/2011.
4. Determination of speeds of fluidization separation of loose materials./Yunusov B. I., Karabayev D. T., Artikov A. A./ТашГТУ, Chemical technology. Control and management. 2/2011.
5. Kasatkin A. G. Main processes and devices of chemical technology. – M: Chemistry, 1971. – 784 p.

Section 5. Physics

Zlobin Igor Vladimirovich,
Higher Technical School «SETMO»,Senior Researcher,
Department of hardware and software support
to the computer centre
E-mail: igor.zlobin@kolumbus.fi

The question of orientability in Time

Abstract: In the article the Hawking and Ellis problem (the question of connectivity at orientability in Time) is considered. For this purpose, we introduce such concepts as: 1) current of Time j_i; 2) function T, in terms of Space-Time; 3) phase angel of Time Ψ_z. In the article the mechanism of correlation between the local currents of Time is described and the hypothesis about mathematical operator generating extrapolation of values of the phase angle to the local currents of Time is stated.

Keywords: Time, Hawking, current, phase angle

1. Introduction

It follows from the postulate on local causality [4], that you can send a signal from one point r of the manifold M (we consider the manifold M connected as there is no information on disconnected parts accessible to us) to the other r' when and only when these points can be connected by not space-like geodesic curve. The concept of manifold responds directly to our ideas of Space-Time continuity. As a matter of fact, the structure of Space-Time is the manifold M allotted with Lorentzian metric and affine connectivity determined by it. The question of orientability in Time is closely connected with the condition of local causality. Here and elsewhere we will write the terms Time, Future, Past and Present capitalized, where they are used with the meaning of real physical objects. Our attention is drawn to the work [1] in which the expanded definitions of the three last-mentioned temporal parameters are given from the point of view of their topological morphogenesis.

If we consider an region of Space-Time Y which is a subset of varieties M ($Y \subset M$), on which the "arrow" of Time [4] is strictly connected with the entropy increment of the quasi-isolated thermodynamic systems, then it may be expected that at each point of $f_i f_i \in Y$ of this region there exists a priori a local "arrow" of Time specified not by an asymptote. For convenience of mathematical analysis of the problem raised in this article we will introduce instead of the term "arrow" of Time a new physical parameter: current of Time. We will denote it with a symbol: j_i. Then it is possible to formulate such definition.

1 Definition

Current of Time j_i is a temporal current representing such period of time Δt, which is defined by stable Time of existence of the randomly chosen material body from the moment of its formation t' until the moment of its decay t''.

From this definition it follows logically that the current of Time j_i is equivalent to Δt, $j_i \sim \Delta t$ and, besides, the following fundamental conditions must be carried out at all times and in all places:

$$\begin{gathered} \Delta t \in [t', t''] \\ \Delta t = [t'' - t'] \\ t'' > t' \\ \Delta t \neq 0 \end{gathered} \qquad (1)$$

So far, the mechanism of the established relationship between the currents of Time in various regions of Space-Time is not quite clear from the physical standpoint. Stephen W. Hawking and George F. R. Ellis have defined this problem rather consistently. Hereafter we will refer to the initial problem as the Hawking and Ellis problem to simplify consideration. This problem is formulated as follows, hereafter according to text: "… It is not quite clear what the relationship is between this "arrow" and the other "arrows" defined by the expansion of the universe and by the direction of electrodynamic radiation…" [4].

2. Analysis of the Hawking and Ellis problem.

This solution of Hawking and Ellis problem will be constructed on the basis of several other conceptual

suggestions rather than those presented in [4]. First of all we will consider the questions connected with temporal aspects.

The Universe, in general, can be considered as global thermodynamic system evolving, both in space and in time. As previously noted, the thermodynamic system of any kind is characterized by entropy, and thus by the strictly set direction in Time. Representing the Universe in the form of a complex multiply connected topological manifold M it is reasonable to suggest that the interior *int M* of this structural formation is filled with the sum of events $\Sigma\, G_n$ of all material bodies. Any event G_n as a physical phenomenon is characterized by the fact that it is happening in Time. Consequent alternation of the set of events is also strictly determined by and complies with causal chronological postulates. Whereby the statement disclosed earlier in [4] is valid: in physically realistic judgements the condition of causality and the chronological condition are equivalent. In accordance with the abovementioned it seems physically reasonable to formulate such suggestion

2.1 Assumption

The beginning of inflation of the Universe [2] and its subsequent evolution in time is directly proportional to the function T acting as a transcendental type of Space-Time [1].

It is needed to introduce function T and relate it to the Universe and therefore with the manifold M (Picture 1) to it is necessary in order to fulfil the stable causality condition [4] that is written as follows: stable causality is identified everywhere in M if and only if the function T, the gradient of which is timelike everywhere, i. e. the metrics g is negative

$$X \in D_p \Rightarrow \exists g(X; X) < 0 \qquad (2)$$

where g is the Lorentzian metric, X is the non-vanishing vector, p is the element of M, where the non-vanishing vector X is timelike, $g(X; X)$ is the scalar square, D_p is space, representing the set of all directions in p, and which are identified as tangents to M vector spaces in p. The function T on the manifold M extrapolates as the Space-Time of the Universe, in the sense that it ascends along each not spacelike curve directed to the Future, therewith $T \in M$ [4]. It is not difficult to notice that T reflects such current of Time of the Past to the Future at which all events G_n along the timelike curve h are determined according to the cause-and-effect relations. By curve h we mean the curve of non-zero extent, besides one point cannot be considered as a curve.

As noted above the interior of the Universe is predicted as a conglomerate of a vast number of material bodies, each of which can be compared to one-to-one correlation in the form of local timelike currents of Time j_i. This model lets us note that in the *int M* there is i number of bodies, for which the condition of bijection of *int M* is satisfied: $i \to j_i$. In this regard, it is not difficult to notice that from the physical standpoint the borders of Space-Time can be expanded continuously, i. e. now function T consists mainly of the integrated additive local currents of Time. It follows that an adequate local current of Time will be found to each material body in the Universe.

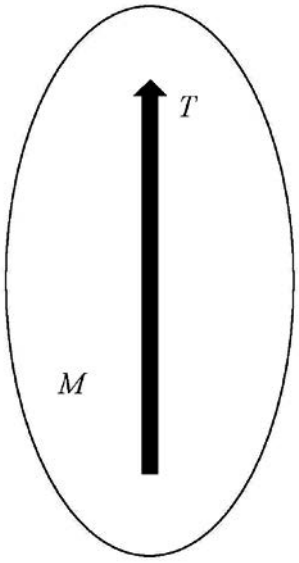

Picture 1. Space-Time *T* mapping onto manifold *M*

Considering this criterion we can write down that the function T is nothing but sum of finite number of local currents of Time (Picture 2).

$$T = \bigcup_i j_i \qquad (3)$$

In the context of the axiomatic analysis it is clear that in case at a certain point of time we have two homogeneous systems, for example, two bodies, comparable by their nature (their physical, chemical, geometrical, etc. properties are identical), then they can have absolutely identical local currents of Time. Please note that such option can be realized only in ideal conditions. And, on the contrary, if two chosen material bodies completely differ according to all the physical characteristics, then their local currents of Time can't be identical. These days, when the Universe is in a dynamic state, it is very difficult to allocate two and more material bodies strictly equivalent to each other in all parameters. And this also causes that in the interior of Space-Time T there is no orientation between local currents of Time j_i that would be connected accurately and systematically. And this also causes that in the interior of Space-Time T there is no orientation between local currents of Time of j_i that would be connected accurately

and systematically. It will be shown below that actually there is a certain physical mechanism that can distinguish descriptively the correlation between one single local current of Time and other local currents. As a matter of fact, one of probabilistic solutions of the Hawking-Ellis problem is formulated a priori.

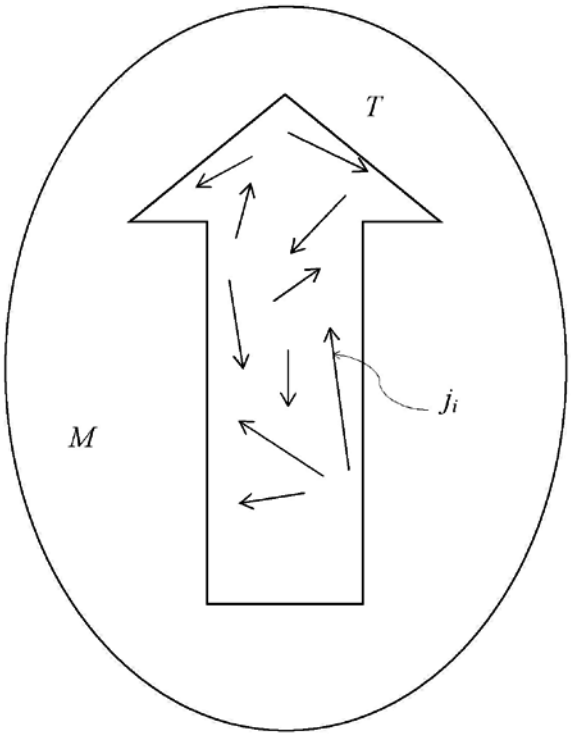

Picture 2. Distribution of local currents of Time j_i as projection on to Space-Time T

Let us assume that in some (already mentioned above) region of Space-Time Y, there are two material bodies U and V, chosen so that they would interact with each other in a certain way. These bodies are chosen so that they don't belong to the same type. It is understood that their physical properties and parameters are heterogeneous. Due to the fact that these bodies influence each other, despite different orientation of their local currents of Time j_U and j_V, functional and physical connection between them still remains. The question is in finding this connection, i. e. it is required to reveal such calibration parameter that would allow establishing correlation between initial local currents of Time.

For solution of this problem it is appropriate to carry out the following mathematical transformations:

1) local currents of Time j_U and j_V are situated relative to each other in such a way that their reference points coincide in point — 0. Theoretically this point represents a pole, such that

$$\{0 \in j_U \cap j_V\} \leftrightarrow \{0 \in j_U\} \wedge \{0 \in j_V\} \qquad (4)$$

2) let us assume that one of the local currents of Time, for example j_U, is set parallel to Space-Time T, $j_U \| T$. Then, local current of Time j_V of the material body V will be oriented in relation to j_U at a certain angle (Picture 3).

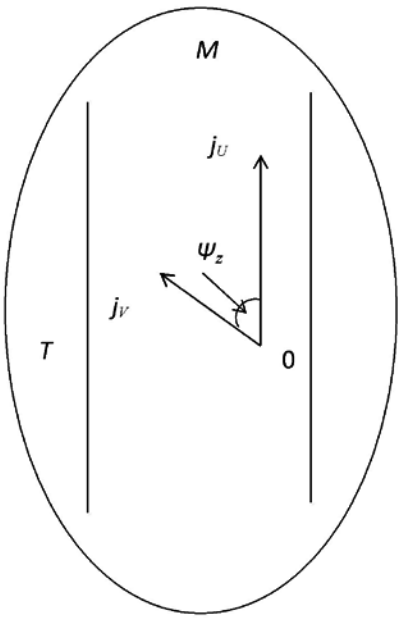

Picture 3 Relative positioning of local currents of Time in a segment of Space-Time with the allocated phase angle of Time

From gnoseological standpoint this is a very important conclusion. Indeed, according to paragraphs 1) and 2) the oriented mapping of local current of Time j_V onto local current j_U can be carried out by means of angular parameter. Let us designate this parameter as *phase angle of Time* and denote it with Ψ_{z_i} then we can write down the following:

$$\Psi_z : j_V \to j_U \qquad (5)$$

where Ψ_z is mapping j_V at $\Psi_z(j_V) \to j_U$.

Index z is needed to allocate this angle from the class of basic geometrical angles. First assumption of possible existence of phase angle of Time has been stated in the article [3].

2.2 Assumption

Phase angle of Time Ψ_z is the angle between local currents of Time j_i (brought to one pole) that identifies connectivity at orientability in the interior of Space-Time T.

It is clear conceptually that numerical borders of the phase angle of Time Ψ_z have variational values. Indeed, basing on the analysis methods applied in mathematical morphology, we define that for a particular configuration of two specific local currents of Time the value Ψ_z is strictly individual and is characterized only by the local currents of reference.

Let us adapt the techniques of mathematical induction to the analysis of system, in which i — number of local currents of Time accumulates. For this purpose let us

take as the frame of reference any of Time currents, and provided that we use the phase angle of Time, it is elementary to determine functional connection (orientability) between the local current of Time of reference and other local currents. Thus, clear probability of understanding of the proceeding processes in Space-Time T with due account for orientation of local currents of Time j_i relative to each other is generated.

Summarizing all the above-mentioned we can draw the following conclusion: Hawking and Ellis problem is solved sufficiently precise in case it is summed up to finding values of phase angle of Time. As angles are measured in degrees or radiant, specific numerical interpolation of these angles is high-priority. it should be also remembered that the algorithm of getting a nonabstract number included in value of the variable Ψ_z correlates with existence of a certain mathematical operator explicitly. The issue of this operator is the key aspect and it also need to be worked out, however doing that within this article is to soon. Further analysis will be made in the subsequent researches. The top priority is verification of the hypothesis of local currents of Time offered in this article.

3. Conclusion

The case considered in this article demonstrates that for solution of the question of connectivity at orientability in Time, it is necessary and sufficient to define the angular characteristic distinguished as a phase angle of Time Ψ_z. The imperative of such mathematical operation is due to the fact that in the inflation Universe it is functional to connect certain temporal regions to each other.

References:

1. Guth A. H., P. J. Steinhardt The Inflationary Universe//V Mire Nauki (In the Science World). – 1984. – № 7. – P. 56–71.
2. Zlobin I. V. Perspective aspects of elaboration of physical and topological concepts on time//European science. – 2016. – № 3 (13). – P. 13–24.
3. Zlobin I. V. Time factor in immanent essentiality of the Universe//Philosophy and cosmology. – 2016. – Vol. 16. – P. 13–24.
4. Hawking S. W., Ellis G. F.R The large scale structure of Space-Time. Cambridge University Press, 1973.

Kaganov William Ilich,
Institute of Radio Engineering
and Telecommunication Systems,
Moscow University MIREA
E-mail: Kaganovwil@yandex.ru

Protection from icing of contact networks railway and tram transport with the help of microwaves

Abstract: Basics of a new method of struggle with icing contact networks wires is discussed. It is shown as a group of waveguide radiators could create a powerful microwave electromagnetic field over fast-moving locomotive or tram. This field will melt the layer of icing on the contact wire.

Keywords: icing, contact wire, microwave radiation, waveguide antenna, antenna array.

1. Introduction. One of the natural phenomena, which negatively affect the functioning of technological systems, is the formation of an ice layer on the metal objects during freezing cold drops of rain or mist. This ice, called icing, occurs under certain weather conditions — ambient temperature between 0–5 °C and high humidity. Icing is a particular danger for industrial sites, the most important element of which is the exposed metal wires of great length. These objects include contact-electric network of rail and tram transport. The consequence of the ice layer is a significant increase in weight contact wires, which leads to their sagging, rocking and even breakage. Also because of the icy conditions significantly affects the communication between the contact wire and pantograph, causing arcing and firing it wires. The result is a reduction in the speed of trains and trams to a complete standstill, and frequent replacement of expensive graphite current collectors.

Use the following method for de-icing: electrical mechanical and chemical.

The first method is the elimination of icing is used, for example, on the high-speed line Paris – Lyon [1]. In this case, 600A current from power voltage 26 kV is passed along the contact wire. Wire at a power of 600 W/m density is heated to +(10 –15) °C and the ice gradually melted.

Chemical protection method catenary ice by using special deicing fluid.

It can be noted that the effective methods and means for de-icing of wires contact network does not exist. It is therefore proposed to consider a fundamentally new method of protection against icing rail and tram transport by means of microwave electromagnetic waves, remote heating wires without touching them.

2. Heat water by electromagnetic field

Let us first consider the physical mechanism of the rapid heating of water under the influence of microwave electromagnetic radiation.

Asymmetrical structure of the water molecules results in the polarization of the electric charge. Therefore, the water molecule is an electric dipole (Figure 1), having a dipole moment [2]:

$$p = ql, \quad D = C \cdot m \qquad (1)$$

where of q – charge, l – length of the dipole, D = 3,335·$\cdot 10^{-30}$ C·m – a unit of dipole moment, called the Debye.

Dipole moment of one molecule of water: p = 1.87 D = 6.24·10^{-30} C·m.

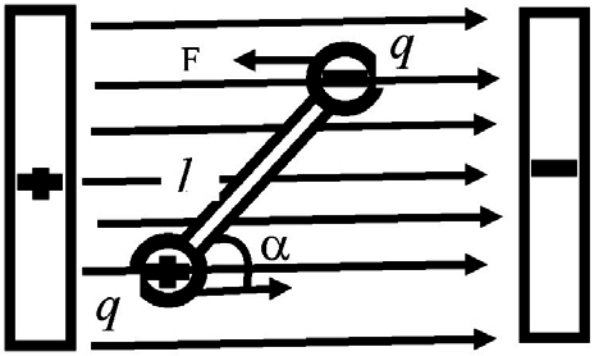

Fig.1. The water molecule in the form of a dipole

Water molecules are arranged randomly in the absence of an external electric field and aligned in one direction, if available. The water molecules under the influence of high-frequency electromagnetic fields are rotated in one direction and then in another direction. The work performed by a single molecule of water in this rotation (Figure 1) for one second:

$$W_L = \int_0^{\pi} qlKE\sin^2\alpha\, d\alpha = \pi\, ql\, f\, E \approx 2\times 10^{-20} f\, E\,[J], \qquad (2)$$

where $K = 2f$ – number of rotations of the molecule in one second, f – frequency electromagnetic field oscillation in GHz; E – is the electric field strength, V/m.

According to the molecular-kinetic theory it is quick, intense motion of the molecules leads to an increase in body temperature. This process is most intense at certain resonant frequencies characteristic of each substance. For water this is one of the resonance frequencies f = 2450 MHz. (It is at this frequency tuned magnetrons in domestic microwave ovens).

At a frequency of f = 2450 MHz and the field strength E = 10 kV/m in accordance with (2) the energy of one of the polarized molecules under the influence of microwave electro-magnetic fields will be 5 10^{-16} J. Millions of such rotating molecules and lead to a rapid, remote heating water. The total energy of the electromagnetic field energy conversion into heat

$$W_{\text{н}} = c\, m\, \Delta T = P_G\, k_{\text{т}}\, \Delta t\ , \qquad (3)$$

where c – thermal capacity of the material taking into account the dipole moment, m– mass of the heated body, ΔT – temperature of heating of the body relative to the ambient temperature, P_G – power of generator irradiating the object, Δt – time of heating, k_T < 1 – coefficient that determines the power of the generator, consumed for heating of the body.

3. Irradiation of the contact wire of the microwave electromagnetic wave

For liquidation the ice layer on the wire is required to generate the electromagnetic field of a certain power over the roof of the locomotive or tram As a result of the under the influence of electromagnetic radiation of the ice will melt quickly. The electromagnetic field may be formed by a certain group of directional type emitters In this case, the best option is a rupornaya antenna or a simple option in the form of an open waveguide with excitation basic wave λ <2a and λ <2b (Figure 2) [3].

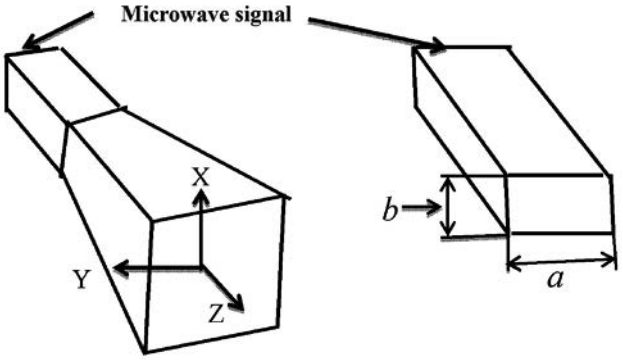

Fig.2 Antenna: rupornaya and as in the form of an open waveguide

Choose a waveguide variant for which the antenna pattern in the planes x-y and x-z defined by the expressions:

$$H(x)=\left|\frac{\cos\left(\pi\left(a/\lambda\right)\sin x\right)}{1-\left(2\left(a/\lambda\right)\sin x\right)^{2}}\cdot\frac{1+\cos x}{2}\right| \qquad (4)$$

$$E(\mathrm{y})=\left|\frac{\sin\left(\pi\left(b/\lambda\right)\sin \mathrm{y}\right)}{\pi\left(b/\lambda\right)\sin \mathrm{y}}\cdot\frac{1+\cos \mathrm{y}}{2}\right|, \qquad (5)$$

where x, y — angle in degrees relative to vertical.

Graphs of these functions for $a=\lambda$ and $b=\lambda$ built in Figure 3.

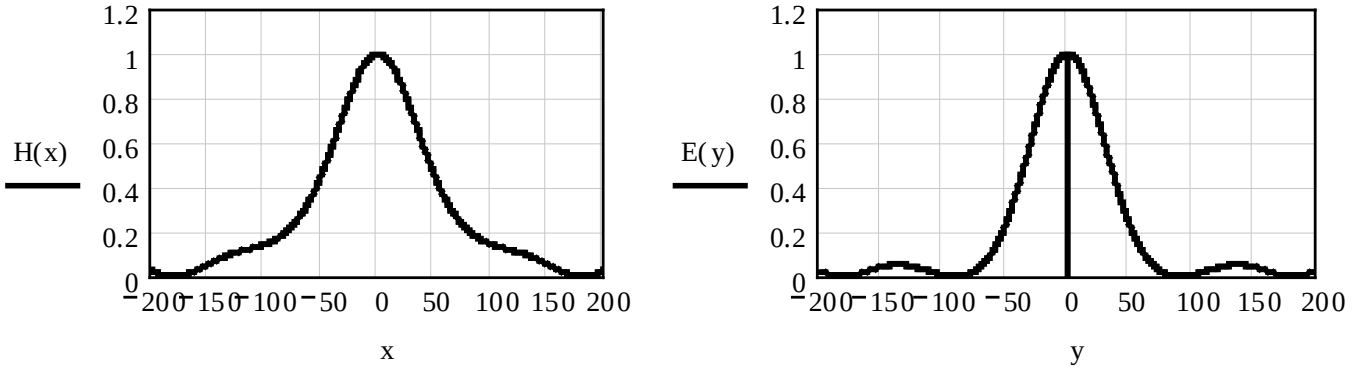

Fig.3. The antenna pattern waveguide radiator

4. The antenna array on the roof of the locomotive

When placing the emitters on the roof of the locomotive or trams should take into account two factors: the curved form of the trajectory of the trolley wire and change the height of the wire with respect to the rail. It is necessary to ensure the constancy of the clearance of 10–15 cm between the contact wire and the edge emitters. Therefore, the radiators are arranged on a special platform associated with a pantograph. This design provides a constant gap.

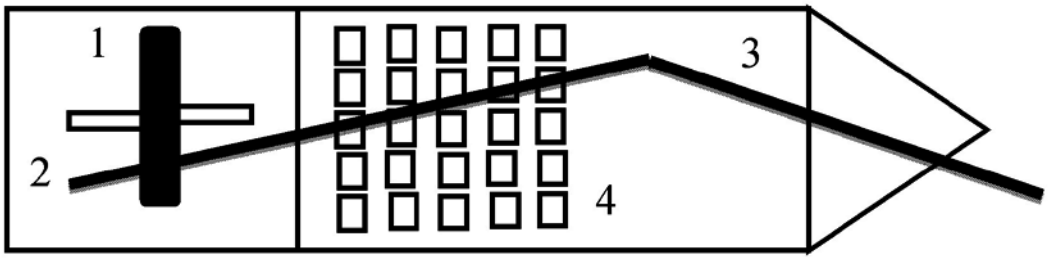

Fig.4. Model Microwave installation of (top view). 1. Grafitovy current receiver 2.Pantograph. 3. Contacty wire 4. The waveguide emitters

At the platform should be arranged in groups of N emitters, creating an antenna array. Number of $N\geq 25$ (Figure 4). Thus, the electromagnetic field is produced over moving locomotive. It drives "field — cloud" melts ice on the contact wire.

5. The laboratorny experiment

Photo of laboratory setup, made based domestic microwave an oven with magnetron power 800 W and frequency 2450 MHz, is shown in fig.5. Irradiation was subjected to the contact wire, spaced at a distance in front of the magnetron 0,2m.. On the contact wire arranged cylinder with a mass of 120 g of water and a thin layer of ice.

The purpose of the experiment: determination of water heating time and melting ice. The result: water heating time to 20 ° K was 60c, the melting of ice — does not exceed 50 c

Thus, the idea of remote heating icing on the contact wire by means of microwave irradiation has been confirmed experimentally.

Fig. 5. Photo of the laboratory setup

6. Full-scale experiment

For industrial application the considered method of struggle against icing on contact wires is necessary to conduct a full-scale experiment. The locomotive must be equipped with a certain number of irradiators and magnetrons frequency 2450 MHz. This frequency according to "Radio Regulations" is designed for use in industrial installations.

This experiment will determine the required power of magnetrons and the number of irradiators depending on the speed of movement of the locomotive and icing at wires. The required total power of radiation of contact wires to melt the layer of icing is calculated by the formula

$$P_{\Sigma} = K_{G} N P_{1} V , \qquad (5)$$

where N – number of irradiators, P_1 – the power delivered by the magnetron to a single irradiator, V – speed of the locomotive, K_G – coefficient determined experimentally during the tests.

The emitted signal is directed upward relative to a moving train. Therefore, only one protection is required on microwave irradiation — closing screen of bridges with help of a metal mesh

7. Conclusions. Developed basics of a new method of struggle against icing wires contact networks railway and tram transport with the help of microwave electromagnetic waves. It requires the creation of an industrial model and its full-scale tests.

References:

1. Menuet J. System of combat de-icing wires contact network. Revue Générale des Chemins de Fer, 2001, – № 4, P. 9–14.
2. Дергольц В. Ф. Мир воды. – Л., Недра, 1979.
3. Jackson J. Classical Electrodynamics. – New York, Wiley, 1975.

Section 6. Chemistry

Abdurakhmanov Ilkhom Ergashevich,
Applicant of the Department of analytical chemistry of the Samarkand state University
Uzbekistan, Samarkand
E-mail: ergash50@yandex.ru
Kabulov Bahadir Jabborovich,
Doctor. chem. sciences, Professor,
Tashkent technical University,
the head laboratories of State unitary enterprise "Science end progress" Uzbekistan, Tashkent,
E-mail: kabulov@rambler.ru

Study of the dynamic and calibration characteristics of semiconductor sensors of Ammonia

Abstract: Revealed a linear territory of the signal of a semiconductor sensor of ammonia provides the definition of concentration in a wide interval. It is found that increasing the concentration of iron compounds in the gas sensing material leads to higher performance sensors. At the annealing temperature of 550 °C response time of the sensor reaches 14 s.

Keywords: Sensor, ammonia, performance, dynamic and calibration characteristics.

The most correct and correct solutions to the task rapid and accurate determination of ammonia in air and process gases is the use of simple and available semiconductor sensors. In this regard, the development of highly effective semiconductor sensors for the determination of ammonia in the environment is an urgent issue. In [1; 2] studied a semiconductor sensor of ammonia.

The aim of this work is to study the dynamic characteristics and calibration of semiconductor sensors of ammonia.

Given the anticipated scope and high toxicity of ammonia, primary and satisfying conditions of use of the sensor should be time fast response. That is, the ammonia sensor should have good dynamic characteristics.

In environmental monitoring and control industrial emissions are usually measured the average concentrations of gas impurities. For such measurements is acceptable time constant of the sensor in tens of seconds or a few minutes.

The performance of the obtained thin cover samples with respect to ammonia was measured on the example of standard gas mixtures of ammonia in air at 200 °C. In the experiments we used the gas mixture (GM) with ammonia concentrations of 50–500 mg/m^3.

A test feature of the sensor of ammonia was accompanied by a continuous record of the transitional process diagram tape recording device KSP-4. The value of the gas sensitivity (S) of the sensor was calculated by the formula

$$S = R_0/R_{gas} \quad (1)$$

Where: R_0 — the electrical resistance of the cover in air in the absence of gas, R_{gas} is the electrical resistance of the cover when exposed to a predetermined gas concentration.

Simultaneously, we measured the response time ($t_{resp.}$) and recovery time ($t_{recov.}$) sensors based on films of gas sensitive material (gas sensitive material) of the composition SiO_2/TiO_2+5%Fe_2O_3, and SiO_2/TiO_2+10% Fe_2O_3.

In experiments, each test point in the measurement range was characterized by six values: three for forward and three for reverse cycle measurement.

The analytical signal of the sensor was monitored with a digital voltmeter V7–35 after the establishment of a constant value (not less than 1 min after the filing of the instrument standard mixtures).

The results of the study. The results of determining the dynamic characteristics of the SCS-NH_3 are presented in table 1.

Table.1. – The dynamic characteristics of the sensor based on the films SiO_2/TiO_2+10% Fe_2O_3 при the effects of ammonia. (T= 600 °C)

The dynamic characteristics of the sensor	*$t_{0,1}$	$t_{0,65}$	$t_{0.9}$	t_p
the response time of the signal S.	1	5	10	15
the recovery time of the signal S.	2	7	14	20

** $t_{0,1}$ — the start time of the response; $t_{0,65}$ — constant time, s; $t_{0.9}$ — time us-development of testimony, with; T_P — full total measurement time, with*

Research of gas sensitivity showed that the change in surface resistance of the cover in the direction of decreasing is observed within 10–15 seconds after receipt of ammonia in the measuring chamber.

Subsequent purging of the chamber with clean air that does not contain ammonia, the resistance returns to the original value.

It is established that the value of the gas sensitivity and $t_{response}$ and $t_{recovery}$ depend on the content of the catalyst in the gas sensitive material (GSM). (Table. 2.).

Table 2. – The dependence of response (sec.) sensor of ammonia from the content of the catalyst (Fe_2O_3) in the gas sensitive material annealed at 350 °C (the concentration of methane in the mixture 500 mg/m^3)

№	Composition sensitivity material	The response time of the sensor ($\tau_{response}$ or τ_{09}), sec.	The recovery time of the sensor ($\tau_{recovery}$ or τ_{01}), sec.
1	SiO_2/TiO_2	63	83
2	SiO_2/TiO_2+1%Fe_2O_3	55	61
3	SiO_2/TiO_2+5%Fe_2O_3	22	27
4	SiO_2/TiO_2+10%Fe_2O_3	16	21

With increasing content of iron oxide in the cover there is a decrease in response time. Recovery time for purging the measuring cell with air ranges from 15 to 22 sec. and decreases with increase in the concentration of iron oxide in the cover. Therefore, increasing the concentration of iron compounds from 5 to 10% leads to increase the performance of gas sensors in 1,2–1,4 times.

Based on the response time of a semiconductor sensor based on SiO_2/TiO_2+10% Fe_2O_3 50 mg/m^3 of ammonia from the annealing temperature of gas sensitive material prividitsya in table.3.

Table 2. – The dependence of response (sec.) sensor of ammonia from the content of the catalyst (Fe_2O_3) in the gas sensitive material annealed at 350 °C (the concentration of methane in the mixture 500 mg/m^3)

The composition of gas sensitive material	Annealing temperature, °C						
SiO_2/TiO_2+10%Fe_2O_3	300	350	400	450	500	550	600
	The sensor response ($\tau_{отк}$ or τ_{09}). sec.						
	34	24	19	16	15	14	14

Cover SiO_2/TiO_2+10%Fe_2O_3 annealed at a temperature of 300 °C are characterized by low gas sensitivity (S=0,06), compared with the samples annealed at temperatures 600 °C (S=0,17). Analysis of the dependence of the response (table.3.) samples of the cover annealed at temperatures 300–600 °C showed that the response time of the sensor depends on the annealing temperature of the cover and decreases with increasing annealing temperature in the temperature range from 300 to 550 °C. The minimum time constant (14 sec.) of the sensor based on SiO_2/TiO_2+10%Fe_2O_3 is achieved at the annealing temperature of gas sensitive material 550 °C. Further improvement of the performance of the sensors was not possible to the fact that at higher temperatures the stability is lost the heater and contacts the sensing layer and the heater. When checking concentrations of ammonia in the air by adjusting the amount of catalyst and increasing the temperature of annealing of a cover of gas sensitive material to the maximum possible managed to achieve the performance of the sensor based on titanium dioxide about 14 sec. It is established that the value of gas sensitivity, as well as $t_{resp.}$ and $t_{recov.}$ sensor of ammonia depend on the content of the catalyst in the gas sensitive material. Increasing the concentration of iron compounds in the gas sensitive material

from 5 to 10% leads to increase the performance of gas sensors in 1,2–1,4 times.

At the annealing temperature of 550 °C response time of the sensor reaches a stable value (14 sec.) above which does not reduce the value of the indices of the sensor. The sensor response in the studied conditions, quite reproducible, and can be used to determine low concentrations of ammonia in air and process gases.

During the experiments, studied the calibration characteristics of the sensor of ammonia based on titanium oxide. To increase the sensitivity to ammonia on the titanium oxide was applied to the iron oxide, which is active and selective catalyst for the oxidation of ammonia by air oxygen.

Table.4. shows the dependence of the signal (S) of semiconductor sensors with different gas sensitive material on the concentration of ammonia.

Table 4. – The dependence of the signal of the semiconductor sensor from the content of ammonia in the air (temperature experience — 350 °C)

The composition of gas sensitive material	**The content of ammonia in the air, mg/m^3**									
	100	**200**	**300**	**400**	**500**	**600**	**700**	**800**	**900**	**1000**
	sensor signal, $\Delta\sigma/\sigma_0$									
SiO_2/TiO_2	1,07	1,1	1,12	1,13	1,14	1,15	1,16	1,17	1,18	1,19
SiO_2/TiO_2+1%Fe_2O_3	1,11	1,15	1,18	1,21	1,23	1,26	1,29	1,32	1,35	1,39
SiO_2/TiO_2+5%Fe_2O_3	1,37	1,61	1,73	1,85	1,96	2,06	2,18	2,29	2,4	2,51
SiO_2/TiO_2+10%Fe_2O_3	1,51	1,82	2,04	2,26	2,49	2,72	2,94	3,16	3,38	3,61

As shown, in a wide concentration range (20 to 1000 mg/m^3) the dependence of the signal of a semiconductor sensor of the concentration of ammonia in the calibration gas has a straightforward character.

The analysis presented in table.4. the data shows that the gas sensitive material based on SiO_2/TiO_2 and SiO_2/TiO_2–1% Fe_2O_3 is characterized by low sensitivity and selectivity to ammonia. The sensitivity threshold of sensors based on thin cover titanium dioxide is 20 mg/м^3 in the air. A sharp rise in the value of the gas sensitivity is observed for the sample with Fe content of 5–10%. Semiconductor sensors based on SiO_2/TiO_2–5% Fe_2O_3, and SiO_2/TiO_2–10%Fe_2O_3 can detect NH_3 gas impurities at the level of the TLV.

The conclusion. Thus, it was found that increasing the concentration of iron compounds in the gas sensitive material from 5 to 10% leads to increase the performance of gas sensors in 1,2–1,4 times. At the annealing temperature of 550 °C response time of the sensor reaches a stable value (14 sec.) above which does not reduce the value of the indices of the sensor. The results of the experiments revealed a linear territory of the signal, which determine the content of ammonia in a wide range of concentration.

References:

1. Abdurakhmanov I. E., Murodova Z. B. Sattarova M. Dj. Highly sensitive automatic gas analyzer VG ammonia — NH_3//The journal "Chemical industry". Russia. V. 92, No. 3, 2015. P. 138–141.
2. Abdurakhmanov I. E., Begmatov R. H., J. B. Kabulov. Study the influence of the amount of TEOS and acid (PH) on the properties of cover-forming solution.//Actual problems of humanitarian and natural sciences. No. 4, 2015. P. 12–17.

Aripova Mastura Khikmatovna,
Tashkent Chemical Technological Institute,
Department of «Technology of silicate materials and rare precious metals»
Dr. Technical Sciences, Professor
E-mail: aripova1957@yandex.ru

Kadirova Zukhra Chingizovna,
Tashkent Chemical Technological Institute,
Center of Excellence,
Dr. Engineering, PhD in Chemistry,
E-mail: zuhra_kadirova@yahoo.com

Mkrtchyan Ripsime Vachaganovna,
Tashkent Chemical Technological Institute,
Innovation Centre, PhD in Technical Sciences
E-mail: mk_hripsime@mail.ru

Computer simulation of interaction between polyacrylic acid and bioglass by molecular dynamics

Abstract: The results of quantum chemical simulation show that the polyacrylic acid exhibits good adhesion properties to a biocompatible glass produced in $Ca_5(PO_4)_3F$-$CaAl_2Si_2O_8$-$Zn_3(PO_4)_2$ system, and the Ca^{2+}, $Zn^{2+}$and Al^{3+} ions form stable metal complex bonds with polyacrylic acid to facilitate the strength during the hardening reaction.

Keywords: biocompatible glass, polyacrylic acid, adhesion.

Computational techniques have been shown to be capable of help in the fundamental knowledge of complex problems in the field of biomaterial research. Bioglass is an object of several experimental studies, though the understanding at a molecular level of the integration mechanism in bones and teeth has not been fully reached yet. Computational modeling of bioinert, resorbable and bioactive glass materials represents a crucial tool to complement and interpret experimental data [1, 1004–1006]. Applying different methodologies, from classical dynamics to *ab initio*, bulk properties of amorphous materials as well as surface reactivity of crystalline structures can be characterized. Structural and dynamical properties of bioglass surface characterization and reactivity of hydroxyapatite were in good agreement with experimental results validated both models [2, 154]. Elucidation of the structural role of fluorine in bioactive glasses by experimental and computational investigation and fluorine environment were modeled by *ab initio* [3, 2038] and molecular dynamics simulations [4, 12730]. Quantitative rationalization of multicomponent glass properties by means of molecular dynamics simulations [5, 1045], evaluation of elastic properties of binary alkali silicate glasses, prediction and interpretation through atomistic simulation techniques were carried out [6, 3144].

The aim of this study is simulation of polymer adhesion to a variety of metal oxide, ceramic, and other materials by construction of an appropriate model in the simplest way. It is possible to consider of polymer interaction with a multi-component system of the $Ca_5(PO_4)_3F$-$CaAl_2Si_2O_8$-$Zn_3(PO_4)_2$ biocompatible glass as adhesion of large number of polymer molecules on solid glass surface by quantum chemical calculations. In this case all the electrons (polymer and glass) are included in the electronic Hamiltonian and this method is a direct generalization of quantum chemical methods developed for individual molecules in large systems consisting of several numbers of individual molecules. Taking into account the interaction of polymer molecules with a large number of structural glass units, calculation of the energetically most favorable conformation of polymer molecules on the glass surface were carried out. The quantum-chemical method must be suitable for study of molecular interactions and adequately describe the whole system.

The polyacrylic acid is well-known component of bio-glass composition, and simulation of polyacrylic

acid adhesion process is quite simple using classical molecular dynamics method based on a number of approximations in Accelrys Material Studio software package, Discover program. Adhesion energy ($E_{Interaction}$) was calculated on basis of calculation of the total energy of the system on the polymer surface (E_{total}) by the formula:

$$E_{Interaction} = E_{total} - (E_{surface} + E_{polymer})$$

where $E_{surface}$ is calculated energy of the free surface without the polymer, $E_{polymer}$ is calculated total energy of polymer uncoordinated to the surface.

The material on the basis of the fluoroapatite, anorthite, zinc orthophosphate R-CaF_2-P_2O_5-Al_2O_3-SiO_2 (R=CaO, ZnO) system was chosen as an object of study. Surface modeling was carried out based on a number of CIF files from X-ray diffraction data base. Simulated adhesion to individual components (anorthite, fluorapatite and zinc orthophosphate) was calculated, as well as, interaction of short-range order was simulated, i. e. polymer adhesion to ZnO, Al_2O_3, CaF_2, CaO, SiO_2, P_2O_5. Besides energy interactions of polyacrylic acid molecules with the Ca^{2+}, Zn^{2+} and Al^{3+}ions were calculated.

The Table 1 shows polyacrylic acid affinity towards long-range and short-range order structural units.

Table 1 – The calculated adhesion energy for glasses in R-CaF_2-P_2O_5-Al_2O_3-SiO_2 (R=CaO, ZnO) system

Modeling surface	Adhesion energy, kJ/mol
Structural units of minerals	
$Ca_5(PO_4)_3F$	–12550,10
$CaAl_2Si_2O_8$	–8370,05
$Zn_3(PO_4)_2$	–42,10
Structural units of short-range order	
ZnO	–2179,86
Al_2O_3	–1439,30
CaF_2	–870,27
CaO	–564,84
SiO_2	–96,23
P_2O_5	–96,23

It is known that glasses are amorphous solids characterized by a network of building blocks, linked together by bridging oxygen atoms [7, 45]. It is known that possible minerals are formed as result of glass crystallization the RO-CaF_2-P_2O_5-Al_2O_3-SiO_2 (R=CaO, ZnO) system [8, 55–56]. While the short-range order is similar to their crystalline counterparts, no long-range order is present in bulk; the high flexibility in the angles and relative orientation determines a high degree of structural disorder except short-range structural unit [2, 148].

Analysis of interaction between polyacrylic acid with the Ca^{2+}, Zn^{2+} and Al^{3+} ions at simple molecular level carried out by calculating electronic structures of polyacrylic acid molecules (n =1–8), metal complexes and polyacrylate anion. All calculations have good correlation between the reactivity indices (atomic charges, bonds orders, HUMO and LUMO parameters for polyacrylic acid molecules, polyacrylate anion, polyacrylate metal complexes (Ca^{2+}, Zn^{2+} and Al^{3+}). The reactivity indices characterize the energy of intermolecular interactions of polyacrylic acid molecules in case of comparatively large distance between each polymer molecules. The energy of intermolecular interactions between polyacrylic acid and metal ions can be divided into three types: coulomb, orbital and steric. The interaction of two molecules of polyacrylic acid with Ca^{2+}, Zn^{2+} ions leads to formation of stable polymeric metal complexes with monodentate coordination of carboxylate group via oxygen atom. Interaction of the three polyacrylic acid molecules with Al^{3+} ion are also thermodynamically favorable and allows a high degree of crosslinking between bridged polymer molecules.

The structures and bulk properties of amorphous materials can be evaluated using classical dynamics applied to reactivity evaluation of the microcrystalline surfaces in different crystal planes. The solid surface was created on the basis of XRD results, and adhesion of individual components, e. g. energy of interaction between polyacrylic acid molecules and different solid surface planes of the short-range order microcrystallites were optimized (Figure 1). It is shown that fluorapatite and anorthite minerals have a very high degree of adhesion (~ 12550–8370 kJ/mol), while zinc phosphate has a weaker affinity (~ 42 kJ/mol) to the polyacrylic acid. At the same time, analysis of the adhesion energy between oxides and the polymer molecules showed that the polymer adhesion on zinc oxide (~ 2180 kJ/mol) is much larger than in the case of calcium oxide (~ 565 kJ/mol). Adhesion energy of polymer to aluminum oxide has an intermediate value (~ 1440 kJ/mol). SiO_2 and P_2O_5 showed identical values of adhesion energy with polyacrylic acid molecules (~ 96 kJ/mol), which explains their good mutual compatibility in the glass ionomer materials.

Thus, quantum chemical simulation shows that the polyacrylic acid exhibits good adhesion properties to bioglass produced in $Ca_5(PO_4)_3F$-$CaAl_2Si_2O_8$-$Zn_3(PO_4)_2$ system, and the metal ions (Ca^{2+}, Zn^{2+} and Al^{3+}) form stable metal complex bonds reinforced the glass by improving material mechanical strength during the hardening reaction.

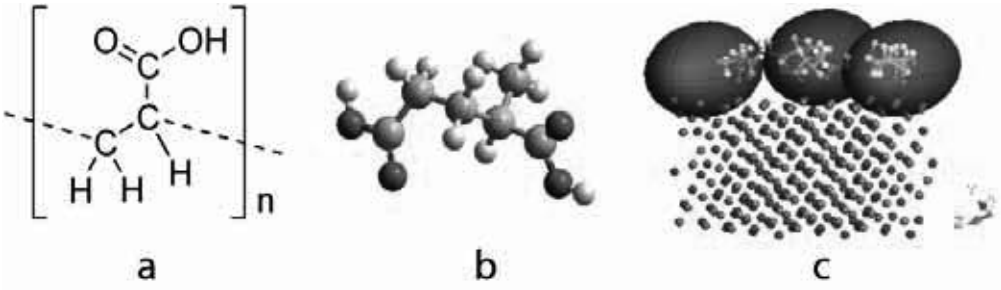

Figure 1–Schematic picture of interaction of polyacrylic acid (a) molecules (n=2) (b)on the solid oxide surface (c)

References:

1. Tilocca A. Structural models of bioactive glasses from molecular dynamics simulations//Proc. R. Soc. A. – 2009. – V. 465. – P. 1003–1027.
2. Pedone A., Corno M. Computer Simulations Techniques for Modelling Bioceramics//La Chimica e L'Industria. – 2010. – N. 9. – P. 146–155.
3. Christie J. K., Pedone A., Menziani M. C., TiloccaA. Fluorine Environment in Bioactive Glasses: ab Initio Molecular Dynamics Simulations//J. Phys. Chem. B. – 2011. – V.115. – P. 2038–2045.
4. Lusvardi G., Malavasi G., Cortada M., Menabue L., Menziani M. C., Pedone A., Segre U. Elucidation of the structural role of fluorine in potentially bioactive glasses by experimental and computational investigation//J. Phys. Chem. B. – 2008. – V. 112. – P. 12730–12739.
5. Malavasi G., Pedone A., Menziani M. C. Towards a quantitative rationalization of multicomponent glass properties by means of molecular dynamics simulations//Molecular Simulation, 2006. – V.32. – P. 1045–1055.
6. Pedone A., Malavasi G., Cormack A. N., Segre U., Menziani M. C. Insight into elastic properties of binary alkali silicate glasses; prediction and interpretation through atomistic simulation techniques//Chem. Mater. – 2007. – V. 19. – P. 3144–3154.
7. Patent of Republic Uzbekistan 04509. C 03 C 10/00, A 61 K 6/02. Glass for biocompatible glass ceramic material/Aripova M. Kh., Mkrtchyan R. V. Rasmiy Akhbarotnoma. – 2012. – N 6. – P. 45.
8. Aripova M. K., Mkrtchyan R. V., Nam T. Synthesis and properties of glasses in $Zn_3(PO_4)_2$-$Ca_5(PO_4)_3F$-$CaAl_2Si_2O_8$ system//Conference of Mendeleev Russian and Moscow Chemical Society on Resource Saving and Energy Saving Technologies in the Chemical and Petrochemical Industries, – M. – 2013. – P. 54–55 (in Russian).

Khayitov Ruslan Rustamjonovich,
Institute of General and Inorganic Chemistry,
Academy of Sciences of Uzbekistan, Tashkent, Uzbekistan,
doctoral student, the Laboratory of Chemistry of Oil
E-mail: leo-bexa@mail.ru

Narmetova Gulnara Rozukulovna,
Institute of General and Inorganic Chemistry,
Academy of Sciences of Uzbekistan, Tashkent, Uzbekistan,
Chief scientific officer, the Laboratory of Chemistry of Oil

Production of activated coal from the pits of apricots and peach for the adsorption purification of the waste Diethanolamine

Abstract: The obtained activated carbons from pits of apricot and peach. Conducted carbonization of the raw material in the temperature range 600–900 °C in a quartz reactor placed in an electric furnace with controlled heating. The resulting activated carbons with water vapor for 1–5 hours. Determined sorption and physical characteristics of the obtained activated carbons were compared with other known sorbents.

Keywords: activated carbon, apricot pits, peach pits, carbon AG-3, activate, carbonizate, alkanolamine, regeneration.

Introduction. The production of activated carbon (AC) has been steadily increasing and their application is continuously expanding. The traditional raw material for the production of AU are wood, peat, peat coke, some coals and polyoxy based on them. In Uzbekistan, despite the large demand for AU, they do not produce. In addition, food enterprises of the Republic annually produce large amount of waste of processing of fruits of apricots and peaches, is widely cultivated on the territory of the Republic. According to available information [1] named waste can serve as a good raw material for the production of AC. There is sufficient information about the kernel processing polyethylene into valuable products [2], but literature data on receipt and use of coal sorbents based on shell pits are scarce [2–4].

AC have a well-developed porous structure and large specific surface area (up to 1000 m^2/g). Carbon adsorbents are used primarily for drying, purification and separation of gases, purification of natural and waste waters in the process of extracting precious metals, decontamination of contaminated fluids, for separation of harmful impurities in the atmosphere in small concentrations, as catalysts and even for the analysis of complex mixtures that differ only in isotopic composition.

In the world practice for cleaning saturated solutions of alkanolamines on the units amine treatment of natural gas from acid components is widely used activated coal brand AG-3. Activated coal brand AG-3 is obtained in the form of granules from coal dust and binder method of treatment with water vapor at a temperature of 850–950 °C.

Uzbekistan has three major gas processing complex Mubarek gas processing factory (mgpf), the washing installation of the enterprise "Shurtanneftgaz" and Shurtan gas and chemical complex. The units amine treatment of natural gas from acidic components higher the number of plants for the purification of saturated alkanolamines used activated coal AG-3.

We must remember that activated coal AG-3 is of foreign origin and imported for currency.

In the present work, the aim was — obtaining activated carbon from local raw materials for the regeneration of alkanolamines in the process amine treatment of natural gas instead of sorbent AG-3.

Objects and methods of research. The object of research was the benchmark of aromatic hydrocarbons (benzene), methylene blue (MB), iodine, water vapor, carbon adsorbents (coconut shells, the shell cedar nut, shell almonds, activated coal brand AG-3), as well as the proposed coal — local activated carbon on the basis of fruit pits (apricot and peach).

In the course of the research were studied the carbonization of the raw material in the temperature range 600–900 °C in a quartz reactor placed in an electric furnace with controlled heating. The temperature in the furnace was controlled using a thermocouple and potentiometer. Processing was subjected to a fraction of 0,2–5,0 mm and dried at 110 °C to constant weight. Released gaseous products of pyrolysis is evacuated from the reactor via the vapor tube and directed into a cooled condenser for condensation of water vapor and tar. To achieve the required temperature of the experiment, the samples were kept in the reactor for 0,5–3,0 hours, and then cooled to room temperature. Chilled carbonizate unloaded from the reactor by standard methods was determined by their absorption properties [3–5]. The activation process of carbonisation studied in the same reactor. This carbon matrix obtained by the pyrolysis of raw materials was charged into the cold reactor, which is purged with a current of nitrogen gas for 15 min to remove oxygen from the reaction zone [6–8]. Then we carried out heating the samples to a final temperature of activation, which was in the range of 600–900 °C.

Upon reaching the desired temperature in the reactor was fed water vapor from the generator within 1–5 h. After heat treatment activity left to cool to room temperature.

The quality of the desired products was monitored by measuring their adsorption activity for methylene blue (MB), iodine, benzene, water vapor [9–11], while it was evaluated their total porosity by boiling in water [12; 13].

Analysis of apricot and peach kernels is established that the mass fraction in them the shell is 85–90, its moisture content is in the range of 20–21, and ash content — 0,27–0,3%. The obtained experimental results are shown in tables 1 and 2, allowed us to note that the optimal conditions of carbonization of the bones to peaches are a duration of 1 h at 750 °C; apricots for 2 h at 600 °C.

Results and their discussion. Upon receipt of the activated carbon from the seeds of apricots and peach obtained the following results (tab. 1 and 2).

Table 1. – The conditions and results of carbonization of apricot pits fragments

Process temperature, °C	τ – the speed of temperature rise, min.	The mass of raw material, g.	The mass of carbonizate, g.	V_{Σ}, H_2O,%	V condensate, ml.	Adsorption activity	
						for C_6H_6, g/100g*	for water vapor, cm^3/g
600	0–90	8,4	2,14	24,86	5,5	1,26	0,6577
650	0–90	10	2,5	24,9	6,5	0,93	0,0268
750	0–90	10,8	2,54	23,52	7,8	0,62	0,1734
850	0–90	10,27	3,72	36	8,7	0,34	0,1233
900	0–90	11,16	2,78	22,4	9	0,09	0,1088

** – capacity determined in dynamic conditions in the liquid phase*

Table 2. – The conditions and results of carbonization of peach pits fragments

Process temperature, °C	τ – the speed of temperature rise, min.	The mass of raw material, g.	The mass of carbonizate, g.	V_{Σ}, H_2O,%	V condensate, ml.	Adsorption activity	
						for C_6H_6, g/100g*	for water vapor, cm^3/g
600	0–90	5,06	0,26	5,14	5,2	0,52	0,2286
650	0–90	5,27	2	38	6,1	0,87	0,2997
750	0–90	5,29	1,54	29,1	8	1,18	0,3383
850	0–90	5,39	1,67	31	8,6	0,46	0,2466
900	0–90	5,36	1,47	27,4	8,9	0,24	0,1966

** – capacity determined in dynamic conditions in the liquid phase*

The resulting carbonizate stone raw material is activated. The conditions and results of activation are shown in tables 3–5.

Table 3. – The activation conditions of carbonizate of apricot

T, °C	The time of exposure, min.	The degree of burning, %	Adsorption activity	
			for MB, m^2/g	for I_2,%
800	60	28,82	5,18	21,7
850	120	27,10	6,39	25,34

Table 4. – The activation conditions of carbonizate of peach

T, °C	The time of exposure, min.	The degree of burning, %	Adsorption activity	
			for MB, m^2/g	for I_2,%
800	60	16,39	4,19	8,52
850	120	15,89	5,38	12,34

Based on the obtained data (tab. 3,4), it was stated that the optimal conditions for the activation of carbonizate stone raw material temperature of 850 °C, duration 2 h.

Compared some of the characteristics of the obtained activated carbons from stone raw materials with other well-known commercial activated carbons (tab. 5).

Table 5. – Some of the characteristics of the carbon adsorbents

Mark of adsorbent	Adsorption activity			Specific surface, m^2/g	Source of information
	for MB, m^2/g	for I_2, %	for C_6H_6, g/100g		
Shell apricot walnut*	6,39	5,34	1,26	800–890	Results of their own experiments
Shell peach walnut*	5,38	12,34	1,18	878–936	Results of their own experiments
Coconut shells	> 2,5	11,0	1,05	~500	PJ, Philippines, Japan
The shell cedar nut	3,18	14,0	0,73	~ 250	Russia, Siberia, Tomsk
Shell almonds	6,3	9,0	1,10	650–700	Central Asia, Kazakhstan, Astana
Activated coal brand AG-3	–	–	1,23	480–500	Russia, Rostov-on-Don

** We received samples of stone active carbon*

Conclusion. Comparison with literature data revealed that the obtained target products for adsorption activity are at the level of the activated carbon from stone raw materials, which is one of the highest quality global industrial activated coals, and far superior to many other carbon adsorbents (table 5). Thus, the studies demonstrate the feasibility of processing described waste of the Republic of Uzbekistan on carbon adsorbents.

Evaluated the prospect of processing the waste pits of apricots and peaches are formed on the enterprises of food industry of the Republic of Uzbekistan on activated carbons.

References:

1. Large-scale controls on potential respiration and denitrification in riverine floodplains./ELSEVIER/Marth, 2012/73–84.
2. Attachment of faecal coliform and macro-invertebrate activity in the removal of faecal coliform in domestic wastewater treatment pond systems./ELSEVIER/Marth, 2012/35–41.
3. Kinle Kh., Bader E. Active carbons and their industrial application (translated from the German). – L.: Chemistry, 1984. – P. 215.
4. Butyrin G. M. Highly porous carbon materials. – M.: Chemistry, 1976. – P. 187.
5. Greg S., Singh N. Adsorption, specific surface, porosity. – M.: Mir, 1970. – P. 408.
6. Dubinin M. M., Radushkevich, L. V.//Rep. of AS of USSR, 1947. – V. 55. – P. 331.
7. Kolyshkin D. A., Mikhailov K. K. Active carbon. Properties and test methods. Directory. – L.: Chemistry, 1972. – 57 P.
8. Active coals. Elastic sorbents. Catalysts, dehydrators and chemical absorbers based on them. Item catalogue under the General editorship of V. M. Mukhin. – M.: Ore and metals, 2003. – 280 p.
9. "Water treatment", No. 8/2010. ID "Panorama".
10. "Treatment" № 9/2010. ID "Panorama".
11. Anurova T. V. Development of technology of active carbons from vegetable waste and their use for the protection of air from vapors of hydrocarbons: dis. cand. tech. sc. – M., 2003. – P. 54–55. – P. 68–102.
12. Mukhin V. M., Zubova I. D., Zubova I. N., Solovyov S. N., Yakovlev E. N. Method of producing active coal//Patent of Russia № 2393990/13, 06.04.2009.
13. Baklanova O. N., Plaksin G. V., Lavrenov A. V., Knyazeva O. A., Likholobov V. A. Technology of production of porous carbon materials//Patent of Russia № 2451547, 31.08.2010.

Sobirov Mukhtorjon Mahammadjanovich,
Junior scientific researcher Academy of Sciences
Republic of Uzbekistan Institute of General
and inorganic chemistry, Tashkent, Uzbekistan
E-mail: fcb_m_2011@mail.ru

Sultonov Bokhodir Elbekovich,
PhD in technique, senior reseacher of laboratory of Phosphorous fertilizers,
Academy of Sciences of the Republic of Uzbekistan, Institute of General
and inorganic chemistry, Tashkent, Uzbekistan
E-mail: i_umbarov@mail.ru

Tajiev Sayfuddin Muhitdinovich,
PhD in chemistry, Head of laboratory of Complex fertilizers,
Academy of Sciences Republic of Uzbekistan
Institute of General and inorganic chemistry, Tashkent, Uzbekistan
E-mail: sayf49@rambler.ru

Suspended sulfur containing fertilizers based on low-grade Kyzyl-kum phosphorites

Abstract: In this article, the principal opportunities for intensive technology of complex suspended sulfur-containing fertilizers wide actions based on unconcentrated phosphorites from Central Kyzylkum

have been given. There has been found the chemical composition of the fertilizers and expansion coefficient of phosphorite flour. In order to obtain optimal ratios and an increase of nutrients in plant during vegetation periods, and improvement of rheological properties of the nitrogen-phosphate slurry, it was added that required amount of ammonium nitrate solution obtained by neutralization of nitric acid with gaseous ammonia.

Keywords: phosphorite flour, ground sulfur, nitric acid, ammonia, ammonium nitrate.

Introduction. In recent years, the global fertilizer market has a high demand for various types of liquid and suspended NPK-fertilizers. Such a situation is caused, primarily, their high agrochemical value, as the fertilizer applied to the soil that allows simultaneously all three of the most valuable nutritional elements — nitrogen, phosphorus and potassium. Recently concentrated liquid complex mineral fertilizers have been replacing the traditional solid.

Among them are very perspective suspended complex fertilizer (SCF) [1; 2]. Suspensions of the complex fertilizer are saturated salt solutions, in which are dispersed fine crystals (particles) of insoluble salts, stabilizing agents and other substances. Concentrated suspended NPK-fertilizers, obtained using concentrated nitrogen fertilizers are the best with consumer point view. Ammonium nitrate and urea, in which the nitrogen content is 35.0% and 46.7% by weight respectively, are used as nitrogen containing components.

Phosphorite is the main industrial source of phosphorus is an important, necessary for the life cycle of all living organisms. However, the phosphorus's reserves in the soil are being depleted, so it is necessary to make this element in the form of natural or chemical fertilizers.

In Uzbekistan, the Central Kyzyl Kum phosphate is the main raw material for phosphate fertilizers [3]. One ways of processing high calcareous phosphate raw material is nitric acid decomposition. The use of nitric acid largely economically justified, as resulting nitric acid suspensions can be used calcium nitrate fertilizer. In this regard, the methods of processing raw phosphate in nitric acid solutions are the greatest interest.

Currently in our country there are practically no technology for complex preparations universal actions for root and for foliar feeding, which are effective fertilizers and insecticides, exterminating spider mites and other sucking plant pests, although the work [4] is devoted to the production of liquid complex fertilizers based on phosphate and nitric acid.

From the above should be noted that the development of complex suspended nitrogen, phosphorus, potassium, calcium, and sulfur containing fertilizers technology based on nitric acid, potassium chloride, ammonia, sulfur, and phosphate raw materials is quite topical.

Objects and Methods. To obtain new types of complex fertilizers in laboratory experiments were used the following: unconcentrated phosphorite flour of Central Kyzylkum with composition (wt.%): P_2O_5–17.55; CaO – 43.68; CO_2–14.83; MgO – 1,68; R_2O_3–2,47; SO_3–1.01; F – 2,17; H_2O – 1.19; insoluble residue – 3.80%; ground sulfur, corresponding to State standard [5]; gaseous ammonia and 58.50% nitric acid. Stoichiometric norm of nitric acid calculated on the decomposition of phosphate and carbonate minerals of the phosphate rock to form monobasic calcium phosphate and calcium nitrate. The norm of nitric acid was varied in the range of 30–70% of stoichiometry.

The mixture of the phosphorite flour and elemental sulfur was prepared at a ratio of 9: 1 to obtain suspended complex fertilizers. This mixture was thoroughly mixed, then it was decomposed by the first portion of nitric acid. The rest of the nitric acid is neutralized with ammonia gas, 64.16% ammonium nitrate solution is formed.

Decomposition of sulfur-containing phosphorite flour with acid is easily feasible. Component interaction occurs within 15–30 minutes. Process temperature, depending on the norm of acid varies in the range of 30–45 °C. To improve the quality and properties of the compound suspended in the resulting sulfur-containing fertilizer nitrogen-phosphoric pulp with constant stirring, the estimated amount of 64.16% solution of ammonium nitrate was added.

The contents of all forms of P_2O_5 (total, acceptable, water-soluble) in the products obtained was determined by photo-calorimetric method as a yellow complex phosphorus-vanadium-molybdenum complex on CPC-3 (= 440 nm) [6; 7]. The nitrogen content was determined by the distillation of ammonia on Kjeldahl and chlorine-amine method in according to [8]. The content of sulphate sulfur defined using barium chloride gravimetric method [9]. Elemental sulfur was determined by subtracting the sulphate form of sulfur of the total elemental sulfur taken to obtain the sulfur containing phosphorite flour. Determination of the content of all forms of calcium was carried out by complexometric titration

volume Trilon B in the presence of calcein or chrome dark blue indicators [10]. Expansion coefficient was calculated according to the formula: $Ke = (P_2O_{5accep.} / P_2O_{5total.}) \cdot 100\%$, where — $P_2O_{5accep.}$ is acceptable form on 2% citric acid, $P_2O_{5total.}$ is total phosphorus content in the fertilizer samples.

Results and discussion. The complex suspended sulfur-containing nitrogen-phosphorus fertilizer (N: P_2O_5 = 1:1) obtained at 30% norm of nitric acid contains 8.69% of total nitrogen, of which 35.09 % is in ammonium and a rest in nitrate, 8 67% of P_2O_{5total}, of which 4.03 is in water-soluble form, 21.64% of CaO_{total}, of which 24.03% is in water-soluble forms of CaO and 5.50% of the added ground sulfur in a hydrophilic state, including 72,73% of elemental, and 27.27% of sulphate form (Table. 1). The fertilizer mainly consists of calcium nitrate — 10.98%, ammonium nitrate — 30.46% of mono- and dicalcium phosphate as well as activated form of phosphorite flour in amount of 34.68% and sulfur — 5.70%. The amount of nutrients NPCaS is 44.71%.

With increasing amounts of ammonium nitrate to 30.46% in the composition of the slurry, i. e. a change in the ratio N: P_2O_5 from 1:1 to 1:0.5 the expansion coefficient (Ke) of phosphorite flour is increased from 38.32 to 40.03%.

With the increase of the nitric acid norm from 40% and 70% the content of water soluble form of phosphorus and calcium are raised from 0.71% to 1.71% and from 6.79% to 11.28%, respectively. Expansion coefficient of phosphorite flour is increased from 49.30% to 79.55%.

Table 1. – The chemical composition of the suspended sulfur-containing fertilizers,%

N: P_2O_5	N			P_2O_5		CaO		S			H_2O	Ke.
	total	nit-te	am-m	total	water	total	water	total	elem.	SO_4		
When norm HNO_3 30%												
1:0.5	12.53	7.21	5.33	6.27	0.28	15.6	3.75	4.11	2.89	1.08	23.65	40.03
1:0.6	11.59	6.82	4.77	6.86	0.30	17.08	4.11	4.50	3.16	1.18	22.49	39.65
1:0.7	10.65	6.44	4.21	7.46	0.32	18.56	4.46	4.89	3.43	1.29	21.34	39.28
1:0.85	9.67	6.05	3.63	8.08	0.34	20.1	4.83	5.30	3.72	1.39	20.14	38.86
1:1	8.69	5.65	3.05	8.68	0.35	21.64	5.20	5.70	4.00	1.50	18.94	38.36
When norm HNO_3 40%												
1:0.5	12.35	7.41	4.94	6.17	0.54	15.37	4.93	4.05	2.43	1.48	24.50	51.05
1:0.6	11.41	7.05	4.36	6.75	0.59	16.8	5.39	4.43	2.65	1.62	23.44	50.67
1:0.7	10.46	6.69	3.77	7.33	0.63	18.24	5.84	4.81	2.88	1.76	22.38	50.34
1:0.85	9.49	6.32	3.16	7.92	0.67	19.72	6.32	5.20	3.11	1.90	21.29	49.87
1:1	8.52	5.96	2.56	8.52	0.71	21.20	6.79	5.59	3.35	2.04	20.19	49.30
When norm HNO_3 50%												
1:0.5	12.17	7.60	4.56	6.09	0.75	15.15	6.07	3.99	2.20	1.65	25,32	61,41
1:0.6	11.23	7.27	3.96	6.64	0.81	16.53	6.63	4.36	2.40	1.8	24,36	60,99
1:0.7	10.28	6.94	3.35	7.20	0.87	17.92	7.18	4.72	2.61	1.95	23.39	60.42
1:0.85	9.32	6.60	2.72	7.77	0.93	19.35	7.75	5.10	2.82	2.1	22.41	59.85
1:1	8.35	6.26	2.09	8.35	0.99	20.78	8.33	5.48	3.03	2.25	21.42	59.16
When norm HNO_3 60%												
1:0.5	12.04	7.82	4.22	6.02	1.11	14.98	7.21	3.95	2.09	1.72	26.21	71.26
1:0.6	11.10	7.51	3.58	6.56	1.21	16.34	7.86	4.31	2.27	1.88	25.34	70.73
1:0.7	10.15	7.21	2.95	7.11	1.30	17.69	8.51	4.66	2.47	2.03	24.47	70.18
1:0.85	9.19	6.89	2.30	7.66	1.40	19.08	9.18	5.03	2.66	2.19	23.58	69.71
1:1	8.22	6.57	1.65	8.22	1.49	20.47	9.84	5.39	2.86	2.35	22.68	68.98
When norm HNO_3 70%												
1:0.5	11.87	8.01	3.86	5.94	1.30	14.78	8.29	3.89	1.99	1.77	27.01	81.31
1:0.6	10.93	7.72	3.21	6.46	1.40	16.09	9.03	4.24	2.17	1.92	26.22	80.96
1:0.7	9.99	7.44	2.55	6.99	1.50	17.41	9.77	4.59	2.35	2.08	25.43	80.54
1:0.85	9.03	7.14	1.89	7.53	1.61	18.75	10.52	4.94	2.54	2.23	24.63	80.08
1:1	8.07	6.85	1.22	8.07	1.71	20.09	11.28	5.29	2.72	2.39	23.83	79.55

We have also studied the change of acceptable form phosphorus and calcium in the obtained suspension of complex fertilizers (Fig. 1) depending on the norms of nitric acid and the ratio of nutrients.

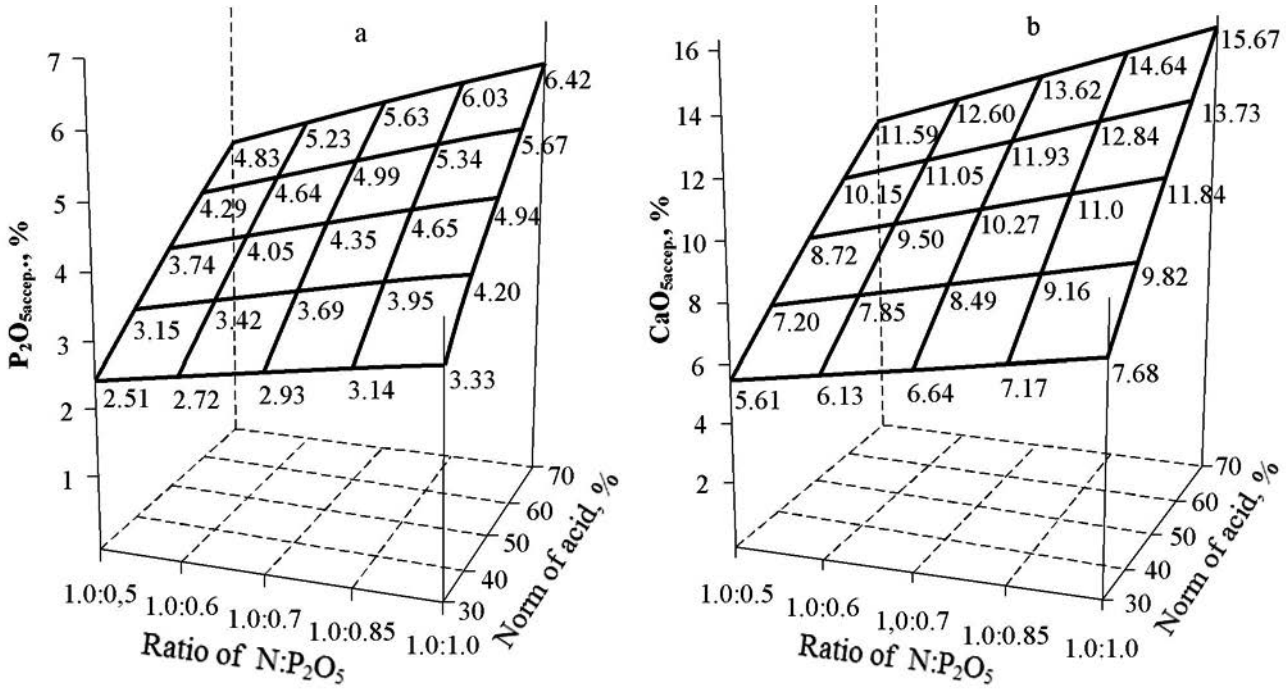

Figure1. The change of acceptable form of P_2O_5 (a) and CaO (b)content on 2% citric acid depending on the norm of HNO_3 and ratio of N: P_2O_5.

It is found that with increasing nitric acid standards acceptable phosphorus and calcium forms increased. For example, at a ratio of N: P_2O_5 from 1: 1 and a norm of 30% nitric acid, content of acceptable phosphorus and calcium is 3.33% and 7.68% and the acid norm 70% equal to 6.42 and 15.67%, i. e. increased 1.92 and 2.04 times, respectively.

Thus, the increase of nitric acid's norm promotes to raise acceptable forms of phosphorus and calcium. However, it should be increased unwisely the norm of acid from this point of view, in this case there is overspending acid. Therefore, we think that the optimal norm of nitric acid is 50–60%. The most widespread N: P_2O_5 in the fertilizer complex for the main crops such as cereals, sugar beet, cotton, potatoes, vegetables, fodder root crops are the following: 1: 0.5; 1: 0.7; 1: 1 [11] and the ratios are optimal.

The suspended complex sulfur-containing fertilizer mainly consists of water-soluble salts –15.24% of calcium nitrate, ammonium nitrate — 17.41% of mono- and dicalcium phosphate as well as 34.68% of activated form of phosphorite flour and 5.70% of sulfur. The amount of nutrients NPCaS makes 44.71% (Table 2).

Table 2. – Salt composition of complex suspended sulfur-containing fertilizers,%

N: P_2O_5	NH_4NO_3	$Ca(NO_3)_2$	mono-, dicalcium phosphate	Activated phosphorite	$CaSO_4$	H_2O
1	*2*	*3*	*4*	*5*	*6*	*7*
When norm HNO_3 30%						
1:0.5	30.46	10.98	4.73	25.00	5.18	23.65
1:0.6	27.26	12.03	5.13	27.37	5.69	22.49
1:0.7	24.06	13.07	5.53	29.75	6.21	21.34
1:0.85	20.4	14.15	5.92	32.21	6.71	20.14
1:1	17.41	15.24	6.28	34.68	7.22	18.94
When norm HNO_3 40%						
1:0.5	28.25	14.43	5.89	21.11	6.88	24.50
1:0.6	24.90	15.78	6.39	23.08	7.56	23.44
1:0.7	21.55	17.12	6.90	25.05	8.20	22.38
1:0.85	18.09	18.52	7.39	27.08	8.88	21.29

1	*2*	*3*	*4*	*5*	*6*	*7*
1:1	14.63	19.91	7.86	29.12	9.52	20.19
When norm HNO_3 50%						
1:0.5	26.10	17.78	6.96	17.34	7.61	25.32
1:0.6	22.62	19.41	7.54	18.92	8.33	24.36
1:0.7	19.13	21.04	8.10	20.51	8.96	23.39
1:0.85	15.54	22.72	8.66	22.15	9.69	22.41
1:1	11.96	24.40	9.20	23.79	10.41	21.42
When norm HNO_3 60%						
1:0.5	24.10	21.10	7.92	13.72	7.90	26.21
1:0.6	20.47	23.01	8.56	14.96	8.67	25.34
1:0.7	16.85	24.92	9.21	16.20	9.31	24.47
1:0.85	13.14	26.88	9.85	17.47	10.07	23.58
1:1	9.42	28.83	10.50	18.74	10.75	22.68
When norm HNO_3 70%						
1:0.5	22.08	24.29	8.90	10.15	8.07	27.01
1:0.6	18.33	26.45	9.64	11.05	8.79	26.22
1:0.7	14.58	28.61	10.38	11.95	9.52	25.43
1:0.85	10.77	30.82	11.12	12.88	10.2	24.63
1:1	6.95	33.02	11.84	13.80	10.92	23.83

As it is seen from the tabulated data that with the change in the ratio of N: P_2O_5 salt composition of the complex suspended fertilizer varies considerably. For example, at a ratio of N: P_2O_5 = 1: 0.5, and 30% nitric acid norm, the suspended fertilizer composition is the following: 10.98% of calcium nitrate, 30.46% of ammonium nitrate, 4.63% of mono- and dicalcium phosphate, 25.00% in active form of phosphorite, and 4.11% of sulfur. By changing the ratio N: P_2O_5 from 1: 0.5 to 1: 1 in the same norm of nitric acid in the obtained complex suspended fertilizer, content of the main component is increased, except the ammonium nitrate.

For example, at a norm of 50% nitric acid with a change in the ratio N: P_2O_5 from 1: 0.5 to 1: 1, the content of calcium nitrate, mono- and dicalcium phosphate, phosphorite flour in an activated form and sulfur increased from 19.41 to 24.40, from 7.54 to 9.20, from 18.92 to 23.79 from 4.36 to 5.48%, respectively, but ammonium nitrate content decreased from 22.62 to 11.96%.

Physicochemical properties of liquid fertilizer: density, viscosity, and crystallization temperature are important as they determine the conditions of production, storage, transportation and introduction into the soil. Therefore, we studied the rheological properties of the suspended complex fertilizers. Studies have shown that with increase temperature, decrease viscosity and density of the fertilizer suspension is observed. The crystallization temperature of the suspended fertilizer varied from –7 to 6.5 °C. The suspended fertilizer containing high concentrations of calcium nitrate, i. e. obtained at excess nitric acid norms has much high crystallization temperature. pH of suspended complex fertilizers depending on the norms and ratios of nutrients is varied in the range 4–6.

Conclusion. There have been shown the principal opportunities for intensive technology of complex suspended sulfur-containing fertilizers wide actions based on unconcentrated phosphorites from Central Kyzylkum, for root and for foliar feeding, which are effective fertilizer and have insecticidal properties, exterminating some agricultural plant pests (spider mites and sucking pests). In order to obtain optimal ratios and an increase of nutrients in plant during vegetation periods, and improvement of rheological properties of the nitrogen-phosphate slurry, it was added that required amount of ammonium nitrate solution obtained by neutralization of nitric acid with gaseous ammonia. Proposed suspended sulfur-containing compound fertilizer compared with standard solid fertilizers has the following advantages: insecticidal properties; simplicity of production technology; meets all the requirements set by agricultural production.

References:

1. Efimova L. P., Malakhov N. N. production of suspended fertilizer. Chemical Industry. 1981. No 2. P. 27–28.
2. Postnikov A. V., Efremov L. N. Suspended fertilizer is a new form. Chemictry in Agriculture. 1992. No 3. P. 28–32.

3. Beglov B. M., Namazov S. S., Phosphorites Central Kyzylkum and processing. Tashkent, 2013. 460 p.
4. Radjabov R., the Tajiev S.M, Tukhtaev S. Suspended liquid complex fertilizer. Achievements and prospects of complex chemical processing of fuel and mineral resources of Uzbekistan: Coll. mat. Rep. scientific. tehn. Conf. 7–8 October 2008. Tashkent, 2008. v. 2 P. 161–163.
5. State standard 127.5–93 sulfur ground for agriculture. Specifications. – M: Standard publication, 1993. 10 p.
6. Methodical instructions perform tests extraction pulp and extraction phosphoric acid. JSC "Ammophos – Maxam", Almalyk, – 2010. 22 p.
7. State standard 20851.2.75. Methods for determination of phosphorus content. – Minsk: Standards Publishing House, 1983, 22 p.
8. State standard 30181.4–94 Methods for determination of total mass fraction of nitrogen in compound fertilizers and nitrate in ammonium and nitrate forms (Devarda method). Intergovernmental council for Standardization, Metrology and Certification. Minsk. 1996. 7 p.
9. Vinnik M., Erbanova L. N., Zaitsev P. M. Methods of analysis of phosphate rock, phosphate and compound fertilizers, feed phosphates. – M.: Chemistry.1975. 218 p.
10. Handbook of chemicalization in agriculture/Ed. V. M. Borisova. – M.: Kolos, 1980, 500 p.

Khayitov Ruslan Rustamjonovich,
Institute of General and Inorganic Chemistry,
Academy of Sciences of Uzbekistan, Tashkent, Uzbekistan,
doctoral student, the Laboratory of Chemistry of Oil
E-mail: leo-bexa@mail.ru

Narmetova Gulnara Rozukulovna,
Institute of General and Inorganic Chemistry,
Academy of Sciences of Uzbekistan, Tashkent, Uzbekistan,
Chief scientific officer, the Laboratory of Chemistry of Oil

Shermatov Bobomirza Eshbaevich,
Uzbek Scientific Research Chemical-Pharmaceutical Institute
named after A. Sultanov UzKFITI,
Tashkent, Uzbekistan, head of the laboratory,
E-mail: bobomirza@mail.ru

Regeneration of activated carbon used in adsorption purification of alkanolamines

Abstract: Studied the methods of regeneration of spent activated carbon. Regeneration of spent activated carbon was carried out in laboratory conditions by high temperature treatment of spent activated carbons in an environment of water vapor and nitrogen at 750±20 °C; 800±20 °C; 850±20 °C temperature regimes.

Keywords: activated carbon, regeneration, adsorption, desorption, reactivation, heat treatment, the specific area, adsorption activity.

Introduction. The adsorption process has wide application in environmental engineering for treating and cleaning gas industrial emissions and sewage. It allows you to quickly and effectively remove from any environmental toxicants. As adsorbents can be used various materials with a certain chemical composition, crystal structure, the mechanism of their action must conform to the following principles [1]:

– have a high adsorption activity directed action;

– do not change the natural balance of substances in all parts of the ecosystem;

– have the ability to regenerate;

– to be able to recycling.

On oil and gas companies to capture hydrocarbons of oil and oil products from waste water is used as a highly effective adsorbent activated carbon, which meets all the

requirements. It has a high specific surface area, adsorption ability (activity) and selectivity to polar components, which is one of the major harmful environmental contaminants specific to the oil and gas industry. In addition, activated carbons can be used not only in water but also dry and wet gas flows, thereby extending the range of their application.

However, the practical use of activated carbon for trapping hydrocarbons of oil and petroleum products is constrained because of problems of regeneration, which is necessary since during the operation of the specific surface and sorption activity of their gradually declining.

Earlier, in our studies the adsorption process was used to regenerate the spent alkanolamine used for purification of natural gas from acidic components by using activated carbon from local raw materials.

The aim of this work was to study the effect of temperature regimes regeneration of spent activated carbon, passivated during regeneration of spent alkanolamine used for purification of natural gas from acidic components, the degree of recovery of their specific surface and sorption activity.

Objects and methods of research. Because adsorption is in principle a reversible process, the contaminants can be removed from activated carbon by desorption (separation of adsorbed substances). The strength of Van-der-Waltz, which is the main driving force for adsorption is weakened, so that the contaminant could be removed from the surface of the coal, there are three technical method [2]:

– the method of temperature fluctuations: the effect of forces of Van-der-Waltz decreases with increasing temperature. The temperature increases due to hot nitrogen stream or by increasing the steam pressure at a temperature of 110–160 °C;

– the method of pressure fluctuations: with decreasing partial pressure, the effect of the forces of Van-der-Waltz is reduced;

– extraction — desorption in the liquid phase. The adsorbed substances are removed by chemical means.

All these methods have disadvantages. Some amount of the pollutant may remain in the pores of activated carbon. With the use of steam regeneration 1/3 of all adsorbed species, is still in the activated carbon.

The chemical regeneration understand the processing of the sorbent liquid or gaseous organic or inorganic reagents at a temperature of usually not higher than 100 °C. Chemically regenerate like carbon, and not carbon sorbents. As a result of this processing, the sorbate is desorbed either unchanged or desorb the products of its interaction with the regenerating agent. Chemical regeneration often occurs directly in the adsorption apparatus. Most methods of chemical regeneration is narrowly specialized for the solutes of a certain type.

Low-temperature thermal regeneration is in the processing of the sorbent with steam or gas at 100–400 °C. this Procedure is quite simple and in many cases it leads directly to the adsorbers. Water vapor due to the high enthalpy are often used for low-temperature thermal regeneration. It is safe and available in production.

Chemical recovery and low-temperature thermal regeneration does not ensure full recovery of the adsorption of coals. Thermal regeneration process is very complex, multistage, affecting not only the sorbate and the sorbent. Thermal regeneration close to the technology of obtaining active coals [3]. The carbonisation of the solutes of various type of coal most of the impurities decomposes at 200–350 °C and at 400 °C is typically destroyed about half of the total adsorbate. CO, CO_2, CH_4 are the main products of decomposition of organic sorbate is released when heated to 350–600 °C. In theory, the cost of such regeneration is 50% of the cost of a new activated carbon. This suggests the need to continue the search and development of new highly effective methods of regeneration of sorbents.

Reactivation — regeneration of activated carbon by steam at a temperature of 600 °C. the Contaminant is burned at this temperature, without burning the coal. This is possible due to the low concentration of oxygen and the presence of large quantities of steam. Water vapor selectively reacts with adsorbed organic matter, having high reactivity in water at these high temperatures, thus there is complete combustion. However, you cannot avoid the minimum combustion of coal. This loss must be offset by new coal. When you reactivate often the case that activated carbon shows a large internal surface and higher reactivity than conventional coal. These facts are due to the formation of additional pores and coking contaminants in the activated carbon. The pore structure also changes — they are increasing.

Reactivation is performed in an oven for reactivation. There are three types of kilns: rotary and shaft furnaces with variable gas flow. Oven with variable gas flow has the advantages of low losses in combustion and friction. Activated carbon loaded in a stream of air and combustion gases can be blown up through the grate. Activated carbon becomes partially fluid due to the intense gas stream. Gases also transporterowych the products of combustion during reactivation of activated carbon in the afterburner chamber. Air is added to the second com-

bustor, so the gases that have not been fully inflamed, can now be burned. The temperature increases to about 1200 °C. After the combustion gas flows to the gas washing apparatus in which the gas is cooled to temperatures between 50–100 °C by the cooling water and air. In this cell, the hydrochloric acid which is formed adsorbed chlorinated hydrocarbons greatly from purified activated carbon, neutralized with sodium hydroxide. Due to the high temperature and rapid cooling is no formation of toxic gases (dioxins and furans).

The most common regeneration technique used in industrial processes is thermal regeneration. The thermal regeneration process consists of three steps [4]:

– the adsorbent is dried at about 105 °C;

– the high temperature desorption and decomposition (500–900 °C) in inert atmosphere without oxygen;

– residual organic gasification by an oxidizing gas (steam or carbon dioxide) occurs at elevated temperatures (800 °C).

The heat treatment stage utilizes the exothermic nature of adsorption and results in desorption, partial destruction and polymerization of the adsorbed organics. The final step aims to remove charred organic residue formed in the porous structure at the previous stage and re-build the porous carbon structure, restoring its original surface features. After this procedure, the adsorption column may again be used. In the process of heat of adsorption the regeneration cycle of 5–15% of the mass of the carbon layer is burned, resulting in a loss of adsorption capacity. Thermal regeneration is energy intensive process due to the necessary high temperatures, making it commercially expensive process. Plants that rely on thermal regeneration of activated carbon, must have a certain power before it is economically feasible to have local funds for regeneration.

Results and their discussion. The process of regeneration, we conducted in laboratory conditions by high temperature treatment of spent activated carbons in an environment of water vapor and nitrogen at the following temperature regimes:

750±20°C; 800±20 °C; 850±20 °C.

As follows from the obtained data, the temperature of the regeneration process has a significant influence on the sorption properties and porous structure of activated carbons.

Thus, the regeneration temperature of 750±20°C the degree of recovery of specific surface area of the sorbent was 72±3% and its sorption activity is 75±3% when the regeneration temperature of 800±20 °C the degree of recovery of specific surface area was 80±3% and its sorption activity — 83±3% when the regeneration temperature of 850±20 °C the degree of recovery of specific surface area was 87±3% and its sorption activity of 90±3%.

Thus, the results of experimental work show that the regeneration of waste activated carbon using high temperature treatment in the range of 750–850 °C leads to effective recovery of the main chromatographic parameters: the specific surface and sorption activity. The degree of recovery of the sorption properties of activated carbon depend on the temperature of the regeneration mode: the higher the temperature, the higher the degree of regeneration of sorption properties. When the regeneration temperature 850 °C maximum recovery of the surface, pore structure and activity of the sorbent.

The obtained data for the development of modes of regeneration of activated carbon used in manufacture, as sorbent, in the engineering protection of air and water basins from contamination sorption method.

References:

1. Keltsev N. V. Principles of adsorption technology. – M.: Chemistry, 1984. – 512 p.
2. Neymark I. E. Synthetic mineral adsorbents and catalyst carriers. – Kiev: Naukova Dumka, 1982. – 216 p.
3. Dubinin M. M. Porous structure and adsorption properties of active coals. – M.: Chemistry, 1965. – 72 p.
4. Chernysheva L. G. Study of adsorption process of separation of condensates of cyclohexane and clean it. Abstract. dis. … Ph. D. – Tashkent, 1970. – 28 p.

Yakhshieva Khurniso,
Gapparov Dilshodbek,
Juraev Ilxom,
Smanova Zulayxo,
National University of Uzbekistan
Uzbekistan, Tashkent
E-mail: yaxshiyeva67@mail.ru

Sorbtion — photometrical Fe (III) determination by immobilized N-methylanabazin-azo-1,8-aminonaphtol-4,8-disulfoacid

Abstract: The abbility N-methylanabazin-azo-1,8-aminonaphtol-4,8-disulfoacid immobilization on the fiber supports of polyacrilonitril type was investigated. Optimal conditions of immobilization and complexformation of immobilization reagent with ions Fe (III) were determined. Method ofFe (III) determination in waters from different sources were elaboraated.

Keywords: ferrum (III), immobilization, N-methylanabazin- -azo-1,8-aminonaphtol-4,8-disulfoacid, natural waters.

Last time the task of rapid determination of heavy and toxical metals has a special actuality in analytical chemistry and it can be solved successfully by application of optical methods with using of organic reagents, immobilized on some polymer sorbents [1–3].

The aim of this work has consisted in improvment of metrological characteristics of optical methods of Fe (III) determination at analysis of different natural objects and industrial materials by using reagents of three phenylemethane raw owing to their immobilization on fiber supports.

Experiment

Solutions, reagents and sorbents. The standart solutions of Fe (III) were preparated by solution on of it`s nitrate in $HNO_3$ with following dilution by distilled water. Solution of reagent — N-methylanabazin- -azo-1,8-aminonaphtol-4,8-disulfoacid (N-MAC) with concentration $1.854 \cdot 10^{-2}$ M was obtained by dissolution of it`s 0.1g in distilled water. Series of buffer solutions were preparated from 1.0M HAc, HCl, NaOH, NH_4OH and NaAc. At N-MAC immobilization sorbents of polyacrylic type modified by different anionchaging groups were used as supports [4]. Sorbents were synthesized on the department of polymer chemistry of chemical faculty of National University of Uzbekistan.

Reagent immobilization was carried out by mixing of support (20–40 mg) with reagent solution (5–10 ml) with concentration $1 \cdot 10^{-4}$ M during 1–10 min with following washing of support by distilled water. Immobilized sorbent was stored in Petry cups in the moist state. Influence of pH, Fe (III) concentration, buffer solution and reagent content in solid phase was investigated at stream rate of solution equaled 10 ml/min.

Reagent concentration on the support was determined by spectroscopic method by of solution absorption at 570 nm before and after immobilization.

Spectrums of diffusion reflection were obtained on spectrometry "Pulsar" giving during one flash of lamp the results on 24 fixed liners lenght of waves (320–760 nm). Electronic spectrums of absorption were obtained on K.F.K.S. an SF-46 (l=1 sm) and pH of solution was controlled on the potenciometr I-130. Data of preliminary investigations have shown the fitness of proposed sorbents of type SMAT as suppoters. At reagent choice we have beloved by demands formulated in work [5]. For immobilization and elaboration of test-method on Fe-ions the reagent N-MAC was shoosed on the base of it`s valuble chemico-analytical properties, accessibility and simplicity of synthesis.

One of the perspective forms of ion-exchange polymers are ion-exchange fibrous materials. In contrast to granulated ionites ion-exchange fibrous materials have possessed the more developed surface what promotes to high velocity of sorption.

Given work is devoted to obtain of anion-exchange materials by chemical modification of industrial poliacrylonitrile fibre "Nitron". The modification of nitronic fibre was realized by interaction of the nitrile groups of the polymer with nitrogen-containing bases — an hydroxylamine (HA), hydrazine (HD), N, N-dimethylhydrazine (DMH), hexamethylenediamine (HMD) and ethylenediamine (EDA).

The sorption fibres were obtained by interaction of fibre "Nitron" with HA in the presence of cross-linking agent-HD.

The kinetics of the chemical modification in water solution was studied within the temperature from 60 ° to 100 ° C at different concentrations HA and HD. On the base of obtained results the acceptable conditions of obtain of ion-exchange fibres with static exchange capacity (SEC) on 0,1 n HCl 5,0–5,5 mg-equ/g were determined.

On the base of IR-spectroscopic and potentiometric studies the following chemical structure of modified nitronic fibre at the treatment with HA in presence.

The chemical modification of poliacrylonitrile fibres with HD and particularly with DMH, in water solution was occurred difficulty. So before modification by these reagents "nitron" was activated by 1% solution of NaOH at 90 ° C during 1–3 mines. A result of such processing formed links of acrylic acid accelerated the reaction -CN groups with HD and DMH. At equal terms of hydrazidation values of SEC of activated fibres were much more than fibres, obtained without activation.

The catalytical action of HA on hydrazidation reaction of nitron was determined. In the presence of HA in reaction mixture the reaction of nitrile groups of the polymer with HD and DMH occurred easier and with more high degree of the conversion.

The ion-exchange fibrous materials containing as weak- and strongalkaly functional groups were obtained by treatment of nitron with HMD and EDA. In these cases the diamines simultaneously execute the function of crosslinking agent and modifier of nitrile groups. The reaction of nitron fibre with HMD without solvent or in the presence of organic solvent was carried out at temperature 130–160 ° C. Obtained in these condition the sorption material (SMA-1) has contained strongalkaly amidine groups. This reaction also can be carried out at in water medium. In this case in ionite composition will contain in more degree a weak-basic- primary and secondary amine groups. It was determined that HA additives to 3% in reaction mixture have brought to sharp growth of SEC in obtained fibres. Consequently in these systems HA also formed with SEC intermediate product, which easy interacted with HMD. Sorption characteristics of the modified fibre were retain after tenfold using of them in processes sorption-desorption.

Method of investigation. Experiments were carried out in statical and dynamic regimes. In case of statical regime in flasks (50,0 ml) 10.0 ml of reagent was introduced and then dishs from support also were introduced and system was mixed during 58 min. After this reagent was removed and immobilized sorbent was washed by distilled water and placed in analyzed solution. In case of dynanic regime the analyzed solution was passed through immobilized disks with rate 10 ml/min and coefficient changing of disk was admited as analytical signal.

Degree of reagent keeping on the support was calculated by formula R=100A/A°, where R-reagent, A and A° — it`s optical density before and after immobilization.

Results and discussion

For immobilization of N-MAC the polyacrylonitrilic fiber, modified by amino-, amido-, and carboxylic groups was used in form of disks with diameter 2 sm. Moist disks with immobilized N-MAC (IMN-MAC) (mass 30–40 mg) were washed by 50 ml 0.1 M HCl, 10 ml acetone and after this they were placed during 10 min in solution of N-MAC and stored in Petry cups in the moist state.

It is shown that reaction of Fe (III)-ions with IMN-MAC is more sensitive and selective in comparation with their interaction with N-MAC in solution.

With aim of metrological estimation of the proposed sorption — photometrical method with IMN-MAC, determination of it`s competition degree and inclusion in arsenal of known and wide used optical methods, the obtained results by determination of Fe (III) in samples of different by nature waters with using of our proposed method were compared with results, obtained by method of atomic adsorption and some GOST method.

From obtained result it is shown that the elaborated method of Fe (III) determination by IMN-MAC has differed by high selectivity and reproducing with Sr didn`t exceed 0.18. And also the obtained results have indicated on the based metrological by recommendation of the proposed method for analysis of different by nature waters.

References:

1. Upor E., Novak D., M. Mir. 1985. P. 359.
2. Amelin V. G., Tretjaykov A. V. J. Analytical chem. 2008., – M. V.61. – № 4. P. 430–436.
3. Shvoeva O. P., Trutneva L. M., Savvin S. B. J. Analytical chem. M. 1994. V.49, – № 5. P. 574–580.
4. Gaphurova D. A., Khakimdjanov B.Sh., Mukhamediev M. G., Musaev U. N. TashGu. 1999. – № 2. P. 27–29.
5. Gevorgyan A. M., Smanova Z. A. Uzb.chem.Jurnal 2007. – № 5. P. 46–48.
6. Dmitrienko S. G., J. Analyt. chem. – M. 2006, V.61. – № 1. P. 18–24.

Contents